NON DESTRUCTIVE TESTING OF STRUCTURES

Part1: Masonry Arch Bridges

Zoltan Orban

University of Pécs Faculty of Engineering and Information Technology

University of Pécs Faculty of Engineering and Information Technology
Department of Civil Engineering

STRUCTURAL DIAGNOSTICS AND ANALYSIS RESEARCH GROUP
www.structuraldiagnostics.eu

Published by University of Pécs Structural Diagnostics and Analysis Research Group

ISBN 978-963-429-834-2

CONTENTS

PREFACE

This textbook has been written to provide civil and structural engineering students and professionals with background information needed to test and assess masonry arch bridges with the help of non-destructive tools.
This textbook focuses on methods of Non-Destructive Testing (NDT) for railway masonry arch bridges primarily but the methodology described can be used on highway structures as well.

Various NDT methods are shown and compared considering several aspects such as cost efficiency, reliability of measured data, easiness of implementation, level of disturbance to traffic, etc. The principles of the methods and the required equipment for their use are briefly described.
Results of field tests are discussed that were performed by the Structural Diagnostics and Analysis Research Group of the University of Pécs in co-operation with Eötvös Loránd Geophysical Institute and ORISOFT Engineering Consulting Ltd., Hungary.
The text also includes descriptions of investigations and experiences gained by tests carried out at European railway administrations Special attention is given to and detailed guidance is provided in this document on the following methods: georadar, seismic tomography, infrared thermography and boroscopy.

This textbook should be considered as an initial document, as it does not fully explore the full range of possibilities for non-destructive inspection of arch bridges. These techniques constitute a continuously developing topic that still require a great deal of research.
It is also recommended therefore that students become thoroughly familiar with the most current recommended practices as well.

The author hopes that this textbook will interest a new generation of young people in considering their careers in bridge engineering and non-destructive testing of historical structures.

Chapter 1
INTRODUCTION

1.1 General

Masonry arch railway bridges still play a significant role in the traffic infrastructure in Europe and worldwide, therefore maintenance and assessment of these structures are of fundamental economic importance. The number of masonry arch railway bridges and culverts is estimated to be around 200.000 individuals in Europe.

In order that the railways accommodate increased loading parameters, it is necessary to assess the load carrying capacity and serviceability of existing masonry arch bridges. Assessment of masonry arch bridges is difficult as there is little knowledge or experience of design of these structures to modern standards, and much of the structure is hidden from view. To provide confidence in the assessment results, reliable input parameters are required for the numerical analyses. Accordingly, effective inspection and testing methods to establish the parameters are necessary.

Several inspection methods are used in civil engineering practice to investigate the condition or to determine the structure of masonry arch bridges. The most common method is still the pure visual inspection. Destructive testing is also used although there is a tendency in recent years towards using non-destructive testing techniques.

Most assessment procedures require the masonry strength and some other mechanical properties as the major input parameters for assessment. Destructive Testing (DT) of masonry bridges is therefore necessary in many instances, although it should be noted that the results of most destructive tests are affected by significant uncertainties and they may provide only local information on some part of the structure, and cannot be directly extended to the whole bridge. While conventional DT methods focus mainly on the mechanical characteristics of the materials, Non-Destructive Testing (NDT) and Semi-Destructive Testing (SDT) methods can provide an overall qualitative view on the arch condition. NDT methods on the one hand seem to be most promising tools for the inspection of masonry arch bridges but on the other hand need a great deal of further study and research.

Monitoring systems are occasionally installed on masonry arch railway bridges in order to follow the evolution of damage patterns such as cracks or deformations. The knowledge of this evolution can help preventing more serious damage or a total collapse of the structure. Monitoring may also provide information that can be used to determine the root causes of the defects. These may be from visual inspection or electronic data collection. Monitoring can be done continuously or via a series of discrete measurements over an extended period.

The following list summarises testing methods that are frequently used on masonry arch bridges:
Destructive Testing Methods: mechanical tests on cored samples, physical and chemical tests on cored samples, tests on soil or backfill properties.

Semi-Destructive and Non-Destructive Testing methods: boroscopy, flat-jack test, hammering (sounding), surface measurements (Hardness, Schmidt hammer, penetration, pull-out tests), georadar, infrared thermography, sonic methods, conductivity measurements.
Monitoring methods: crack monitoring, deflection and relative displacement measurements, dynamic tests, load tests.

1.2 The role of NDT in the assessment of masonry bridges

Masonry arch bridges rarely have accurate or perhaps any drawings of their construction or early repair details. The internal structure of arch bridges may be unknown from external appearance, and may include features such as haunching at support, vaulting, internal spandrel walls, ribs or the presence of saddle over the arch barrel. It may, therefore, be difficult to determine the physical dimensions of the main structural elements of the bridge (*Fig. 1* shows typical structural elements of a railway masonry arch bridge).

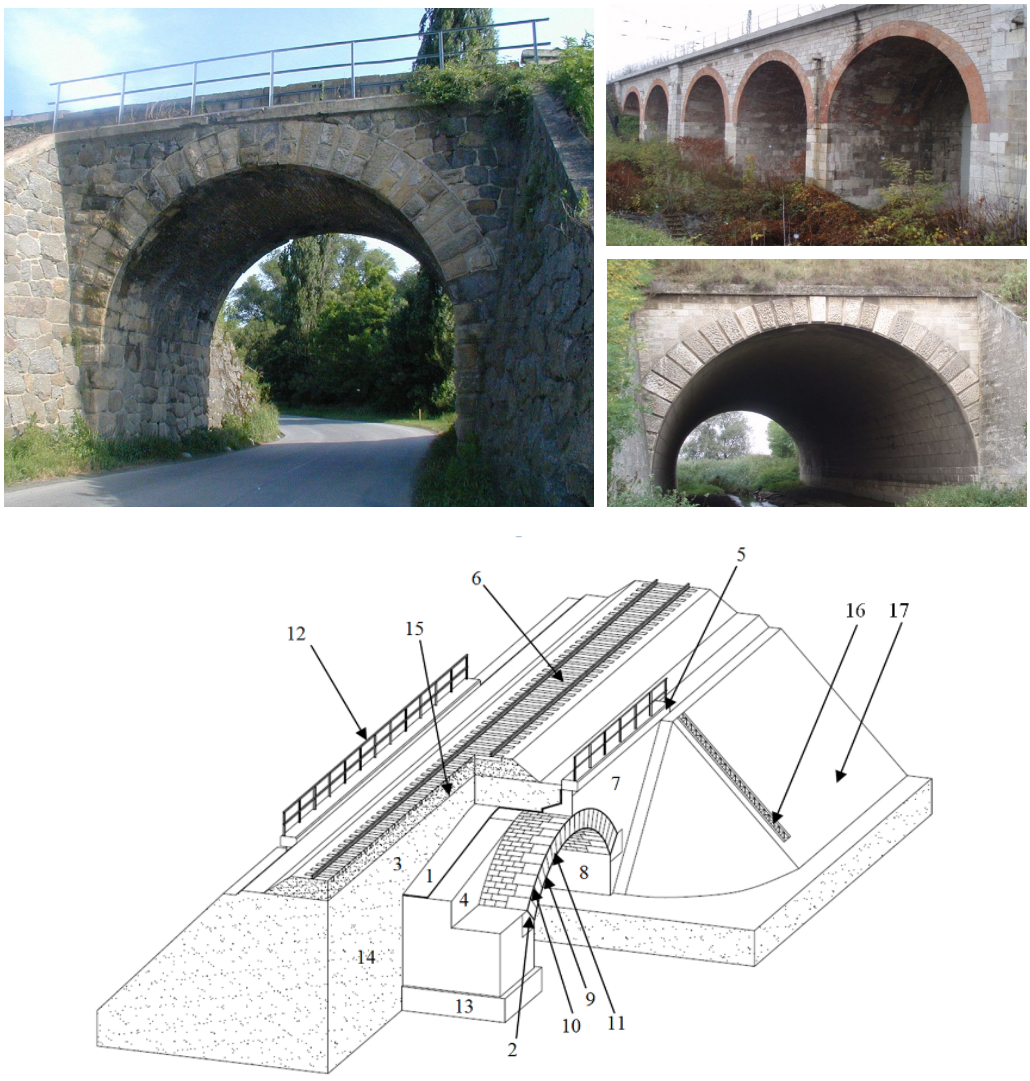

1-waterproofing 2- springing 3- fill 4- backing/haunching 5- edge beam 6- railway track 7- spandrel wall 8- abutment 9- intrados 10- extrados 11- arch stone 12- railing 13- foundation 14- backfill 15-ballast 16-inspection stairs 17-slope

Fig. 1 Elements of typical Hungarian masonry arch railway bridges

Moreover, materials used for the abutment, barrel, spandrel and backfill are variable, and interact. The thickness of the barrel may be greater at the springing than at the crown that might not be visible at the edge of the barrel. The arch barrel thickness across a width may be reduced locally under the external spandrel walls or increased under the track. The material and geometry of backing or haunching and the way they are connected to the arch are often unknown and are rarely visible (see example in *Fig. 2*). This inadequate knowledge of geometry and materials used complicates the problem of accurate modelling of behaviour. Further complication is the possibility of ring separation or the presence of other hidden defect and irregularities such as voids in the granular backfill immediately above the extrados, areas of reduced density and stiffness in the fill adjacent to the extrados, and cracking in the arch ring. Bridge repairs and strengthening require sufficient knowledge on existing defects and their causes too. Hence it is essential that some information of the internal structure and condition of a bridge is obtained before any remedial work or strengthening can be carried out. In this respect NDT methods can play an important role both in the inspection and assessment process and later when the result of the strengthening process has to be checked.

Fig. 2 Left: Stone backing of brickwork arch (bridge under demolition, Hungary), Right: Haunching between piers (bridge under construction, Hungary)

Assessment of masonry arch bridges is carried out at various levels. Higher level assessment is necessary when the load carrying capacity cannot be justified by simple assessment tools, when the structural system of the bridge is complicated or when the presence of defects require sophisticated models. It can also be proposed that where a bridge fails the load-carrying capacity assessment by a small margin, and it looks to be in good condition without significant deterioration, further analysis is carried out that utilise the results of additional investigation using NDT methods.

The condition, construction material and depth of the foundations of existing masonry arch bridges are often unknown although the knowledge of these information is essential for their assessment. The inspection of foundations is difficult in most cases as they are not directly accessible. Non-destructive investigation of existing bridge foundations has gained ground in recent years. These techniques are deemed quick and effective tools in mapping foundations without causing damage or disruption to traffic.

NDT methods provide a means to evaluate masonry without causing observable damage. In spite of the recent advances in NDT technology, it is important to understand that, at the present time, there is no single technique that is appropriate for all situations, and that careful application of complementary techniques often provides the most useful information. NDT methods do not provide a direct measure of material properties, such as strength or stiffness,

and correlations between NDT results and material properties are often based on tenuous relationships. It is possible however to gain a general understanding of the relative quality of the material being investigated. Thus destructive investigative approaches, such as removal of masonry at probe holes for visual examination or drilling cores for further analysis in laboratory, may not be eliminated, but can be reduced through the use of NDT procedures.

1.3 The test programme for case studies

Due to the fact that the number of references and projects that have utilized NDT methods on masonry arches is very low and only a few calibration tests have been carried out until now there was a need to establish what NDT techniques are available and how applicable they are for the specific inspection purposes of masonry arch bridges.

A test programme has been therefore carried out that was aimed at working out an inspection system for masonry arches with the utilisation of the potential in non-destructive testing. The objective of the programme was to determine whether the selected NDT techniques could be used in order to give information which would not be possible using the traditional inspection methods. The following testing methods were involved in the programme: georadar (GPR), infrared thermography and seismic methods, together with calibratory core drillings and boroscopy survey. Besides testing the efficiency of the above mentioned methods on masonry arches it was also important to find forms of representing measured data that are meaningful for assessor engineers.

In the first part of the test programme GPR survey has been carried out on masonry wall specimens made from used bricks. The objective of the test was to help calibration of GPR technique for the investigation of brickwork constructions. Cavities and other anomalies were artificially created in the brickwork specimens in order to test the efficiency of the radar technique in detecting these anomalies.

GPR investigation has been performed on selected masonry structures. These include both brickwork and stonework arch structures and bridge abutments. Some of the test results have been calibrated and confirmed by boroscopy survey and other tests carried out on cores taken out from the structure.

Seismic tomography has been experimentally used at one of the structures but due to difficulties in the interpretation of measured data this type of testing has not been repeated at other structures.

Series of tests have been performed with the use of infrared thermography on four masonry arch bridges. The aim of the survey was to explore the application possibilities of this remote sensing method. The significance of research is confirmed by the fact that during the periodical inspection of masonry arch bridges, especially those with difficult or costly access, more and more importance must be given to remote sensing methods.

The foundations of two structures have been investigated by the borehole radar and parallel seismic methods.

The field tests were carried out between 2004 and 2016 on Hungarian railway masonry bridges. Some of the results and conclusions of the test programme are summarised in Case Studies. Full details of the tests performed are found in separate reports (see Literature).

Chapter 2

REVIEW ON NDT AND MONITORING METHODS

This chapter gives an executive summary on the available NDT methods that can be used for the inspection of masonry bridges. In order to complete the list information are provided on semi-destructive testing (SDT) and bridge monitoring methods too. A summary review is given in a table format at the end of the chapter for each test families (*Chapter point 2.4*).

2.1 Non-Destructive Testing (NDT) methods

2.1.1 Sonic methods

Description:
The technique is based on the generation of sonic impulses at a point of the structure. A signal is generated by a percussion or by an electrodynamics or pneumatic device (transmitter) and collected through a receiver which can be placed in various positions of the structure. The resulting data is based on the wave velocity by measuring the time the impulse takes to cover the distance between the transmitter and the receiver. The velocity of the stress wave passing through the masonry material is proportional to the density, dynamic modulus and Poisson's ratio of the material. The quality of some materials is related to their elastic stiffness so that measurement of sonic pulse velocity in such materials can often be used to indicate their quality as well as to determine their elastic properties.
Some further developments of the method: *seismic tomography*, *seismic reflection, impact-echo method.* The *parallel seismic* method is used for mapping foundations. Further information is given in Appendix 1 – A1.3.

Instrumentation:
A typical sonic transmission system setup would consist of a control unit run from a laptop or similar computer connected to a series of geophones (accelerometers) and to an instrumented hammer source.
The systems are normally ruggedised and portable being powered from a 12V power supply. The geophones can be attached directly to the structure using brackets and expansion bolts into the mortar beds. This enables many travel paths to be recorded simultaneously (tomography can additionally build up a 3D image of the internal structure). The system is triggered by an instrumented hammer and records the arrival of the sonic pulse through the structure. Several records can be stacked together from a single point in order to improve the quailty of the data.

Test results are used for:
- Detection of cracks, voids, flaws within the masonry,
- Finding voids and poor consolidation within the fill material,
- Finding damaged structural parts,
- Mapping foundations,

- Controlling the effectiveness of repair intervention.

Advantages:

- Can give information on the integrity of the barrel without direct access to the barrel itself,
- Provides data not only on the local but also on the overall condition of the structure.

Disadvantages, limits:

- Interpretation of the results is complicated,
- Finding correlation of the sonic parameters to mechanical characteristics is difficult,
- The information provided is rather qualitative than quantitative,
- A large number of measurements should be carried out in order to obtain estimable data therefore the measurement is expensive,
- Different masonry types need different calibration,
- Ultrasonic tests only useful for homogeneous materials, like natural stones. In case of heterogeneous materials (masonry) the penetration depth is too small.

2.1.2 Ground Penetrating Radar (GPR)

Description:

The method is based on the propagation of electromagnetic impulses, which are transmitted into the material using a dipole antenna. The impulses are reflected at interfaces between materials with different dielectric properties. The results are based on the correlation between the dielectric constants and the material characteristics. Sampling is so rapid that the collected data is effectively a continuous cross section, enabling rapid assessment of thickness and condition over large areas.
Further information is given in Appendix 1 - A1.1

Instrumentation:

The system consists typically of a control unit powered by 12V supply, with a transducer head connected by a cable. Different frequency antenna are used, with the higher frequencies giving maximum resolution and lower frequencies giving a greater penetration. The systems are often linked to an electronic distance measuring wheel in order to control the scan rate and increase positional accuracy.

Test results are used for:

- Detecting voids, inclusion of different materials, detachment of rings,
- Detecting backfill conditions (compact and loose areas),
- Defining hidden geometry, e.g. presence of internal spandrels, haunching, saddle over the arch,
- Detecting the state of damage, structural irregularities, unfilled joints,
- Defining the presence and level of moisture,
- Controlling the effectiveness of repair intervention.

Advantages:

- Provides data not only on the local but also on the overall condition of the structure,
- Has large penetration depth,
- Can penetrate multiple layers and accurately measure the depth of defects (when calibration has been carried out prior to the measurements),

- Relatively quick measurement, can cover large areas rapidly,
- The continuous recording in real time permits preliminary assessment of the findings.

Disadvantages, limits:

- The interpretation of data requires a highly skilled expert,
- Not all measured data are of engineering significance,
- High resolution only achievable at shallow depth,
- The correlation of the measured data to mechanical properties is tenuous,
- The radar wawes cannot penetrate conductive materials such as metal, clayey and highly saline soil.

2.1.3 Infrared thermography

Description:

The measurement is based on the thermal conductivity of the masonry material. The thermal radiation is collected by a camera sensitive to infrared radiation. Measured surface radiation can be converted to surface temperature if the surface emissivity is known (emmisivity ranges from 0 for a perfect reflector, to 1 for a perfect black body). The result is a thermographic image where each tone corresponds to a temperature range. Advanced thermal imaging systems are capable of detecting differences in surface temperature as small as 0.08˚C and can therefore be applied to structures where temperature variations are relatively small. Correlation to masonry mechanical and physical properties of the masonry can be established by calibration tests.
Further information is given in Appendix 1 – A1.2.

Instrumentation:

A typical thermographic imaging system comprises of a hand-held infrared camera. The system is self powered and is operated in a similar fashion to a typical video camera. Data can be recorded as both stills and video images. Post processing is possible on still images.

Test results are used for:

- Survey of delamination, cavities,
- Detection of inclusions of different materials, cracks and unfilled joints,
- Detection of thermally conductive pipes and services,
- Detection of vegetation on the surface,
- Detection of moisture (the camera finds the cold parts where is a continuous evaporation, transpiration).

Advantages:

- Applicable to wide surfaces,
- The method has a high thermal and spatial resolution,

Disadvantages, limits:

- Has a low penetration depth. It is impossible to locate anomalies which are hidden in the internal parts of the structure.
- Not all measured data are of engineering significance,
- Effective interpretation requires appropriate software,
- Often sensible to boundary conditions,
- Detection of anomalies are only possible when they effect surface emmission.

2.1.4 Conductivity measurement

Description:
Electromagnetic fields are propagated into the structure and the variations are monitored. The instrument produces a constantly changing magnetic field that induces a small electrical current (called an eddy current) within the structure. Eddy currents, in turn, produce a constantly changing magnetic field that induces a current in the receiver coil of the instrument. These provide geometrical and electrical information on the materials investigated. The method is based on the principle that the electromagnetic conductivity of a material is a function of the degree of its moisture content and other properties such as porosity, temperature and clay content. In addition, the measured conductivity will be affected by the presence of strongly magnetic and strongly conductive materials, such as metalwork.

Instrumentation:
The system uses an Electrical Conductivity Meter which can work in two orientations: vertical (relative to the structure) and horizontal (relative to the structure). The different orientations allow different depths within the structure to be investigated. The vertical orientation measures between cca. 0.5m and cca. 1m depth, while the horizontal orientation measures from the surface to a depth of cca. 0.5m.

Test results are used for:
- Defining the presence and level of moisture,
- Defining the presence and level of salt content,
- Defining geometry, composite construction of the masonry wall,
- Defining presence and location of voids, metalworks and services.

Advantages:
- Provides data not only on the local but also on the overall condition of the structure,
- Has a high penetration,
- Very quick and cheap measurement,
- System does not require intimate contact with the surface (although it should be held as close as possible).

Disadvantages, limits:
- The interpretation of data requires a highly skilled expert,
- Results are adversely affected by metalwork within a structure,
- The correlation of the measured data to mechanical properties is tenuous.

2.2 Semi-Destructive Testing (SDT) methods

SDT methods are based on in-situ localised measurements of the masonry structure. Although slightly destructive, the measurements can provide approximate values of some mechnaical or physical properties.

Most SDT methods are considered as a surface or small penetration techniques which can provide only qualitative information on the masonry condition and be used only for preliminary investigation.

2.2.1 Coring and analysis of small diameter cores

Description:
Small diameter cores (cca. 50mm) are drilled from the structure, perpendicular to the masonry surface. The cores are visually analysed and/or taken to laboratory for further testing. The drilled borehole can be utilised for other inspection purposes such as *boroscopy* (*3.2.2*) investigation or *borehole radar* testing.

Instrumentation:
A drilling is usually carried out with a water-cooled diamond-tipped core barrel. The drilling operation requires rigid support platform, generator, water pump and skilled personnel. Analysis of the cores require specific equipment depending on the purpose.

Test results are used for:

- Identifying materials used for construction, determining their internal composition and condition,
- Determination of unknown structural dimensions and features (such as barrel thickness, presence of haunching or saddling, backfill material),
- Testing material properties on cores (mechanical, physical, chemical),
- Calibration of other testing methods.

Advantages:

- The results are transparent and do not rely upon uncertain interpretation of data.

Disadvantages:

- Provides only localised information,
- The cores are not taken in the direction of principal stress that exist in the structure therefore the samples are usually not ideal for testing strength properties. The results of the test must be interpreted accordingly and treated as approximate values.
- Slightly destructive, the signs of coring will remain at the structure,
- Requires heavy machinery.

2.2.2 Boroscopy, endoscopy

Description:
Boreholes are drilled in representative parts of the structure. A small camera is inserted into the borehole allowing a detailed study of its surface. The results of this study can be recorded for further analysis.
Further information is given in Appendix 1 – A1.3.

Instrumentation:
There are two systems used: boroscopes and flexible imagescopes. Boroscopes have a rigid tube and usually use optical fibres to illuminate the subject and conventional lenses to transmit the images. Flexible imagescopes have a flexible tube which is steerable and able to follow a more tortuous path than the rigid boroscopes thus it can extend to a much greater depth within the structure than with a rigid boroscope. The diameter of the insertion tube ranges from 5mm to 50mm. Larger dimeter systems can provide better view of the surface of the borehole but require wider boreholes which is more destructive. In both systems the images can be recorded directly on to a video system or hard disc of a computer.

Test results are used for:

- Detection of large cavities and defects (such as delamination, mortar loss, ring separation, cracks, voiding behind the barrel and in the fill)
- Identifying materials used for construction, determining their internal composition and condition (e.g. layering condition, state of decay in masonry, type of fill, presence of moisture within brickwork and fill),
- Identifying materials used for construction, determining their internal composition and condition,
- Determination of unknown structural dimensions and features (such as barrel thickness, presence of haunching or saddling, backfill material),
- Calibration of other testing methods.

Advantages:

- The operation is simple,
- Provides a permanent digital record of the results,
- The results are transparent and do not rely upon uncertain interpretation of data.

Disadvanteges, limits:

- Provides only local information and a stratigraphic view of the section investigated.
- The measurement requires boreholes to be drilled which can be destructive depending on the diameter and length of the borehole.

2.2.3 Flat-jack test

Description:

The flat-jack test is used to determine in-situ the stress state and some mechanical characteristics (e.g. strength and elastic modulus) of existing masonry structures.

Single flat-jack test is carried out by introducing a thin flat-jack into the mortar layer. The determination of the state of stress is based on the stress relaxation caused by a groove perpendicular to the surface. When pressurized, the flatjack exerts stress on the surrounding masonry and, by measuring surface deformations, information on the existing state of stress can be obtained. The displacement caused by the slot and the ones subsequently induced by the flat-jack are measured by removable extensometers.

In double flat-jack test a second groove is made parallel to the first one and a second flat-jack is inserted, at a distance of approximately 40-50 cm from the other. When pressurized simultaneously, the flatjacks impose a state of compressive stress on the masonry between them. The in situ deformability results are typically presented in the form of a stress–strain plot, from which the masonry compression modulus can be calculated. Measurement on the deformability characteristics are usually carried out with removable extensometers.

Instrumentation:

A flatjack is a hydraulic pressure cell manufactured to be very thin, for insertion into cleared masonry mortar joints. Various shapes and sizes of jacks are manufactured ranging from simple rectangular jacks to different types of segmental jacks. The groove is usually made with a steel disk with a diamond cutting edge.

Test results are used for:

In single flat-jack test:

- Determination of in-situ stresses,

- Determination of stress variations due to external effects.

In double flat-jack test:

- Determination of deformation characteristics (E modulus, Poisson's ratio) under uniaxial compression.
- If the test is continued until damage the compressive strength can also be measured (but it is then destructive).

Advantages:

- When a good calibration is made the method provides quantitative information on the stresses.
- The test provides more realistic information on the behaviour of the structural materials in their original location.
- In the double flat-jact test the compression test is carried out on an undisturbed sample of large area (together with lateral constraints and confinement that would not been possible to reproduce in tests under laboratory conditions)

Disadvantages, limits:

- Gives results only for the outer rings,
- The exposed face of the brickwork in an arch is most subject to weathering resulting in softening of the bricks and/or mortar resulting in lower elastic modulus values. This is not always representative of the mass of brickwork in an arch.
- In case of stress concentration the measurement gives unrealistic values.
- In order to avoid damage for the structure only elastic mechanical parameters can be determined.
- In case of inelastic deformations the equilibrium relationship used for calibration yields to incorrect results.

2.2.4 Schmidt hammer rebound test

Description:

The method based on a principle that the rebound values from the masonry surface is correlated to its strength. Rebound hardness measurements are affected by a number of variables, including surface roughness, specimen mass and geometry, vicinity of nearby edges, and hammer orientation.

Instrumentation:

The equipment used is similar to that was developed for testing concrete structures (known as Schmidt hammer) but with a reduced impact energy.

Test results are used for:

- Identifying variations in masonry material uniformity,
- Providing qualitative information on surface conditions and mortar joints,
- With careful laboratory calibration, it is possible to relate rebound hardness to the elastic properties or compressive strength of the masonry.

Advantages:

- The operation is very simple,
- Testing for rebound hardness is rapid and requires only a few seconds for each reading.

Disadvantages, limits:

- The equipment which was set up to be used on concrete or cement mortars has too high energy for weaker mortars (e.g. lime mortar),
- The properties of the mortar surrounding and the degree of bond between the bricks and the mortar have large effect on rebound values. Therefore the level of uncertainty in testing brickwork structures can be high and the interpretation of the results difficult.

2.2.5 Penetration test on mortars

Description:
The test is carried out by using Schmidt hammer with an adjustable head or by dynamic hardness tester. Correlates the depth of penetration to the mechanical properties of masonry.

Instrumentation:
Schmidt hammer with an adjustable head,
Dynamic hardness tester.

Test results are used for:

- Providing qualitative information on the condition, strength and elastic properties of mortar joints.

Advantages:

- The operation is very simple,
- Testing is rapid and requires only a few seconds for each reading.

Disadvantages, limits:

- The calibration of the test is difficult because the correlation is almost impossible to be found to the real strength of low strength mortars, especially near the surface.
- The depth of penetration is low, so in most cases only the repointing mortars are tested.

2.2.6 Pull-out test

Description:
Threaded bolts are placed on the tested surface using a power-actuated tool. The bolts then pulled out from the surface with a calibrated testing machine while the pullout force is measured. Correlation is made between the pulling-out force and the condition and mechanical properties of the masonry.

Instrumentation:
Power-actuated tool, threaded bolts, cartridges, pullout testing machine.

Test results are used for:

- Providing a rough idea of the masonry condition and strength.

Advantages:

- Testing is rapid and requires only a few minutes for placing the bolts and for reading the pullout results.
- The results considered more reliable than those from Schmidt hammer rebound test as the bolts penetrates deeper into the masonry surface.

Disadvantages, limits:

- Slightly destructive,
- Informs about near surface conditions only,
- Can not be used on mortar joints (only for thick joints),
- Not reliable when applied to rubble masonries.

2.3 Tests for monitoring

2.3.1 Hammer tapping

Description:
During the measurement the masonry surface is tapped with a hammer. Voiding and delamination cause lower pitch than that of a solid surface.

Instrumentation:
Standard equipment is used in order to increase the repeatability of the technique. The standard hammer is mounted on a rod. Scaffolding is needed when the surface is not accessible from the ground.

Test results are used for:

- Providing a rough idea of the masonry condition on the surface,
- Detection of delamination, loose bricks and voids behind the surface (only when these defects are close to the surface)
- Detection of ring separation at multi-ring arches.

Advantages:

- The operation is very simple and inexpensive.

Disadvantages, limits:

- Informs mainly about near surface conditions,
- Needs direct access to the surface under investigation,
- Investigation of the full structure can be time-consuming,
- Cannot be applied on frozen brickwork.

2.3.2 Acoustic emmission

Description:
The method is based on the phenomena that discontinuities (such as cracks and micro-cracks) in a material developed under stress or temperature result transient acoustic stress-waves that travel through the material at a speed of sound. Analysis of these signals can provide information concerning the detection and location of discontinuities and the structural integrity. The signals can be detected by accelerometers attached to the surface of the structure under investigation. By attaching sensors to the underside of arch it is possible to locate cracking events under either forced or ambient loading. Another important feature of accoustic emmission is its irreversibility. If a material is loaded to a given stress level and then unloaded, usually no emissions will be observed upon immediate reloading until the

previous load has been exceeded. This irreversibity has important practical implications because it can be used in the detection of sub-critical growth of flaws.
The accuracy of this application depends on the spacing of the sensors as on masonry the accoustic emmission signal gets dispersed by the mortar joints. In monitoring projects the system can permanently be attached to the structure.

Instrumentation:
The same technique can be used on different materials but with different signal processing. There are different sensors that can be used on different materials as they emit different frequency of acoustic emissions. The signals are acquired and stored by a waveform analyser coupled with a computer.

Test results are used for:
- Monitoring the propagation of cracks in the material,
- Providing a qualitative view on the level of deterioration,
- Identifying the previous maximum load the bridge has been subjected to (under forced loading).

Advantages:
- The method gives information on what is happening inside materials, real-time,
- The method is very sensitive,
- The method can be used for permanent monitoring.

Disadvantages, limits:
- The instrumentation can be quite expensive,
- The data analysis is not always trivial, requires a skilled operator and lots of computer memory,
- High level of background noise makes interpretation of data difficult,
- Although accoustic ammission systems can locate defects and cracks they cannot determine the absolute size only the latest crack growth increment.

2.3.3 Crack monitoring

Description:
When a progressive crack growth is suspected in the structure a crack monitoring system can be installed in order to follow the evolution of the crack pattern. In many cases the knowledge of the crack pattern evolution can help understanding the root causes of damage, raise attention to accelerated damage process and help preventing the collapse of the structure.
Crack monitoring can be carried out in many ways with a variety of instrumentation.

Instrumentation:
There are many ways exist for the monitoring of cracks in masonry. These include manual systems where the results should be read manually, and automated systems where data can be read remotely via a data logger. Many automated systems also have a thermometer and are able to log temperature as well as displacement.
Typical elements of crack monitoring sytems are:
- strain gauges,
- crack width gauges,

- extensometers,
- thermometers,
- cement patches (perpendicular to the crack width),
- bolts placed on each side of the cracks (serves as permanent measuring points for long term measurements).

Test results are used for:

- Evolution of the crack pattern when a progressive crack growth is suspected in the structure.
- Monitoring movement at joints or cracks to give indications of performance problems.

Advantages:

- The instrumentation is easy to install and inexpensive (expecially the manual systems),
- Automated systems can be read remotely after installation for many months with no need for visiting the site.

Disadvantages, limits:

- Manual systems require direct access and regular inspection to read off the results,
- The results can be misleading if no recordings on temperature variations are made,
- Automated systems can be quite expensive,
- The systems are often broken off.

2.3.4 Laser profiling

Description:

Laser profiling can be split into two catagories: the relatively simple 2-dimensional prifiling of an arch to give the shape in one plane and the 3-dimensional laser scanning which creates a complete image of the structure. Both 2-dimensional and 3-dimensional laser profiling systems use a time-of-flight method to measure how long it takes for each laser pulse to hit a surface and return to the scanner. The laser scanning uses a laser cloud principle which is collecting scans containing millions of points which are then converted by specialist software into 3-dimensional images which can be viewed in a CAD environment.

Instrumentation:

A simple 2-dimensional profiling system consists of a laser ranging equipment connected to a computer which records measured data and controls the movements of the laser equipment. An appropriate software is used to determine the bridge profile in a coordinate system.
An automated scanner system is a fully enclosed unit which can be targetted towards the object under investigation and left to run. User defined parameters dictate the area to be scanned with the system recording all the range and angle information necessary to recreate the 3-dimensional image. Geodetic surveying is often used to tie the readings into a true 3-dimensional coordinate system.

Test results are used for:

- Determination of arch profile and geometry,
- Monitoring deformations of arch profile,
- Making digital record of defects such as bulges, cracks and missing brickwork.

Advantages:

- The method can give information on any deformation in the shape of the arch over time,
- The accuracy of the measurement is cca. ±1mm which is enough for most assessment purposes,
- Does not require direct access to the surface of the arch.

Disadvantages, limits:

- 3D systems need to collect a large volumes of data which requires prolonged data processing,
- Obstructions may result in areas not covered.

2.3.5 Moisture monitoring

As a result of the range of problems associated with increased levels of moisture a number of techniques have been developed to monitor moisture levels of masonry structures. Many of these techniques cannot be relied upon to give absolute measurement of moisture levels but can give relative moisture content and as such can be used, along with an understanding of the mechanisms involved in the movement of moisture.
Various electrical, thermal and chemical properties of water are used to test for its presence in a number of techniques including timber plugs, electrical resistance, electrical conductivity, electrical capacitance, calcium carbide meters, oven drying method, Ground Penetrating Radar (GPR) and infrared thermography. The principles, benefits and limitations for each of these are briefly described as follows.

Timber plugs:
The method is based on a principle that timber is a hygroscopic material and will eventually reach an equilibrium moisture content at a given ambient condition. The timber plugs are inserted into sealed holes in the masonry and its moisture content can be deduced from the timber properties. The moisture content of the timber plug is determined by gravimetric methods using oven drying or by monitoring the resistance between two probes inserted into the timber plug.
The method is not very accurate at extremes but accuracies of ± 3% over the range of 10 to 90% RH are claimed.

Electrical Resistivity method:
This technique supplies relative moisture content using the electrical resistivity of moisture. The method is inexpensive and uses a small hand held device. Limitations of the method are that direct hand access is required so that two probes to be inserted or drilled into the material under investigation, thus the procedure is slightly destructive. Results heavily effected by levels of contaminants such as salts.

Electrical Conductivity:
This technique supplies relative moisture content within 2 to 3cm of the surface using the electrical conductivity of moisture. Its benefits and limits are similar to those of the Electrical Resistivity method.

Electrical Capacitance:
This technique supplies relative moisture content within 2 to 3cm of the surface using dielectric properties of moisture. Further benefit of the method compared with the previous two that the results are largely independent of contaminants such as salt. On the other hand a

large multi-component equipment and the off site interpretation of the results are generally required which increases the cost of the measurement.

Calcium Carbide Moisture Meters:
This technique supplies moisture content using calcium carbide powder to convert free water in a drilled sample to acetylene gas. Advantage of the method that measurements can be taken from samples drilled from different depths of the structure, and provides on site absolute measurement of moisture. It is a disadvantage that drilling is required and is therefore partially destructive.

Oven Drying Method:
This simple technique supplies moisture content by weighing a sample before and after drying in oven. The method means simple and accurate measurement of the absolute moisture content of samples removed from different depths of the structure. Disadvantage that the procedure is partially destructive and requires off-site measurements on the samples taken out.

Ground Penetrating Radar (GPR):
Description of the method is found in 2.1.2.

Infrared Thermography:
Description of the method is found in 2.1.3.

It should be noted that while the electrical resistivity, conductivity and capacitance tests along with calcium carbide and oven drying methods are relatively cheap and simple they all require access to the surface under invesitgation, some are partially destructive and they only give point measurements. Thermography and GPR, on the other hand, are both relatively expensive systems that often require off site processing to produce patterns in moisture variations. They both, however, offer rapid progress over large areas, and in the case of GPR variations in moisture content can identified at depths up to 1m in the right conditions.

2.3.6 Monitoring deformations and displacements

Deflection measurements:
The measurement of deflection at the crown forms an important element of the serviceability assessment of arches. In many cases these tests are complemented by measurements at the quarter or third points of the arch. Information provided by the measurements is also used for calibrating analytical models or checking and predicting structural behaviour under loading.
Instrumentation:

- extensometers,
- geodetical appliances.

Relative displacement measurements:
The measurements can provide information on the relative horizontal movements between the springings or their rotation.
Instrumentation: The measurements can be carried out by the use of dynamic oscillating methods, removable extensometers or invar wire. Invar wire is used for an accurate measurement of the distance between two fixed points on a structure and the evolution of the distance in time.

Strain measurements:
Strain measurements provide information on the fluctuation of stresses under loading within the elastic limit of the material. Measurements are usually taken at the crown, quarter points and the springings of the arch.
Instrumentation: The most common methods and device used for the measurements are strain gauges, inductive transducers and dynamic oscillation methods.

2.3.7 Dynamic monitoring (vibration tests)

Description:
The principal objective of the dynamic tests is to investigate the behaviour of the structure to vibration. Vibration tests are carried out to detect the frequencies, the modal shapes and the correspondent modal damping of the structure. These parameters are the characteristics of the local and global behaviour of the structure. The modal frequencies are representative of the global behaviour of the system, while the modal shapes allow detection of the local performance. In passive test the vibration is made by traffic loading (environmental vibration), while in active test by local hammering (forced vibration).

Instrumentation:
A typical system would consist of several monitoring units each containing three orthogonally placed geophones to measure displacement in 3-dimensions. The monitoring units would contain a processing module as well as a data storage unit. Chart printouts can be printed off in real time from some systems.
Other systems may consist of an array of geophones that could be mounted on the structure and either listen continually or record data when vibration levels reach a pre defined threshold.

Test results are used for:
- Localisation of damaged areas by the analysis of the modal shapes,
- Monitoring the arch behaviour over time,
- Verifying the results of a theoretical model,
- Verifying the effectiveness of strengthening intervention (by comparing the structural response prior and after intervention)

Advantages:
- Passive method gives vibration levels for the environment without any need to introduce energy into system.
- The system can be left for weeks to obtain a large volume of data for statistical analysis.

Disadvantages, limits:
- Requires complex processing of information to relate to condition and construction of the arch,
- Very little research has been done on applications associated with masonry structures.

2.4 Summary review

The following tables provide a summary review on the available NDT, SDT and monitoring methods with respect to their principle, the usability of measured data and the advantages or disadvantages of application.

	Name of method	Description	Results are used for	Advantages /disadvantages
NON-DESTRUCTIVE TESTING METHODS	**Sonic methods**	Sonic vawes are transmitted through the structure. The velocity of the waves is proportional to its properties.	Detection of voids and cracks; Hidden geometry; Structural integrity.	Has high penetration; Gives an overall qualitative view; Calibration and interpretation are difficult; Slow in progress.
	Georadar	Electromagnetic impulses are transmitted into the material and recorded by a receiver.	Detection of voids; Hidden geometry; Moisture distribution in masonry and fill.	Has high penetration; Gives an overall qualitative view; Relatively quick in progress; Interpretation is difficult; Not applicable in conductive environment.
	Infrared thermography	The thermal radiation from the surface is collected by an infrared camera.	Survey of cavities and delamination; Remote identification of materials; Detection of wet areas.	Gives an overall qualitative view; Requires no direct contact with the surface; Has low penetration depth; Sensible to boundary conditions.
	Conductivity measurements	Electromagnetic fields are propagated into the structure and the variations are monitored.	Detection of voids, metal objects; presence and level of moisture.	Very quick and cheap; Requires no direct contact with the surface; High penetration; Gives an overall qualitative view; Interpretation is difficult.

Table 1: Summary review of NDT techniques

	Name of method	Description	Results are used for	Advantages /disadvantages
SEMI-DESTRUCTIVE TESTING METHODS	**Coring and analysis of small diameter cores**	Small diameter cores are drilled from the structure and further analysed visually or in laboratory.	Identifying materials; Hidden geometry; Testing material properties; Calibration of other tests.	The results are transparent and reliable; Provides only localised information; Slightly destructive.
	Boroscopy	A small camera is inserted into boreholes drilled in the structure allowing a detailed study of its surface.	Identifying materials; Detection of cavities and defects; Calibration of other tests.	The results are transparent and reliable; Provides only localised information.
	Flat-jack test	Flat-jacks (single or double) are inserted into slots and pressurised with a hydraulic device while stresses and deformations are measured.	Determination of in-situ stresses (single test) and deformation properties (double test).	Can provide quantitative information on the stresses; Calibration is difficult; Gives results only for the outer rings.
	Schmidt hammer rebound test	The method is based on a principle that the rebound values from the masonry surface is correlated to its strength.	Providing qualitative information on surface conditions and strength.	The operation is very simple and quick; The uncertainty in testing brickwork can be high.
	Penetration test on mortars	Based on a principle that the depth of penetration is correlated to mechanical properties.	Providing qualitative information on strength and elastic properties of mortar joints.	The operation is very simple and quick; Calibration is difficult, uncertainty is high.
	Pull-out test	Threaded bolts are pulled out from the surface while the pullout force is measured.	Providing a rough idea of the masonry condition and strength.	The operation is simple and quick; Informs about near surface conditions only.

Table 2: Summary review of SDT techniques

	Name of method	Description	Results are used for	Advantages /disadvantages
MONITORING METHODS	**Hammer tapping**	The masonry surface is tapped with a hammer and listened to.	Providing a rough idea of condition.	The operation is simple and inexpensive; Informs mainly about near surface conditions.
	Accoustic emmission	Stress waves cased by the development of micro-cracking in masonry are detected and monitored by accelerometers.	Monitoring the propagation of cracks; Providing a qualitative view on the level of deterioration.	The method can be used for permanent monitoring; Interpretation of the results can be difficult.
	Crack monitoring	Manual or automated monitoring systems are used to follow the evolution of the crack pattern in the structure.	Monitoring movement at joints or cracks to give indications of performance problems	Easy to install; Automated systems can be read remotely; Manual systems require direct access.
	Laser profiling	Laser ranging equipment or scanner connected to a computer are used in 2D and 3D profiling systems in order to create the profile or the complete spacial image of the arch.	Determination of arch profile and geometry; Monitoring deformations of the arch in time.	Does not require direct access to the surface of the arch; Accuracy is enough for assessment purposes; 3D systems require prolonged data processing
	Moisture monitoring	Various electrical, thermal and chemical properties of water are used to test for its presence in the structure. A large variety of techniques are used including remote sensing and point measurements.	Mapping the presence of moisture in masonry and fill material; Point measurements are able to determine moisture content while remote sensing methods provide an overall view on mositure distribution.	Point measurements are usually simple and cheap; Remote sensing methods are quick, but provide only a qualitative result.
	Monitoring deformations and movements	Manual or automated systems are used for measuring or monitoring the deflection at crown, the relative horizontal movements between the springings or their rotation and the fluctuation of stresses under loading.	Serviceability check of arches; Calibrating analytical models; Monitoring movements and deformations can give indications of performance problems.	Easy to install; Automated systems can be read remotely; Manual systems require direct access.
	Dynamic monitoring (vibration test)	Vibration tests are carried out to detect the frequencies, the modal shapes and the modal damping of the structure. These provide information on local and global behaviour of the structure.	Monitoring arch behaviour over time; Verifying theoretical models and the effectiveness of strengthening.	The system can be used for long-term monitoring; Interpretation of the results can be difficult; Only a few experience exist on masonry bridges.

Table 3: Summary review of Monitoring techniques

Chapter 3

SELECTION OF TEST TECHNIQUES

3.1 General aspects of selection

The final objective of a testing programme is to quantify the parameters that are required for the assessment procedure or to provide information for the evaluation of condition. As a large variety of methods is available the choice of the most appropriate method for a specific problem can be rather complex. Masonry arch bridges are highly variable in their geometry and construction. Different test methods will be appropriate to different structures and not all techniques will work in all situations.

Although measurements may be carried out with the help of specialists, it is the bridge engineer who is responsible for the complete assessment procedure. In each individual case therefore the assessor engineer must be able to select between the available test methods in order to build up a test programme that leads to a reliable knowledge of the condition of the bridge or the input parameters for assessment. The optimal choice is always a balance between the costs and the benefits of tests with regard to the importance and reliability of information they deliver.

The following chapters are aimed to give information for bridge assessors on the availability and reliability of the non-destructive and semi-destructive investigation and monitoring techniques for masonry arch railway bridges. Guidance on the selection between the methods for specific inspection purposes is provided and comparison of the methods in varios aspects is made.

3.2 Data required for the assessment of arches

Reliability of assessment heavily depends on the reliability of input parameters that are required by the analysis. The importance of various geometrical, mechanical and physical parameters varies with the type of structure, purpose and method of assessment.

The following list summarises parameters that are generally taken into account in the assessment of load carrying capacity or condition apparisal of masonry arch bridges. The availability and importance of these parameters are evaluated according to an average case. The evaluation aspects are considered as follows:

[A] Source and availability of information:

1: Usually available information from bridge files or can be reliably determined by visual investigation or simple in-situ measurements as part of a routine inspection.

2: Often not available information from bridge files. Visual investigation and simple in-situ measurements may provide an approximate value but accurate determination of its characteristics would require further tests (e.g. DT, SDT, NDT).

3: Often not available information from bridge files. Details are hidden therefore further tests are needed to determine its characteristics (e.g. DT, SDT, NDT).

[B] Importance of parameter in the assessment procedure:

1: Very important parameter

2: Important parameter

3: Supplementary parameter

4: Usually not important parameter

	Parameter	[A]	[B]	Additional aspects to consider
Geometry	**Arch span**	1	1	
	Arch rise	1	1	
	Arch profile	2	1	Due to long-term creep and load imposed distortions the arch profile may differ from its designed shape.
	Barrel thickness	2	1	Barrel thickness may differ from that visible at the arch side faces and vary in the span direction.
	Effective width	2	1	The effective width is influenced by longitudinal cracks in the barrel and the level of force distribution in the fill and the barrel.
	Fill depth	1	1	The depth of fill over the arch may change in time as a result of track maintenance operations.
	Skew	1	1	
	Abutment geometry	2	3	Internal parts of abutments may have lower quality masonry than that of the facing stone or brickwork.
	Pier geometry	2	2	Piers might be solid or shell constructions. Internal parts may have lower quality than that of the facing stone or brickwork.
	Depth of foundations	2	2	Depth of foundation may differ from that indicated on original drawings or bridge files.
	Presence and geometry of haunching	2	2	Usually not available information. In some cases thorough visual inspection may reveal the level of haunching from drains and water penetration marks.
	Thickness of spandrel walls	2	3	
	Presence and geometry of internal spandrels	3	1	Internal spandrels (ribs) cannot be seen from the intrados. There may be stone slabs spanning across the spandrels or, alternatively, transverse arches. Between the internal ribs there may be voids or they may have been in-filled
	Presence and geometry of other hidden features	3	2	Location and size of buried services such as ducts cannot be seen from the intrados. Notching of the barrel to fit a duct across a bridge can weaken the arch locally
	Extent and nature of any previous strengthening or repair	3	2	It can be difficult to ascertain the extent of any previous widening or strengthening. Particular problems could be: no information on the presence and thickness of saddling, no information on the level of bond between new constructions (e.g. arch widening, shotcrete lining) and the original arch.
Material properties	**Type, strength and condition of units**	2	2	Properties of units may vary widely throughout the structure influenced by workmanship or weathering effects. There may be lower quality masonry in internal parts compared to those in outer rings.
	Type, strength and condition of mortar	2	2	Properties of mortar may vary widely throughout the structure. Mortar near the surface may differ from that in internal parts due to repointing. Internal scour may erode homogeneity of mortar locally.
	Density of masonry	2	2	Density of masonry may vary throughout the structure due to variations in material or moisture content.
	Density of fill	3	2	Density of fill may vary throughout the structure due to variations in material or moisture content.
	Moisture distribution and content in masonry	3	3	Moisture content of masonry may vary throughout the structure. It effects density and mechanical properties.
	Moisture distribution and content in fill	3	3	Moisture content of fill may vary throughout the structure. It effects density and mechanical properties.
	Fill mechanical properties	3	2	Mechanical properties of fill may vary throughout the structure. There may be layers with different properties, compact and loose areas.
Defects	**Loss or displacement of units**	1	2	
	Cracks at the arch intrados	2	1	Although intrados cracks are visible, it is not always trivial to decide weather they are surface cracks or through cracks.
	Cracks at the arch extrados	3	2	Extrados cracks are invisible from intrados.
	Detachment of spandrels	2	3	
	Deformation of barrel	2	1	Deformation of barrel is usually observable but the determination of distorted profile throughout the structure may require measurements.
	Ring separation	3	2	The extent of ring separation is usually not visible.
	Flaws, cavities inside masonry and fill	3	3	Irregularities such as flaws and cavities can modify properties locally.
	Surface delamination	2	2	
	Loss of joint material	2	2	The depth and extent of mortar loss cannot always be seen by visual inspection. Mortar loss has an effect on masonry strength and on the effective thickness of arch barrel.
	Weathering of stones, bricks	2	3	
	Foundation problems	2	1	The survey of causes of settlement, movement and scour of foundations may require tests apart from visual investigation.

Table 4: Overview of parameters required for the assessment of arches

3.3 Evaluation of methods

The following table gives an overview on the level of usefulness of various testing methods for the determination of input parameters for assessment and condition apparisal of arches.

Properties	Parameters \ Test Methods	NDT				SDT						MONITORING						
		Sonic methods	Georadar	Infraded Thermography	Conductivity measurement	Coring and analysis of cores	Boroscopy	Flat-jack test	Schmidt hammer rebound test	Penetration test on mortar	Pull-out test	Hammer tapping	Accoustic Emmission	Crack moinitoring	Laser profiling	Moisture monitoring	Monitoring deformations	Dynamic test
Geometry	Arch profile														1			
	Barrel thickness	2	2		3	1	1											
	Abutment geometry	2	2		3	1	1											
	Pier geometry	2	2		3	1	1											
	Depth of foundations	2	2		3													
	Presence and geometry of haunching	3	3		3	1	1											3
	Thickness of spandrel walls	2	2		3	1	1											
	Presence and geometry of internal spandrels	2	2	3	3	3	2											3
	Presence and geometry of hidden features	2	1	3	3	3	1											
	Extent and nature previous strength. or repair	3	3	3	3	1	1											3
Material properties	Type, strength and condition of units			3		1	2	2	2		2	2				3		
	Type, strength and condition of mortar			3		2	2			2						3		
	Density of masonry	3	3		3	1	2		3									3
	Density of fill	3	3		3	1	2											3
	Moisture distribution and content in masonry		2	2	2	2	3									1		
	Moisture distribution and content in fill		2		2	2	3											
	Fill mechanical properties	3	3		3	1	2											3
Defects	Loss or displacement of units			3			3					2			1			
	Cracks at the arch intrados	2	3	2			3						3	1	3			3
	Cracks at the arch extrados	2	3				3						3					3
	Detachment of spandrels	2	3			3	2						3					3
	Deformation of barrel														1		1	
	Ring separation	3	2			3	2					3	3					3
	Flaws, cavities inside masonry and fill	2	2	3	3	3	2					3						
	Surface delamination	3	3	2		2	2		3		3	2						
	Loss of joint material	3	2	2	3	3	2			2		3			2			
	Weathering of stones, bricks			3		2	2		2		2	2						
	Foundation problems	2	2		3	3	3										2	3

1: Can provide very useful information. Measured data are mainly quantitative and reliable.

2: Can provide useful information. Measured data are mainly qualitative but generally reliable.

3: Can provide only supplementary information. Measured data are mainly qualitative with limited reliability

Left blank: Cannot provide any useful information

Table 5: Summary of available techniques with respect to the usefulness of measured data for the assessment of arches

The evaluation of the test methods in various aspects are given in *Table* 6. The evaluation marks were estimated considering an average bridge project.

	Method	Evaluation aspects					
		[A]	[B]	[C]	[D]	[E]	[F]
NDT METHOD	Sonic methods	3	3	2	2	3	3
	Georadar	3	2	2	2	2	2
	Infrared thermography	2	3	3	1	1	1
	Conductivity measurements	3	3	3	2	2	1
SDT METHODS	Coring and analysis of small diameter cores	3	1	1	3	3	3
	Boroscopy	2	1	1	2	2	2
	Flat-jack test	3	2	2	2	3	2
	Schmidt hammer rebound test	1	4	3	1	1	1
	Penetration test on mortars	1	3	3	1	1	1
	Pull-out test	2	3	3	1	1	1
MONITORING METHODS	Hammer tapping	1	3	3	1	2	1
	Accoustic emmission	3	3	2	1	2	2
	Crack monitoring	2	1	1	1	2	2
	Laser profiling	2	1	1	1	2	2
	Moisture monitoring	2	4	2	1	2	1
	Monitoring deformations and movements	3	1	1	2	2	2
	Dynamic monitoring (vibration test)	2	2	2	2	2	2

[A]: Easiness of implementation
1: easy, 2: fairly easy, 3: moderately difficult, 4: very difficult

[B]*: Importance of data provided by the measurements (in bridge assessment)
1: very important, 2: fairly important, 3: moderately important , 4: only supplemental information

[C]: Reliability (accuracy) of measured data
1: accurate, 2: moderately accurate, 3: fairly uncertain, 4: very uncertain

[D]: Disturbance to traffic during measurements or sampling
1: no disturbance, 2: low disturbance, 3: moderate disturbance, 4: high disturbance

[E]: Quickness of sampling, measurements
1: very quick, 2: moderately quick, 3: fairly slow, 4: very slow

[F]: Cost-efficiency
1: low cost, 2: medium, 3: high, 4: very high

* The following aspects were considered: importance and the availability of parameters that the test is targeted to, usefulness of information gained by the test.

Table 6: Evaluation of test methods

3.4 Recommendation for the use of test methods

The following table gives recommendation for the use of test methods according to various purposes of measurement.

Type of method	Name of method	Purpose of measurement									
		Determinatin of construction materials	Testing mechanical properties	Testing physical or chemical properties	Survey of geometry (arch shape)	Survey of hidden geometry and features	Survey of defects	Validation of models	Overall view on bridge condition	Condition monitoring	Evaluation of the effects of intervention
NDT METHODS	Sonic methods	3	3	3		2	2		2	3	2
	Georadar	3	3	2		2	2		2	3	2
	Infrared thermography	2	3	3		3	2		2	3	3
	Conductivity measurements	3	3	2		3	3		2	3	3
SDT METHODS	Coring and analysis of small diameter cores	1	1	1		2	3		3	3	1
	Boroscopy	1	3	3		1	2		3	3	1
	Flat-jack test		2					2	3	3	3
	Schmidt hammer rebound test	3	2				3		3		
	Penetration test on mortars	2	2	3			3		3	3	3
	Pull-out test	2	2	3					3		3
MONITORING METHODS	Hammer tapping	3	3	3		3	2		2	2	3
	Accoustic emmission						3	2	2	2	2
	Crack monitoring						3	3	3	2	3
	Laser profiling				1		2	3	2	2	
	Moisture monitoring		3	2		3	2		3	3	2
	Monitoring deformations and movements				3		2	2	3	2	2
	Dynamic monitoring (vibration test)						3	2	2	2	2

1: Recommended as routine application

2: Recommended as supplementary application together with other methods

3: Recommended only in special cases or experimentally

Left blank: Not recommended

Table 6: Recommendation for the application of NDT, SDT and monitoring methods for various purposes of inspection

BIBLIOGRAPHY

Binda, L., Saisi, A., Tiraboschi, C. Investigation procedures for the diagnosis of historic masonries, Construction and Building Materials, 14, 199-233, (2000).

Binda, L., Saisi, A., Tiraboschi, C. Application of sonic tests to the diagnosis of damaged and repaired structures, NDT&E International, 34., 123-138, (2001).

Brencich, A.: Guide to the high level assessment of masonry bridges, *Project Report*, UIC International Union of Railways, Paris (2008).

Harvey, W.J.: A guide to the assessment of masonry arch railway bridges, *Project Report*, UIC International Union of Railways, Paris (2008).

McCann, D.M., Forde, M.C.: Review of NDT methods in the assessment of concrete and masonry structures, *NDT&E International* 34 (2001), pp. 71–84

Orbán, Z.: RECOMMENDATIONS TO THE NON-DESTRUCTIVE TESTING OF MASONRY ARCH BRIDGES - Part 1: Case studies and reports on field tests', *Project Report*, UIC International Union of Railways, Paris (2008).

Orbán, Z.: UIC Project on Assessment, Inspection and Maintenance of Masonry Arch Railway Bridges – Keynote lecture, *ARCH 07: 7th International Conference on Arch Bridges*, Madeira, Portugal, 12-14 September 2007. pp. 3-12.

Orbán, Z. Assessment, Reliability and Maintenance of Masonry Arch Bridges in Europe, ARCH 04: 4th International Conference on Arch Bridges, eds: P. Roca, C. Molins, Barcelona, 2004, pp. 152-161, ISBN: 84-95999-63-3.

Orbán, Z (ed.). Assessment, Reliability and Maintenance of Masonry Arch Bridges. State-of-the-Art Research Report of the International Union of Railways, Paris, 2004.

Orbán, Z., Gutermann, M.: Assessment of masonry arch railway bridges using non-destructive in-situ testing methods, *Engineering Structures*, Vol 31 (2009), pp. 2287-2298.

Orban, Z.: Assessment, reliability and maintenance of masonry arch bridges - State-of-the art study, *Project Report*, UIC International Union of Railways, Paris (2003)

Orban, Z.: Testing material properties – Assessment with the help on NDT methods, *UIC Workshop on Masonry Arch Bridges*, Bristol, UK (2018).

Orban, Z.: Recommendations for determining material properties, dimensional parameters and construction details of masonry arches by non - destructive methods, *Project Report*, UIC International Union of Railways, Paris (2008).

Pattantyús-Á., M., Neducza, B., Prónay, Zs., Törös, E. Technological development of GPR measurements at Eotvos Lorand Institute of Geophysics (In Hungarian), Magyar Geofizika, 35. 1., pp. 32-41, (1999).

Prónay, Z. The applicability of the ground penetrating radar method (In Hungarian). *Technical Report (2003).*

Reynolds et. al., An Introduction to Applied and Environmental Geophysics. *Simon Fraser University, EASC 307 (2002).*

Sadri, A. Application of impact-echo technique in diagnoses and repair of stone masonry structures, NDT&E International, 36., 195-202, (2003).

Törös, E., Hermann, L., Prónay, Zs., Geotechnical Applications of Seismic Tomography, EEGS-ES presentation, Turin, (1995).

UIC Code 778-3R: Recommendation for the inspection, assessment and maintenance of masonry arch bridges. *UIC International Union of Railways*, (2011).

Ulriksen, 1982., Application of Impulse Radar to Civil Engineering. *Doctoral Thesis, Lund Universiy of Technology* (1982).

Notes of the Working-Group Meetings of the International Union of Railways project (UIC I/03/U/285: Improving Assessment, Optimisation of Maintenance and Development of Database for Masonry Arch Bridges, project manager: Z. Orban, 2003-2008)

APPENDIX 1

Advice notes for the use of specific NDT methods

APPENDIX 1: Advice notes for the use of specific NDT methods

A1.1 Ground Penetrating Radar (GPR)

General description of the method

The GPR equipment consists of a transmitting antenna, a receiving antenna, data collecting and control unit and a computer that stores the collected data. The transmitter sends series of high frequency impulses (10 MHz – 5 GHz) into the ground or other medium under investigation. The reflected signals are received and digitalised by the receiver related to time and are stored by the computer (*Fig. 1*).

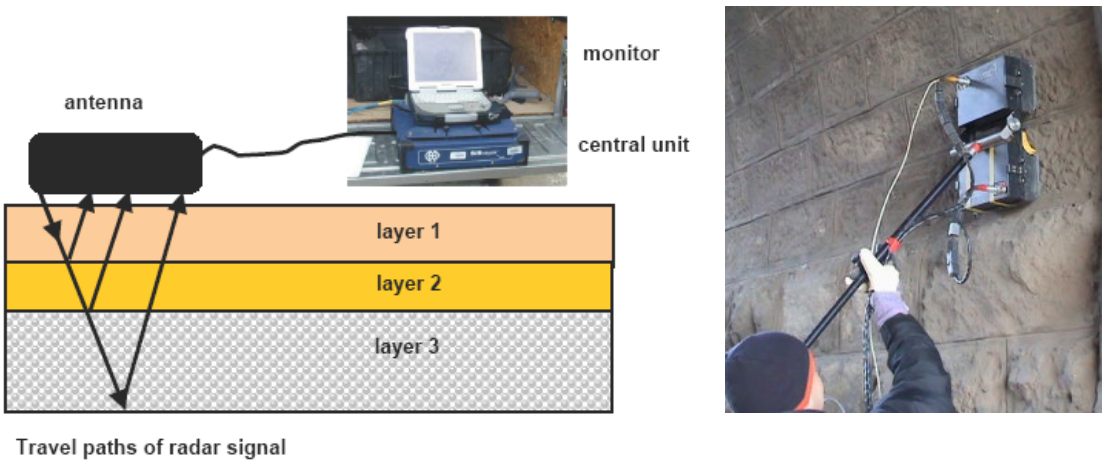

Fig.1. Principle of GPR measurements

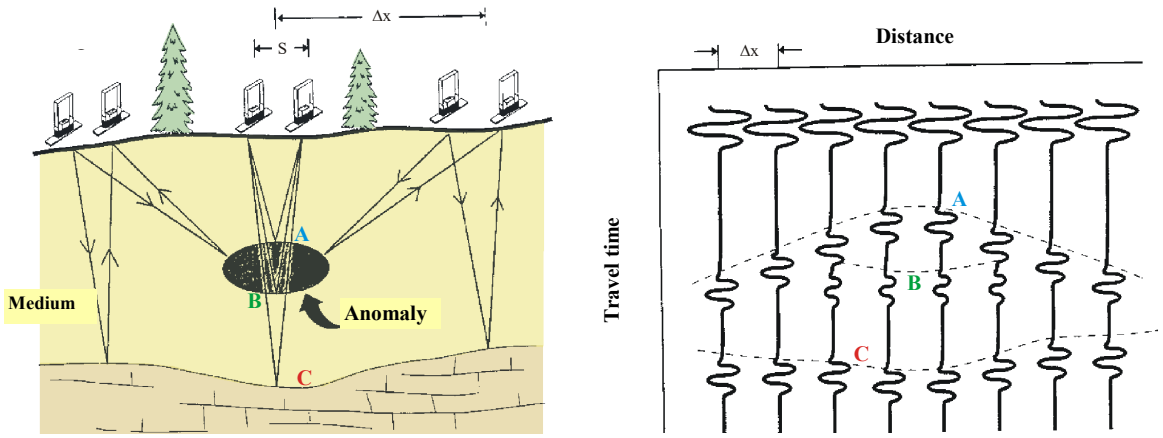

Fig. 2. A draft of GPR measurement and the related time section

The propagation of radar signals in different types of materials depends on the physical characteristics of the medium. The dielectric constant determines the speed with which the wave travels and the electrical conductivity determines the attenuation of the electromagnetic signals. If any of these two parameters changes on a boundary surface, a certain part of the

signal is reflected and the remaining part penetrates into the next layer. If the physical contrast makes it possible, one can follow the geological structures or different structural layers on "real-time" images and can recognise subsurface structures and objects (*Fig. 2*).

For the reliability of the radar equipment it is of great importance that the travel time of the signals is measured accurately. Due to the high measurement frequencies sampling rates are very high as well, 5-2000 ps (picosecond = 10^{-12} s). The travel time depends on the velocity of the waves in the medium and the depth of the layers. The waves travel from the transmitter to the reflection point and back to the receiver, therefore a two-way time is registered. The propagation speed of the waves can be determined, or estimated in the different layers. This way timescales can be converted into depths.

In the course of the measurements the frequency of the transmitted signal can be adjusted by the antennas. Better resolution can be obtained by using higher frequencies but at the same time the detectable depths will be reduced. The main characteristics of the investigated area, the penetration depth and the resolution are determined by the frequency, the band-width and the characteristics of the material.

The measurement produces systems of digital time series which can be further analysed. The objective of the analysis is the improvement of the signal-to-noise ratio where noise means any data that is not reflected from the investigated object.

The measurements carried out by GPR are usually constant-offset (the distance between the transmitter and the receiver) surface reflection measurements, therefore unless stated otherwise it should be understood that this configuration is used.

Advantages of the method:
- high resolution,
- effective field work.

Disadvantages of the method:
- sensitive to external factors (e.g. electric cables),
- small degree of penetration in unfavourable geological environment (e.g. clay surface),
- measured data can not easily be evaluated by non-experts.

The physical basis of the method

In the case of finite conductivity Maxwell's equations for the electric component in one dimension in the frequency range is the following (Reynolds, 2002):

$$\frac{\partial \underline{E}}{\partial x^2} = i\omega\mu\sigma\underline{E} - \omega^2\mu\varepsilon\underline{E}$$

This is a wave equation where $\underline{E}\ (x,t)$ is the vector of the electric field, ε is the dielectric constant σ is conductivity, μ is magnetic permeability and ω is circular frequency.
A similar equation can be applied to the magnetic component.

Based on the equation one can draw the following consequences:

- At low frequencies ω^2 value is low compared to ω, the wave characteristic can be neglected.
- At high frequencies ω^2 value is high compared to ω, the first term can be neglected.
- In case of high conductivity the significance of the first term increases.

The frequencies used by the GPR system are on the verge of two different ways of propagation, therefore one should calculate using both of them depending on the medium. The equation determines both the velocity of the wave in a given medium and the value of attenuation:

$$V_m = \frac{c}{\left\{\frac{\varepsilon_r \mu_r}{2}\left[\left(1+P^2\right)^{1/2}+1\right]\right\}^{1/2}} \qquad \alpha = \omega\left\{\left(\frac{\mu\varepsilon}{2}\right)\left[\left(1+P^2\right)^{1/2}-1\right]\right\}^{1/2}$$

Where c is the velocity of light in vacuum, p is the loss factor, the r index relates to the relative value. In a non-magnetic medium with low loss value, the formula of velocity becomes simpler:

$$V_m = \frac{c}{\sqrt{\varepsilon_r}} = \frac{0.3}{\sqrt{\varepsilon_r}} \qquad \text{[m/ns]}$$

The reflection coefficient of the radar wave i.e. how much of the incoming energy is reflected from the surface, is given by the following formula:

$$R = \frac{V_2 - V_1}{V_2 + V_1} = \frac{\sqrt{\varepsilon_1} - \sqrt{\varepsilon_2}}{\sqrt{\varepsilon_1} + \sqrt{\varepsilon_2}}$$

where the index relates to the number of the layer.

In loose sediment or other porous material the amount of water is of great importance. On the one hand it is the water that influences conductivity (electrolytic conductivity, polarisation) and at the same time attenuation, on the other hand it has a significant effect on the velocity of the electromagnetic waves due to the fact that its dielectric constant is bigger than that of the matrix of the rock or masonry material by a magnitude order.

Length of the impulse (ns)	**Centre-frequency (MHz)**	**Average penetration (m)**	**Resolution (m)**
0.5	2000	< 0.25	0.025
1.0	1000	< 0.5	0.05
2.0	500	< 1.0	0.1
4.0	250	< 2.0	0.2
8.0	125	< 4.0	0.4
16.0	63	< 8.0	0.8
32.0	31	< 16.0	1.6

Table 1: Expected penetration depending on resolution and frequency

Based on the data of the "European GPR Association (EGPRA)" *Table 1* represents the penetration depth and resolution that is expectable at the frequencies normally used in the course of GPR system surveys. These are average values, depending on the local circumstances the values may deviate from those shown in the table to a great extent.

Methodology

Data acquisition

Data are usually collected along a series of vertical and horizontal profiles spaced at 0.5m – 1m centres over the investigated surface. It is recommended to use and electronic distance measuring wheel for controlling the scan rate of the system.

Data acquisition, is only the first step in a radar survey. It is followed by data processing and interpretation, during which the information contained within radar data is extracted and converted into a format meaningful to the bridge engineer. The availability of information obtained by other methods such as cores or sonic methods is always useful and often necessary to produce reliable and accurate results.

Data processing

On return from site the data are downloaded from the central unit to a PC. Data processing is usually made by using an appropriate software.

Typical steps of data processing are:
- Declipping
- Start-time correction
- Dynamic correction
- Noise removal

Representation of data

Data may be analysed as a one-dimensional ‘wiggle’ trace or scan, generated at each pulse of the transmitting antenna. More practical is the recording of multiple wiggle traces as the antenna is moved along a line, thus generating a two-dimensional view of the cross section as shown in *Fig. 3*. The vertical axis on a recorded image is the time axis. It denotes the time required by the signal to travel first to the reflector and then back to the antenna again. It is therefore referred to as two-way-travel time. In order to obtain depths, the signal velocities in the different materials under investigation have to be known (e.g. by a comparison of the radar data and core information).

Different antenna types emitting and recording different ranges of frequencies are available. Using high frequency antennae results in high-resolution data, but reduces the depth of penetration. Low-frequency antennae provide greater depth of penetration at the expense of lower resolution. Most GPR manufacturers offer antennae with centre frequencies ranging from approximately 50 MHz to approximately 1.5 GHz. For masonry bridge inspections, typically antennae with centre frequencies between 225 MHz – 1,5 GHz can be used.

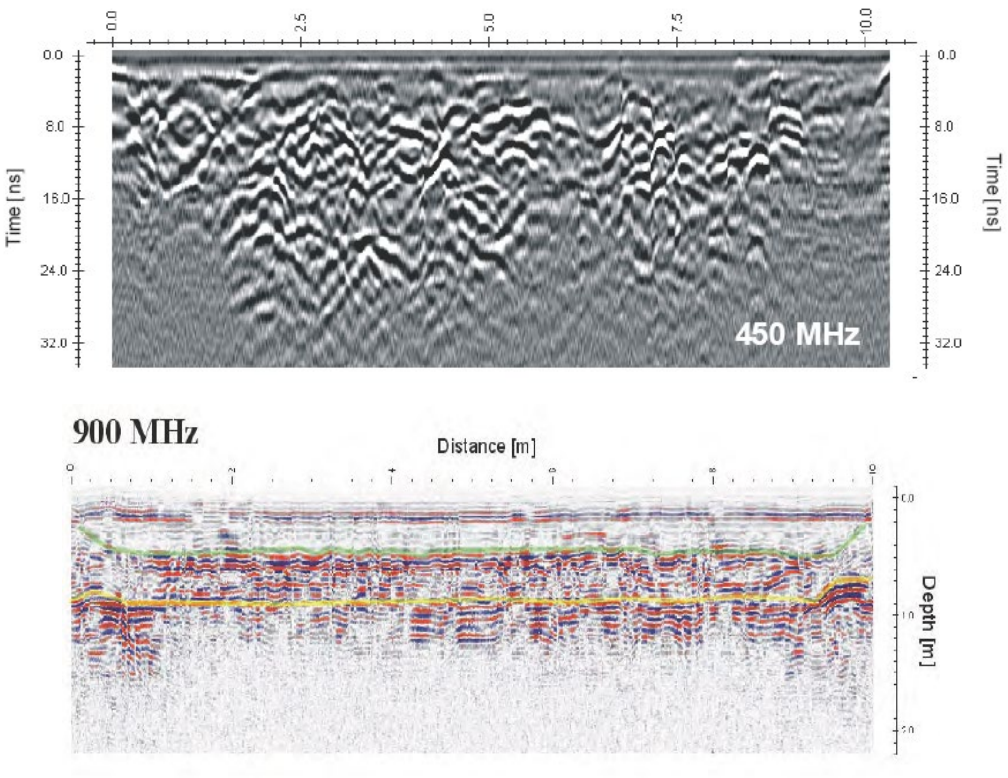

Fig. 3: Typical representation of radar measurements

The relation between resolution and frequency are shown by a practical example in *Fig. 4*.

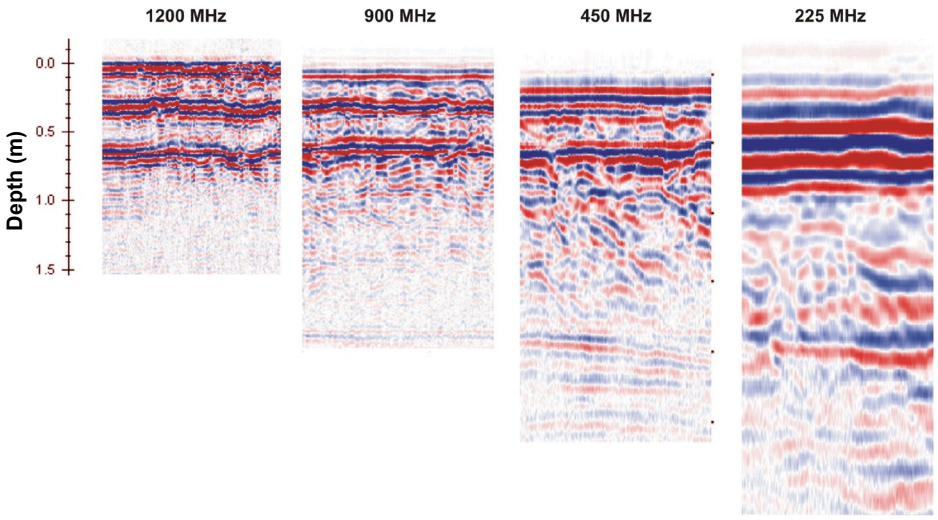

Fig. 4: Measurements at the same location using different frequency antennas

Three-dimensional images can be produced by recording a series of adjacent two-dimensional traces. They are often referred to as 'anomaly maps'. *Fig. 5.* shows anomaly maps of an arch barrel represented in flat sheets. Higher amplitudes (seen in reddish colours on the map) refer to cavity or other highly reflecting material, e.g. larger blocks of stone while lower amplitudes (in bluish colour) generally refer to an increase in moisture level or material with smaller compactness (e.g. fill material).

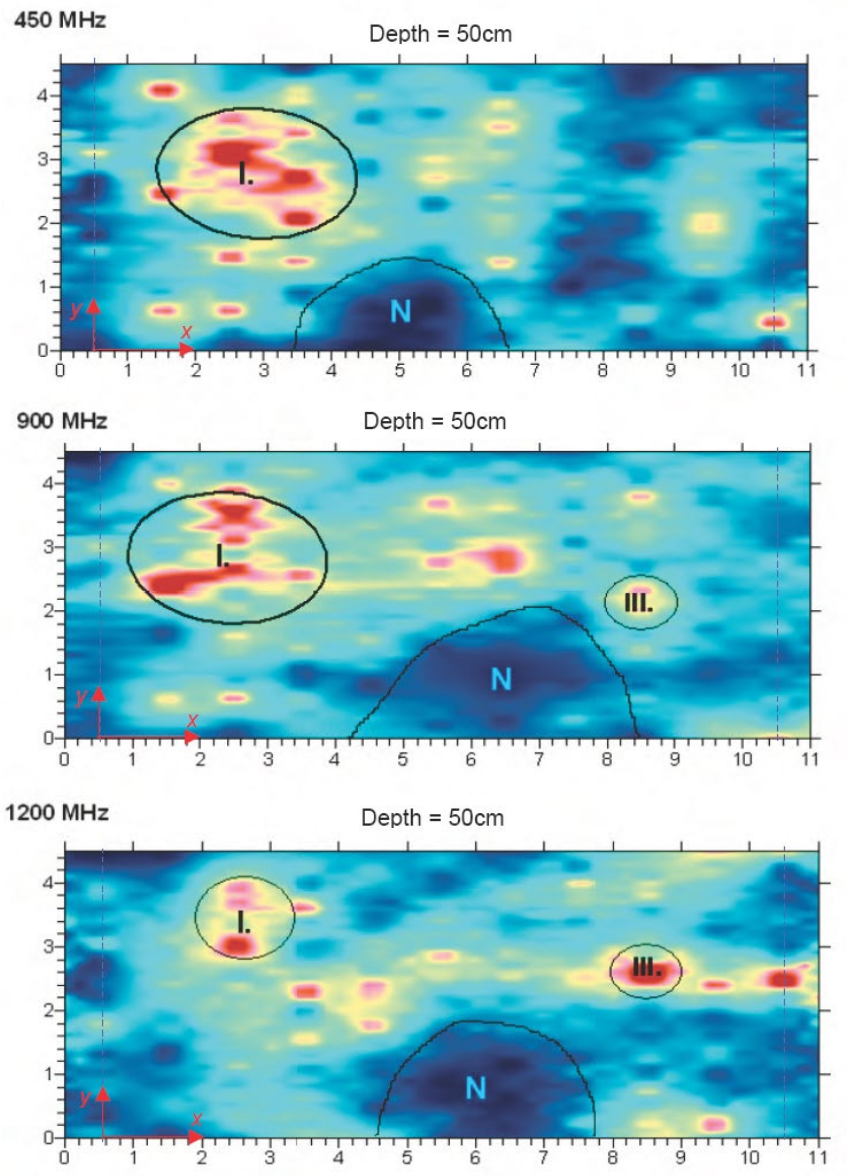

Fig. 5: Anomaly map of an arch barrel taken with various frequency antennas represented on flat sheet (horizontal: longitudinal profiles, vertical: transversal profiles)

Though requiring considerable time to record data as well as extensive computational effort, three dimensional representations are the most meaningful way of representing data of radar measurements.

Accuracy of measurements

The measurement of thickness or depth relies on multiplying the measured two-way travel time by the velocity of the radio signals passing through the materials under investigation.

According to comparisons with boroscopy survey and core data analysis the system is likely to be capable to determine structural thickness with an accuracy of 5-15%. This accuracy is very much dependent upon the type of material, the moisture content and its anomalies and the frequency of antennae used.

Other considerations

Care must be taken when interpreting radar traces, owing to the many reflective interfaces present in masonry construction. Mortar and grout interfaces, as well as geometric interfaces, will refract microwave energy, having a tendency to mask energy reflected from targets of interest. The multiple echoes and localized reflections resulting from this effect can be only partially overcome by data processing.

A1.2 Infrared thermography

General description of the method

Infrared thermography is a remote temperature mapping system which may be successfully used in the inspection of masonry bridges. Infrared thermography is a technique for converting a thermal radiation pattern, which is invisible to the human eye, into a visual image. To achieve this, an infrared camera is used to measure and image the emitted infrared radiation from an object (*Fig. 1*). An infrared camera is a non-contact device that detects infrared energy (heat) and converts it into an electronic signal, which is then processed to produce a thermal image on a video monitor and perform temperature calculations. Heat sensed by an infrared camera can be very precisely quantified, or measured, allowing the inspector to monitor thermal performance.

There are two systems of cameras are used. While short wavelength systems are more effective to test objects where high temperature differences are present long wavelength cameras are able to detect small temperature differences. As the temperature variations of bridges in the field are relatively low a long wavelength camera is required for most surveys on bridges.

Fig. 1. Instrumentation of infrared thermography. FLIR system (left), AGEMA system (right)

The physical basis of the method

Thermal, or infrared energy, is light that is not visible because its wavelength is too long to be detected by the human eye; it's the part of the electromagnetic spectrum that we perceive as heat (*Fig. 2*). Unlike visible light, in the infrared world, everything with a temperature above absolute zero emits heat. Even very cold objects emit infrared. The higher the object's temperature, the greater the IR radiation emitted.

Objects emit energy proportional to their surface temperatures. However, the energy actually detected (by the infrared detector) depends on the emissivity of the surface under measurement and on the environment. In fact, a fraction may be either absorbed by the medium between the object and the camera, either added as reflected by the surface from the surroundings. To take into account these factors, calibration of the system by simulating real operating conditions has to be performed.

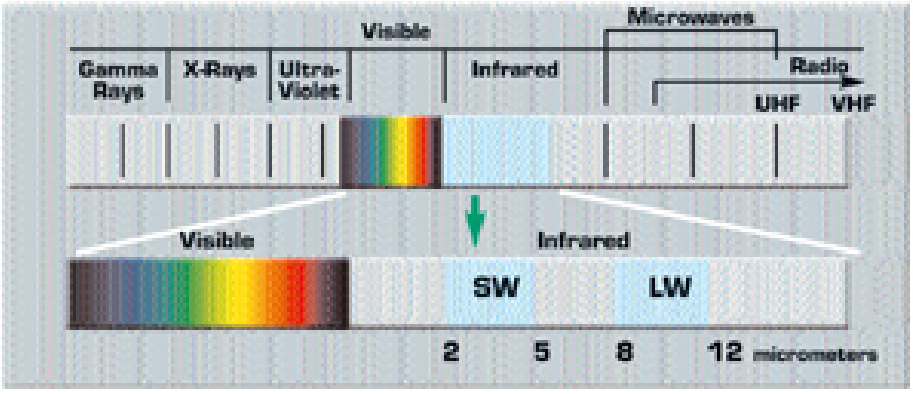

Fig. 2. The electromagnetic spectrum (by www.flir.com)

Different materials have different surface temperatures, since they have different emissivity values. *Table 1*, shows the different emissivity values for some materials that may be found in masonry arch bridges.

Material	**Temperature (ºC)**	**Wavelength (□m)**	**Emissivity value**
Cement	20	8-14	0,54
Concrete	20	8-14	0,92
Plaster	17	2-5	0,87
Sand	20	2-14	0,90
Limestone	36	5	0,96
Sandstone	36	5	0,67
Granite	21	5	0,45
Brick (red)	20	2-14	0,90
Brick (yellow)	20	2-5,6	0,72
Lime mortar	38	5	0,92

Table 1: Emissivity values for masonry components

Methodology

Infrared scans may be conducted by either an active or passive approach. Active thermography relies on homogeneous forced heating of the surface using an external heat source such as sunlight or other heat radiators. Imaging during heating or cooling (after removal of the heat source) provides information on near-surface anomalies. Passive investigations are more useful for locating defects deeper within the masonry.

Interpretation of infrared images relies on interpretation by the inspector to determine the meaning of temperature anomalies. Operator experience is essential as well as an understanding of the physics behind heat transfer processes and the performance of masonry wall assemblies. Under different heating and cooling conditions, for example, sections containing internal voids or delamination may show as either warmer or cooler regions. Temperature variations may also arise due to differences in material moisture content, surface texture, the temperature of the surrounding materials, the atmospheric temperature, the ambient temperature, the weather, the stress-induced temperature change and absorption of infrared radiation. Consideration needs to be given to the fact that outdoors many factors alter the surface temperature of the object under investigation. The weather can have a major effect

as sunlight may increase the temperature, wind may decrease the temperature of an object. Rain, which will lower the temperature of an object through both conductivity and evaporation, will also cause a change to the emissivity. However, any factor which highlights changes in temperature actually helps identify anomalies and features.

The most common representation of the radiated heat is a thermal image where different colours represent different radiated temperatures (see examples on *Fig. 3*). Besides the 2D thermal image temperature distribution can be displayed along horizontal or vertical segments (*Fig. 4*) or on 3D image (*Fig 5*). A difference in the temperature or radiated heat may be due to a number of different factors e.g. delamination, build up of water behind the surface, voids or cracks.

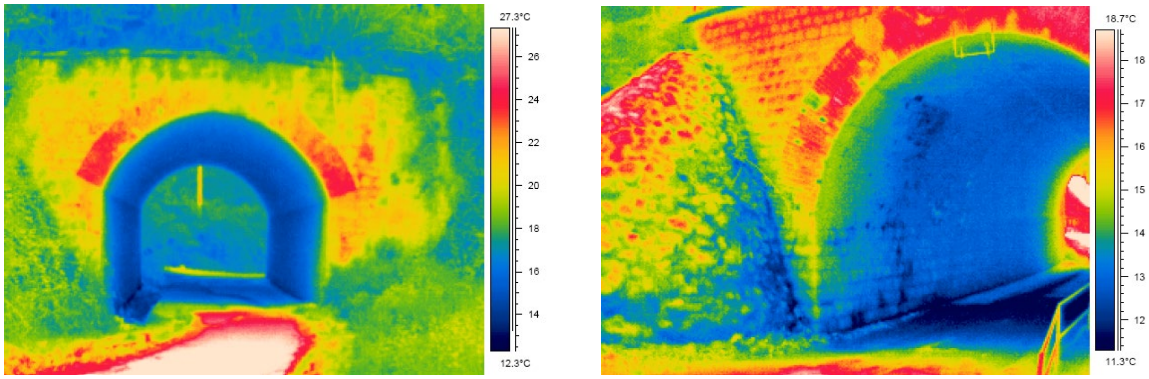

Fig. 3. Typical thermal images of masonry arch bridges. Different construction materials, patch repairs, wet areas and vegetation are clearly visible.

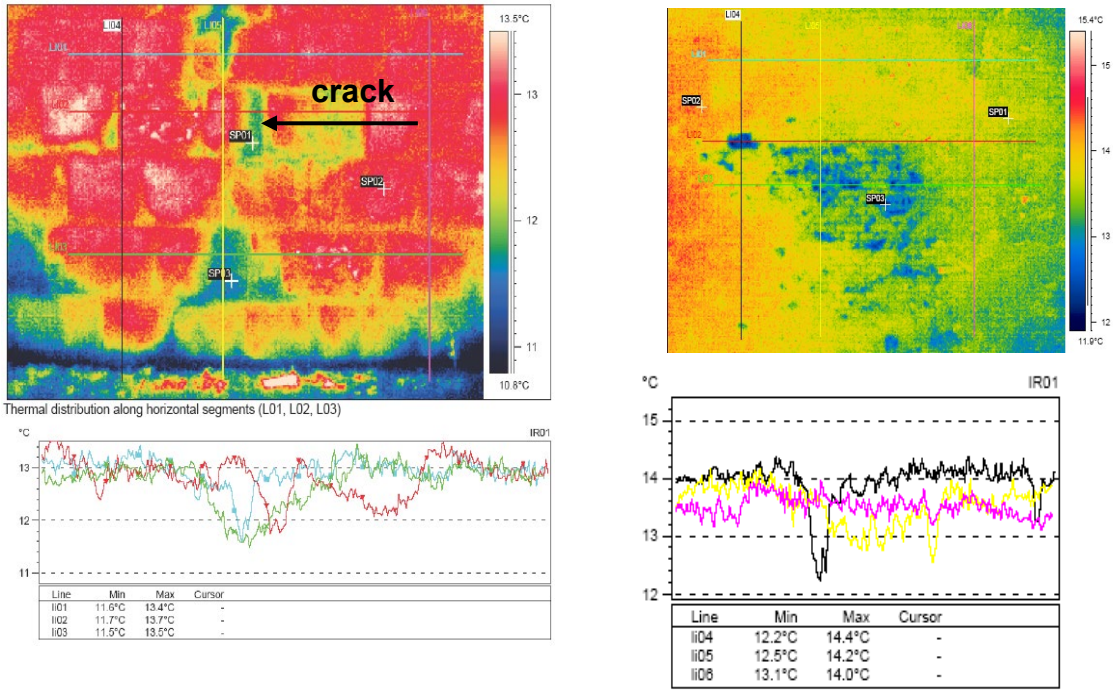

Fig. 4. Wet areas are visible on thermal images. Temperature intensity charts are represented along horizontal segments.

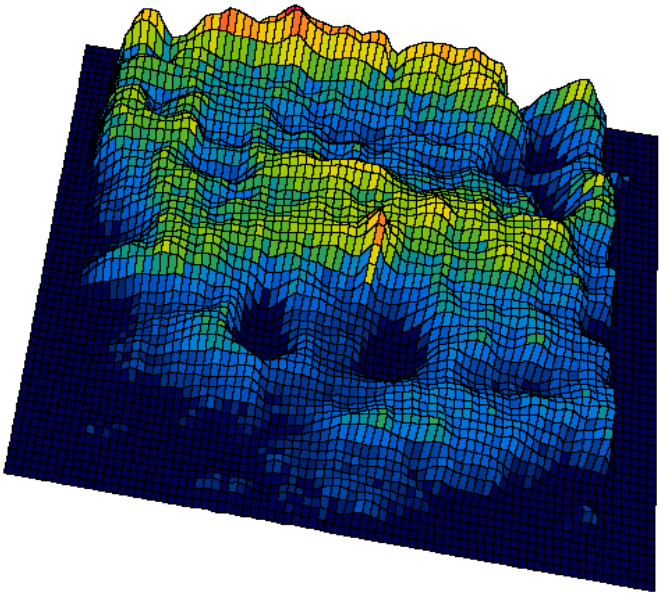

Fig. 5. 3D representation of thermal distribution on masonry surface. Low temperature refer to presence of wettness on the surface

Efficiency of the method

Infrared thermography has proven an effective tool in the determination of surface temperature anomalies of masonry bridges and indirectly provides qualitative information on surface conditions and near surface defects.

- Infrared thermography is able to identify some of the characteristics of masonry structures and to differentiate between construction materials such as various type of stones, bricks and mortars. Locations of patch repairs where materials different from the existing ones were used can also be recognised.

- Anomalies can be recognised such as wet regions, cracks, weathered stones or bricks and remarkable mortar loss in the joints. In may cases these anomalies, referring to damages, are not perceivable by the human eye from the same distance as the measurement is made with the infrared camera.

- Areas were also clearly detected, where undesirable plants and roots were incorporated into the structure, which later on could cause damages due to frost or expansion.

- On the other hand interpretation of the temperature variations on the images is sometimes difficult due to the boundary effects caused by direct solar radiation or air motion.

- It is also recommended that the method is not used by itself but together with other inspection methods that help interpreting the results and calibrating the measurements.

A1.3 Boroscopy

Boreholes are drilled in representative parts of the structure. Coring can be done with a rottary driller using a diamond cutting edge. A small camera is inserted into the borehole allowing a detailed study of its surface. The results of this study can be recorded for further analysis. Typical boroscopy images of brickwork masonry structures are demonstrated on the following photo series.

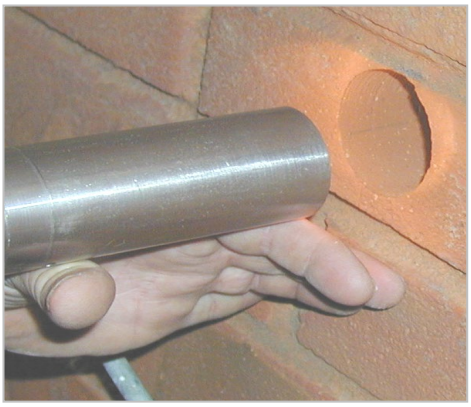

Boroscopy mesurement on masonry structures

Masonry without defects
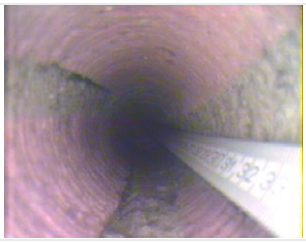 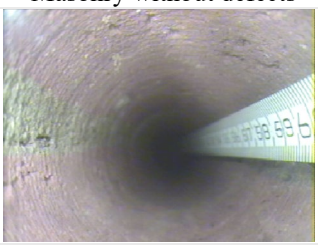 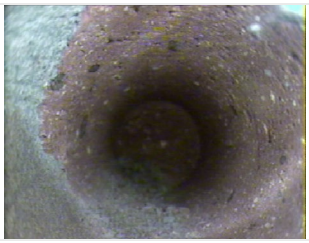
Detection of voids and cracks
  
Survey of backfill conditions
  
Control of injection
 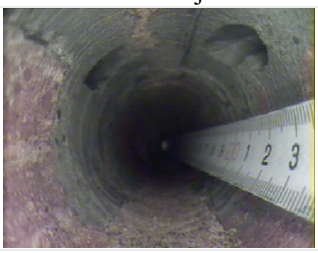 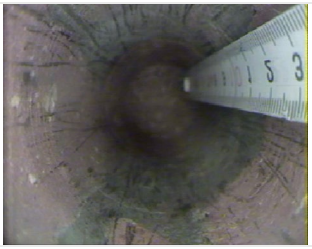

APPENDIX 2

Case Studies

Case Study 1

Radar investigation of brick masonry specimen walls

1. Introduction

Experimental Ground Penetrating Radar survey have been performed on 1.35 m x 1.35 m masonry wall specimens made from used bricks having dimensions of 29 cm x 14 cm x 7 cm. The objective of the test was to help calibration of this non-destructive technique for the investigation of brickwork railway constructions such as bridges, tunnels, culverts and abutments. The purpose of the measurements was to investigate how detectable artificially created defects and damage were in a brick settings and to create a measurement method that can be used in optimal and real circumstances based on the results and experience gained.

2. Survey equipment

In the course of the measurements two types of radar devices and four types of antennas were used. The main parameters of the radar equipment are shown in *Table 1*:

Manufacturer	**GSSI**	**Sensors & Software**
Country	USA	Canada
Equipment	SIR-20	PulseEkko 1000
Minimum sample time (ps)	5	20
Max. scan rate (channel/s)	800	100
Number of channels	2	1

Table 1: Parameters of the radar equipment

The parameters of the antennas are shown in *Table 2*:

Manufacturer	**GSSI**		**Sensors & Software**	
Type	5100	3101D	900	1200
Frequency	900 MHz	1.5 GHz	900 MHz	1.2 GHz

Table 2: Characteristics of antennas

In the second round of the measurements only GSSI radar system and antennas were used due to its higher measurement speed (*Photos 1-3*).

Photo 1. The central unit of GSSI radar system

Photo 2. The GSSI 1.5 GHz antenna

Photo 3. The GSSI 900 MHz antenna

3. Description of the measurements

The measurements were carried out using two different types of GPR equipment and four types of antennas. In the course of the first experiment we defined the equipment to be used and tested the different survey parameters. Next, we applied the optimal parameters and scan density and direction that had been defined in the course of the first survey.

After finishing the survey of the walls in their initial configuration various modifications were made in their internal structure or physical condition. In some cases the gaps of the walls were filled in with gravel or sand. In other cases two walls were pulled together and the gap between the walls was filled with brick fragments, gravel and sand. After these modifications the measurements were repeated. In several cases the measurements were carried out after wetting the parts filled up with various amounts of water.

To make sure that the radar can "see through" the wall a steel plate we put on the opposite side of the wall. Metal entirely reflects radar waves, therefore the steel plate has to show a strong reflection compared to the original recordings. If this signal is present in the recorded section, the penetration of the radar wave is enough for the survey, if not, a lower frequency has to be chosen.

Table 3 summarises the parameters of the measurements:

Number	Wall	Equipment	Antenna ferquency (MHz)	System	Density	Direction	Remark
1.	F1	GSSI	1500	mesh	10 cm	horizontal	
2.	F1	GSSI	1500	mesh	10 cm	vertical	
3.	F2	GSSI	1500	mesh	10 cm	horizontal	
4.	F2	GSSI	1500	mesh	10 cm	vertical	
5.	F3	GSSI	1500	mesh	10 cm	horizontal	
6.	F3	GSSI	1500	mesh	10 cm	vertical	
7.	F4	GSSI	1500	mesh	10 cm	horizontal	
8.	F4	GSSI	1500	mesh	10 cm	vertical	
9.	F4	GSSI	1500	segment	10 cm	horizontal and vertical	steel plate
10.	F3	GSSI	1500	segment	10 cm	horizontal and vertical	steel plate
11.	F2	GSSI	1500	segment	10 cm	horizontal and vertical	steel plate
12.	F1	GSSI	1500	segment	10 cm	horizontal and vertical	steel plate
13.	F2	GSSI	900	segment	10 cm	horizontal and vertical	steel plate
14.	F1	GSSI	1500	segment		horizontal and vertical	denser measurement
15.	F1	GSSI	1500	segment		vertical	dry
16.	F1	GSSI	1500	segment		vertical	wetted (5 l water)
17.	F1	GSSI	1500	segment		vertical	wetted (10 l water)
18.	F1	GSSI	1500	segment		vertical	5 min after wetting
19.	F1	GSSI	1500	segment		vertical	10 min after wetting
20.	F1	GSSI	1500	segment		vertical	15 min after wetting

Number	Wall	Equipment	Antenna ferquency (MHz)	System	Density	Direction	Remark
21.	F3	GSSI	1500	segment		vertical	dry
22.	F3	GSSI	1500	segment		vertical	water stored in plastic bag
23.	F3	GSSI	1500	segment		vertical	wetted (5 l water)
24.	F3	GSSI	1500	segment		vertical	wetted (10 l water)
25.	F3	GSSI	1500	segment		vertical	wetted (20 l water)
26.	F3	GSSI	1500	segment		horizontal	same as 25.
27.	F2	S&S	900	mesh	20 cm	horizontal	
28.	F2	S&S	900	mesh	20 cm	vertical	
29.	F2	S&S	1200	mesh	20 cm	horizontal	
30.	F2	S&S	1200	mesh	20 cm	vertical	
31.	F1	GSSI	1500	mesh	5 cm	vertical	
32.	F3	GSSI	1500	mesh	5 cm	vertical	
33.	F1	GSSI	1500	mesh	5 cm	vertical	dry sand in the gap
34.	F4	GSSI	1500	cross		vertical	brick fragments in hollow
35.	F2	GSSI	1500	mesh	5 cm	vertical	gap between the two wall parts
36.	F4	GSSI	1500	mesh	5 cm	vertical	gravel in hollow
37.	F1	GSSI	1500	mesh	5 cm	vertical	sand + water
38.	F2	GSSI	1500	mesh	5 cm	vertical	gravel in hollow
39.	F4	GSSI	1500	cross	5 cm	vertical	wet gravel
40.	F2	GSSI	1500	mesh	5 cm	vertical	wet gravel
41.	F1&3	GSSI	900	mesh	10 cm	vertical	dry
42.	F1&3	GSSI	900	mesh	10 cm	vertical	wetted (5 l water)

Number	Wall	Equipment	Antenna ferquency (MHz)	System	Density	Direction	Remark
43.	F1&3	GSSI	900	mesh	10 cm	vertical	wetted (10 l water)
44.	F1&3	GSSI	900	mesh	10 cm	vertical	wetted (20 l water)
45.	F1	GSSI	1500	mesh	5 cm	vertical	after injection, denser sampling along lines
46.	F4	GSSI	1500	mesh	5 cm	vertical	denser sampling along lines
47.	F2	GSSI	1500	mesh	5 cm	vertical	denser sampling along lines
48.	F1	GSSI	900	mesh	10 cm	vertical	denser sampling along lines
49.	F4	GSSI	900	mesh	10 cm	vertical	denser sampling along lines
50.	F2	GSSI	900	mesh	10 cm	vertical	denser sampling along lines

Table 3. Parameters of the measurements

4. Results

4.1 Comparison of the two radar systems

In order to compare the two radar systems measurements were made using two radars and four antennas along the same path. The two figures below show some characteristic record sections made by using Sensors & Software (S & S) PulseEkko 1000 radar device with 900 and 1200 MHz antennas, and then using the two GSSI antennas. As an example, in *Figure 1*, the bottom to top direction recorded sections are shown measured on the wall marked F2 with thickness of 3 brick widths. The left and right hand side radargrams show the boundary between the lower and upper parts of the wall. The lower half of the wall is a solid masonry with complete fill of the joints while the middle layer of the upper part consists brick fragments without filling the joints (see description of the wall in *4.3.2*). The difference is shown by a distinct change in the characteristics due to the fact that the reflection is stronger from the brick-air boundary surface than from the brick-mortar boundary. The 2nd cavity in the brick wall can be identified in the middle radargram of *Figure 1* in the lower part of the wall. This artificial cavity is half a brick long, 1 brick high and 1 brick wide (see *Figure 11* and *Photo 5*). The time axis (in ns) is on the vertical while the distance (in metres) are on the horizontal axis of the radargrams.

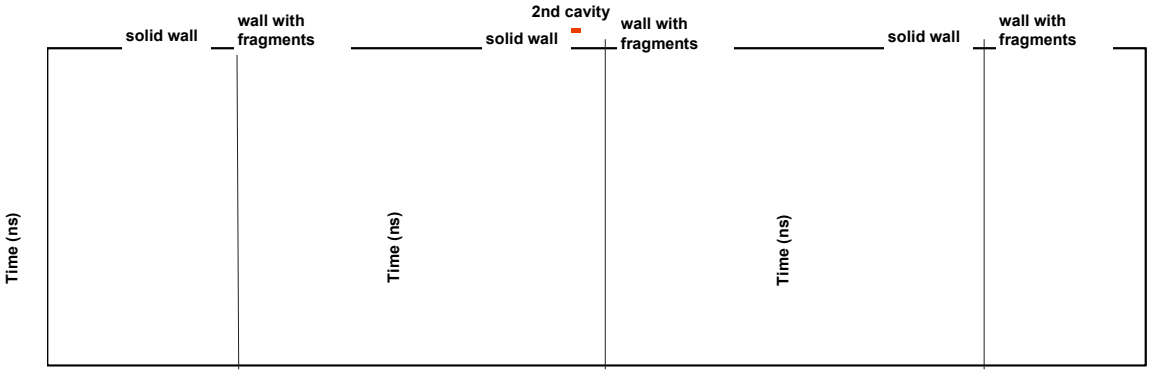

Figure 1. Radargrams of wall F2 recorded with 900 MHz-es antenna (S & S)

In *Figure 2* those sections are shown that were recorded from the same place by a 1.2 GHz antenna.

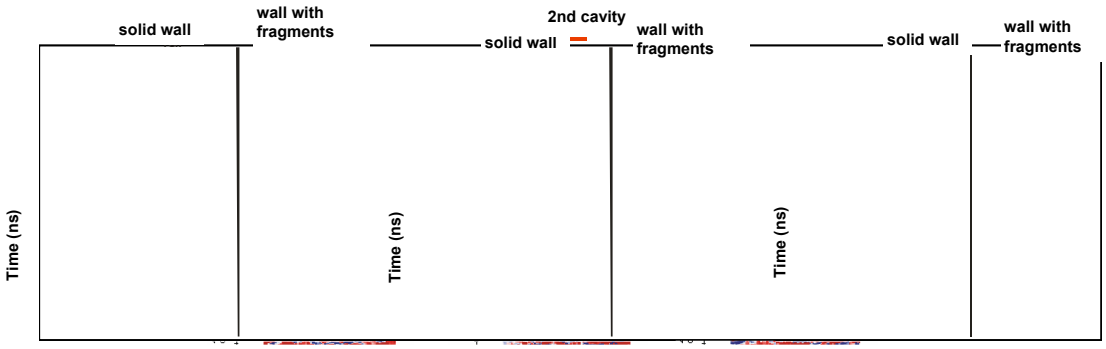

Figure 2. Radargrams of wall F2 recorded with 1200 MHz-es antenna (S & S)

In *Figure 3* the same sections are shown measured by a GSSI device and 900 MHz antenna.

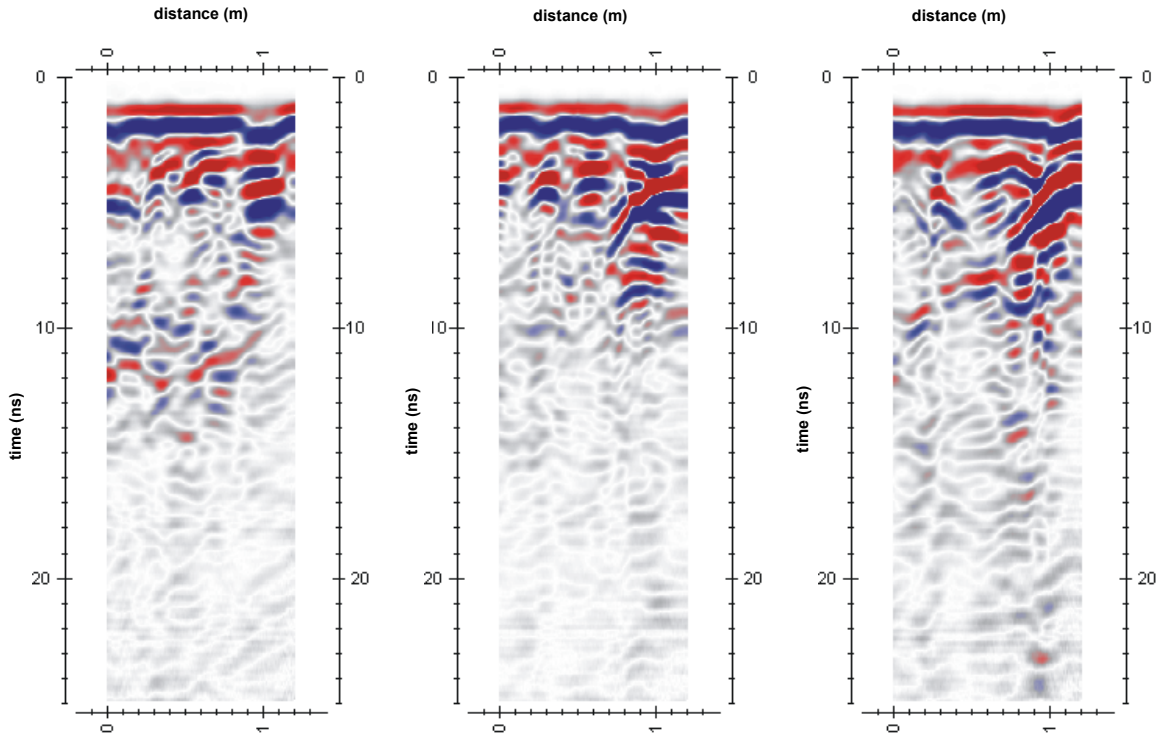

Figure 3. Radargrams of wall F2 recorded with 900 MHz-es antenna (GSSI)

In *Figure 4* the sections were recorded on the same path by a 1.5 GHz antenna.

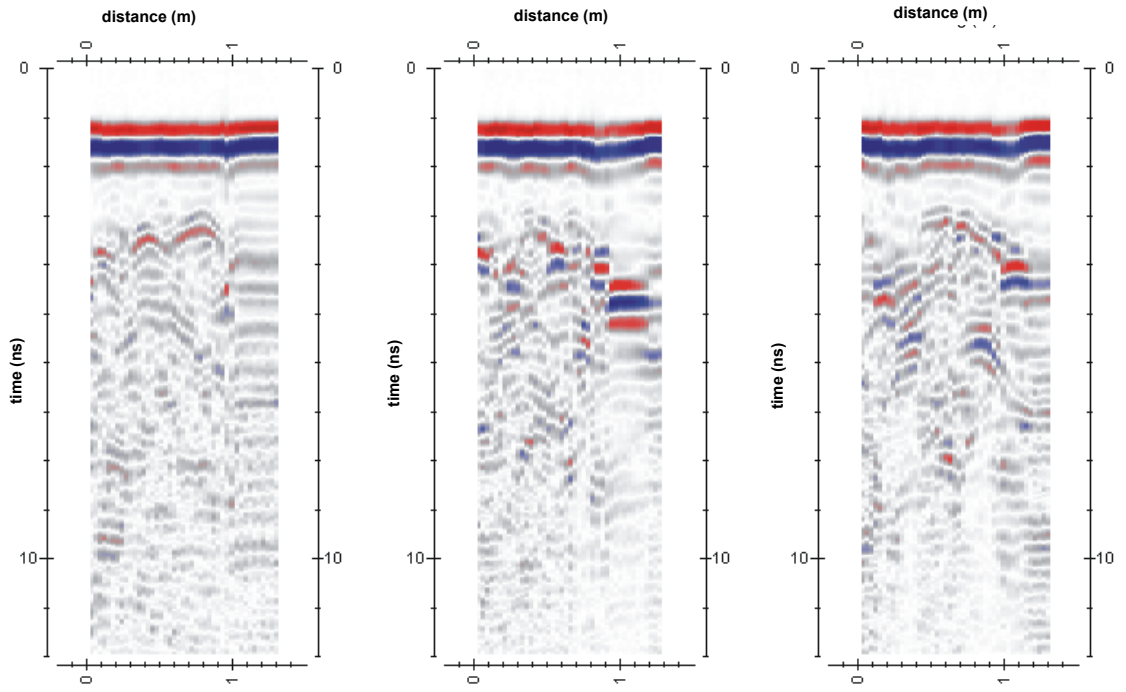

Figure 4. Radargrams of wall F2 recorded with 1200 MHz-es antennae (GSSI)

The starting point (0 m) of the sections are not exactly the same in the case of the different antennas due to the fact that the actual measurements started at different points on the bottom of the wall because the physical sizes of the antennas were different.

Comparing the recorded sections we have come to the conclusion that it is advisable to use the GSSI 1.5 GHz antenna where its penetration ability is sufficient for the given task. For deeper investigations the optimal antenna is the GSSI 900 MHz antenna. In both cases it can be stated that there was no significant difference regarding the quality of the measurements carried out by different types of radar, but since the GSSI radar works with bigger scan rates this equipment was used in further experiments.

4.2 Penetration depth

The first question that comes up with any radar investigations is how deep can the radar "see"? This question cannot really be answered looking at the measurements recorded on the test walls. In these cases the signal got reflected from the front and rear sides, from the air-brick boundary surface, it bounced there and back between the two which resulted in incoming signals over time in accordance with the thickness of the wall.

To answer this question initial measurements were made on each wall and then the measurement were repeated along the same paths putting a steel plate on the back side of the wall thus changing the characteristics of the reflecting surface. If the changes could be seen on the sections it could be stated that the radar was able to survey the area equivalent to the thickness of the wall with the antenna being tested.

The procedure is shown in *Figure 5* when the third (F3), one-brick-thick wall was tested. The effects of the steel plate can be clearly seen in the section.

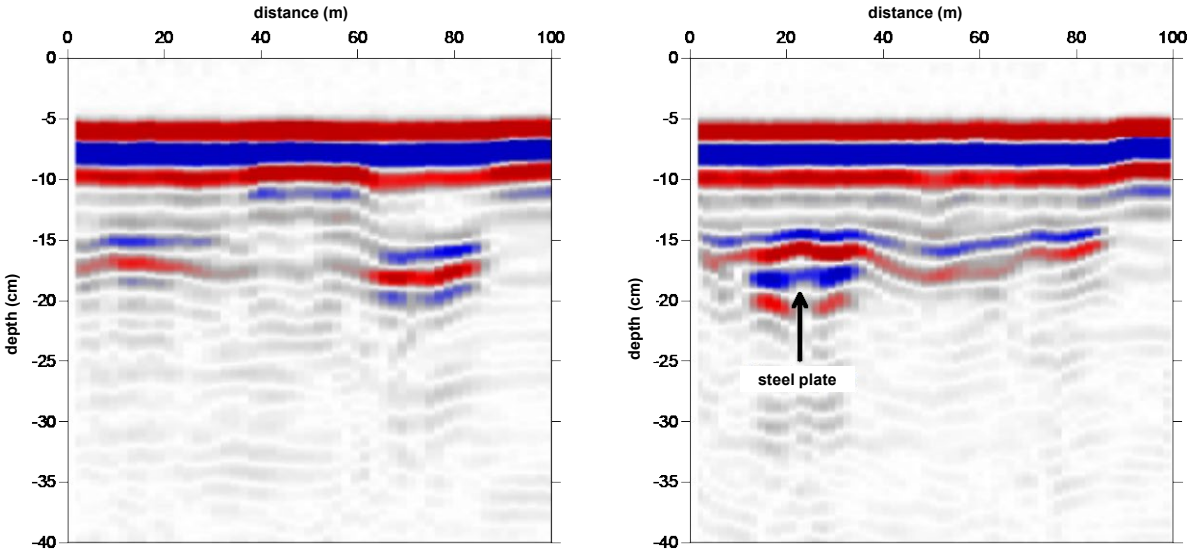

Figure 5. Effect of steel plate on the radargrams (reflections from the rear side)

4.3 Investigation of artificial anomalies

The term: artificial anomaly relates to brick defects, air cavities between courses and differences in construction configuration. Non-deliberate inhomogeneities, such as natural anomalies will be dealt with in a latter chapter.

The presented sections were recorded by using a 1.5 GHz antenna that provides better resolution. Although the measurements were made along vertical lines, for the sake of comparison horizontal measurements were also made on some of the walls. In the sections recorded horizontally, the difference caused by whether the line was running on bricks or wall joints was significant, so it was decided to use the vertical measurements.

The radar measures travel times, therefore the depths indicated in the sections are only approximate values, that was calculated with an average speed of 0.1 m/ns, a value taken from the literature. The actual velocity may change inside the test walls depending on the moisture content and to what extent the joints are filled with binding material.

In the drafts next to the recorded radargrams, the direction and the place of the section being recorded is marked by red arrows. The location of the anomalies in the test wall is also indicated with their related serial numbers.

In the figure height means the height measured from the bottom of the wall, while depth means the distance between the surface of the wall and the anomaly.

4.3.1 Investigation of the 1st test wall (F1)

The wall consists two individual brickwork courses. At the bottom half of the wall the gap between the two brick courses is well filled with mortar while at the upper part there is no filling, the air gap is 1.5 cm wide. The artificial anomalies formed during construction are shown on *Figure 6* and *Photo 4*.

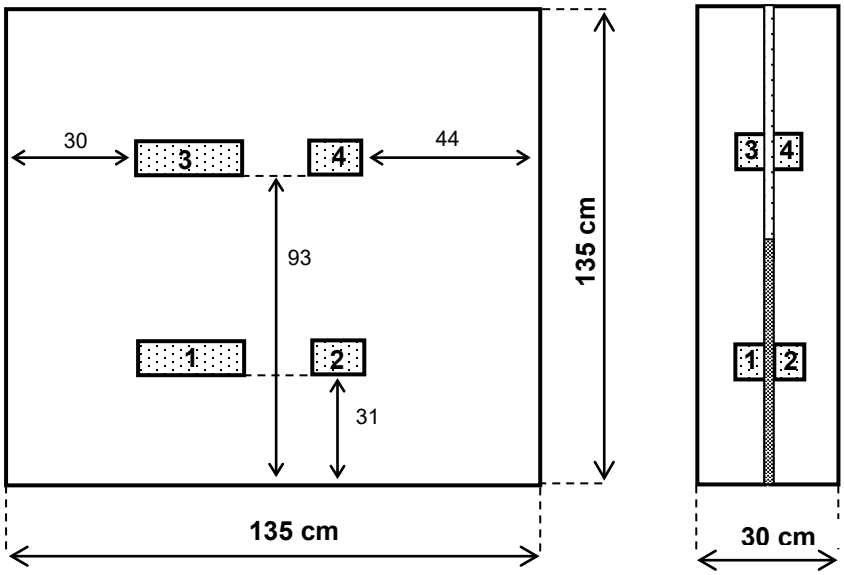

Figure 6. The configuration of the F1 test wall with artificial anomalies

Photo 4. Construction of F1 test wall

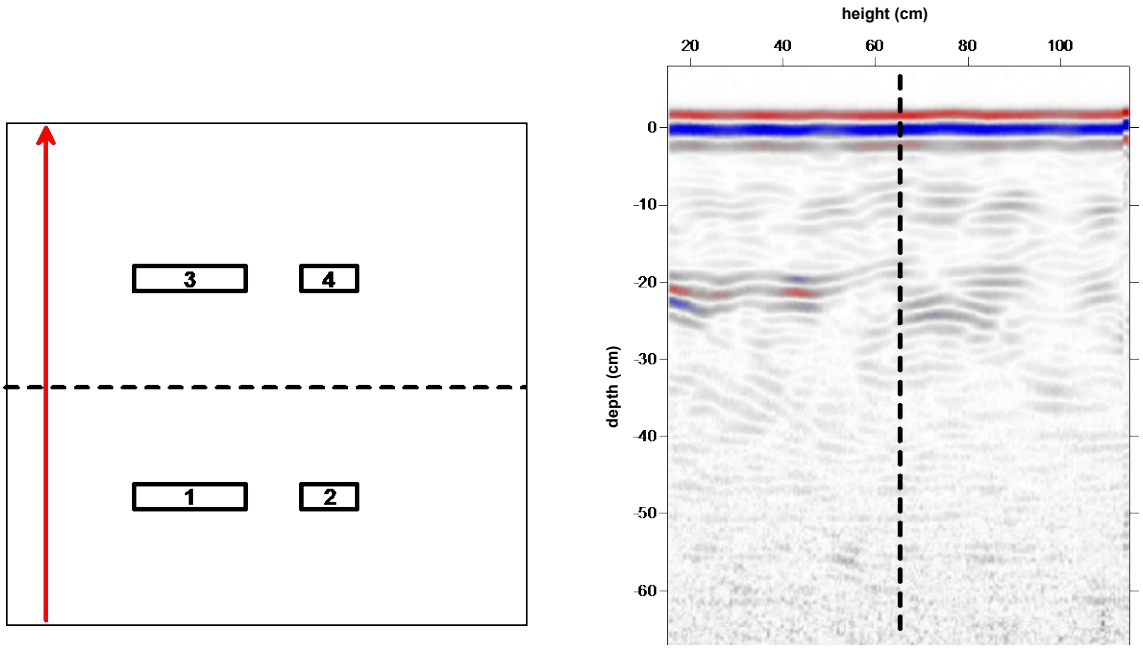

Figure 7. Radargram of the undisturbed part of F1 wall

The boundary between the mortar filled part and the empty part is marked by a broken line in *Figure 7*. This boundary is clearly visible in the recorded section, although, interestingly, it is mainly noticeable on the reflection from the back side of the second brick course. Some amplitude increase can also be noticed on the reflection coming from the air gap, but this increase is not significant due to the interference of the signals reflected from the beginning and the end of the gap. It is visible on the back wall, that at the boundary of the two brick courses well-filled with binding material there is only a slight loss of the signal, therefore the reflection from the back side of the wall is strong. This phenomenon cannot be observed in the case of the air gap. Due to the loss of energy in this area, the amplitude of the signal reflected from the back side is lower.

1st and 3rd anomalies:

1 brick long, 1 brick high, ½ brick thick cavity in ½ brick depth in the first brick course.

On *Figure 8* one can see the effect of the 1st and 3rd anomalies that are situated on the same line. The amplitude increases in both cases in the wall. In the recorded section one can recognise the boundary of the first brick course and the entire thickness of the wall.

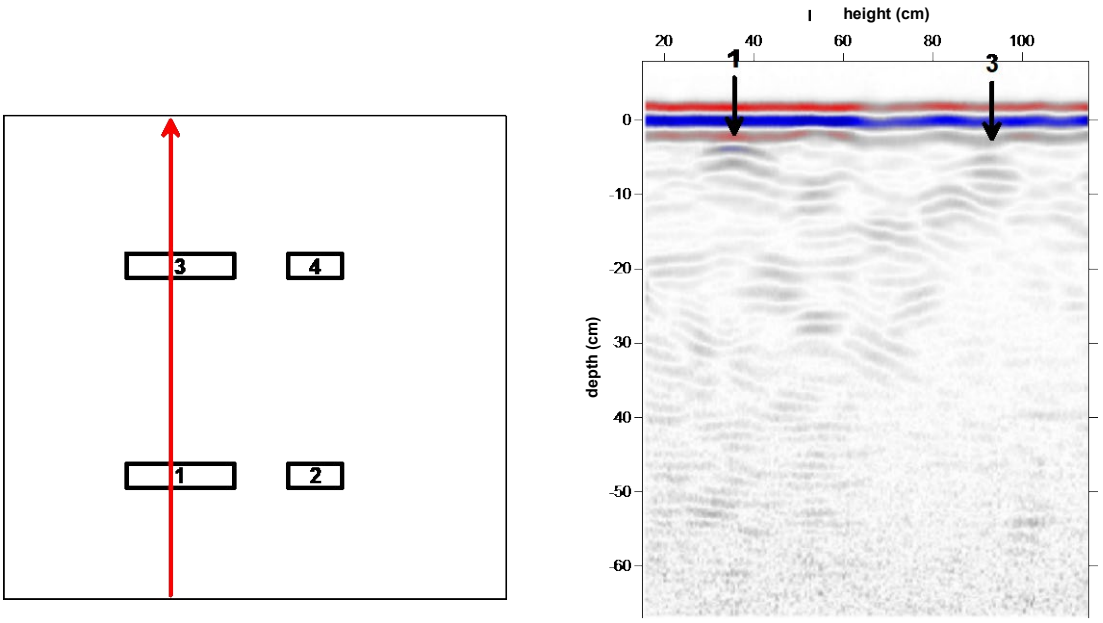

Figure 8. The effect of the 1st and 3rd anomalies on the radargram of F1 wall

2nd anomaly:

A ½ brick long, 1 brick high, ½ brick thick cavity in the second brick course.

4th anomaly:

A ½ brick long, 1 brick high, ½ brick thick cavity in ½ brick depth in the second brick course.

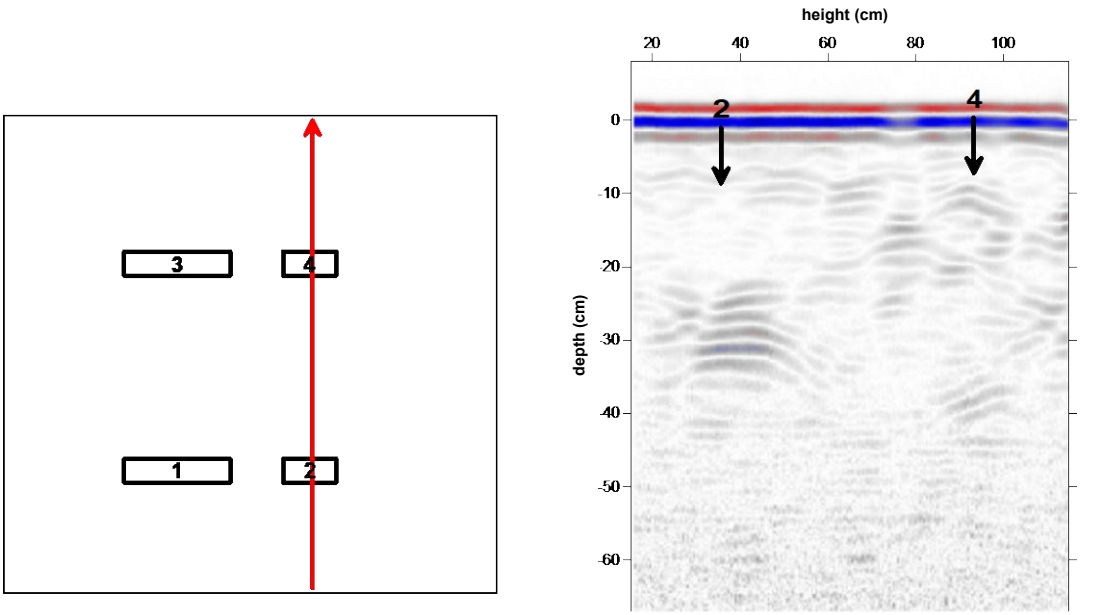

Figure 9. The effect of the 2nd and 4th anomalies on the radargram of F1 wall

In *Figure 9* the 4th anomaly is clearly visible with an amplitude increase while the 2nd one is hardly noticeable, although in theory the 2nd anomaly should be stronger. It is also clearly visible that there are other reflections in the recorded section, the origin of which are not enterely clear.

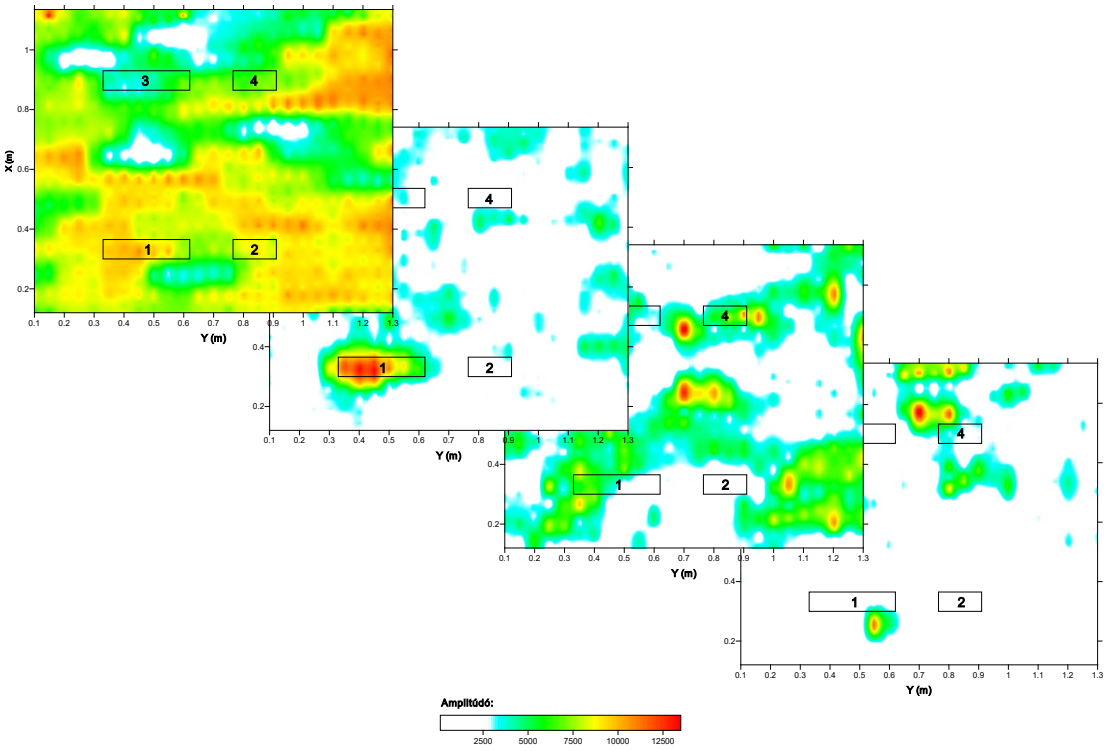

Figure 10. Time slices of the F1 wall

Based on the densely measured sections time slices were also made along planes parallel with the surface of the wall. The amplitude anomalies here also give a picture of the inner structure of the walls, similarly to the recorded sections. The time slices can be transformed into depth-sections by calculating with the average velocity. In the second section from the left in *Figure 10*, the high amplitude caused by the 1st anomaly in F1 test wall can be seen clearly (at 7ns time). These calculations and presentations were done with each wall, but the variety of amplitudes is rather high due to attenuation in the medium and interference phenomena, therefore we could not show all the anomalies in adequate quality in one colour in the time slices and that is the reason why we decided to represent the anomalies in the recorded radargrams that give clearer pictures.

4.3.2 Investigation of the 2nd test wall (F2)

The thickness of the wall is three brick courses, at the bottom part of the wall the joints and the gap between the courses are well-filled with mortar, while the middle course is missing at the upper part of the wall and the gap is filled with brick debris. The location of the artificial anomalies and the construction of the wall is shown in *Figure 11* and *Photo 5*.

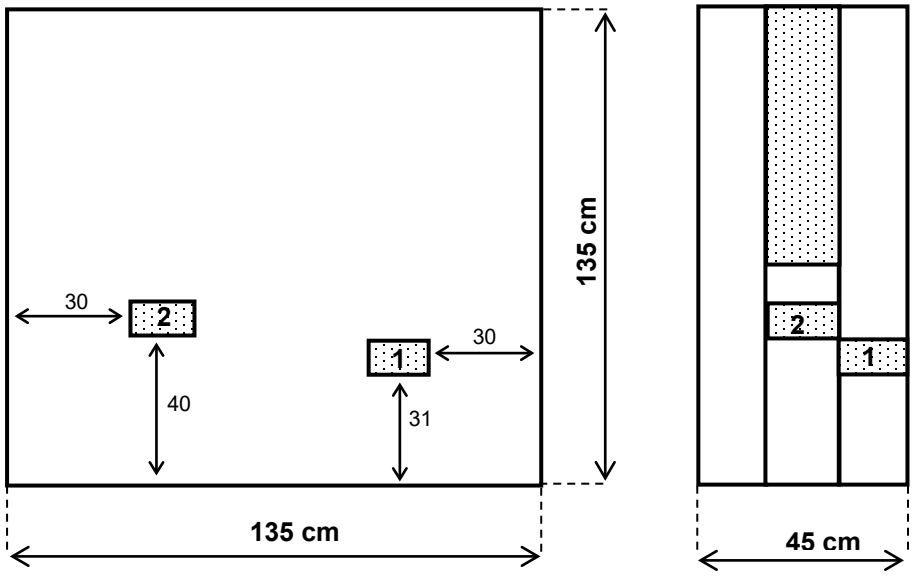

Figure 11. The configuration of the F2 test wall with artificial anomalies

Photo 5. Construction of F2 test wall

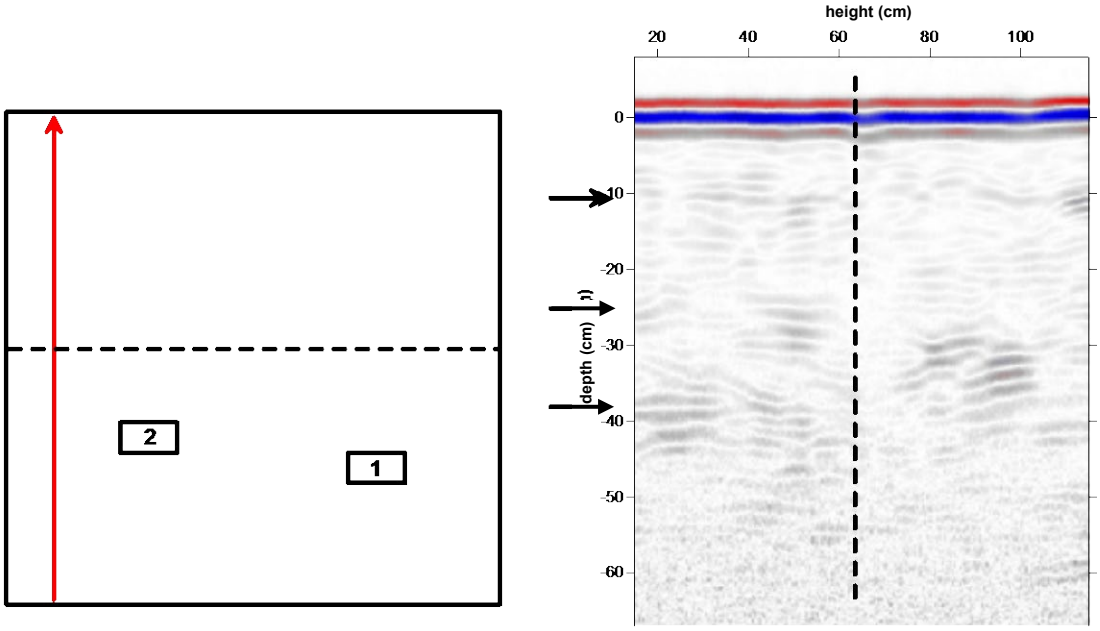

Figure 12. Radargram of the undisturbed part of F2 wall

The radargram in *Figure 12* shows the part of the 2nd wall that is free from defects. The boundaries of the different brick courses are marked by black arrows on the left hand side of the section. It is clearly visible that the 1.5 GHz antenna can "see" three brick courses deep into the wall and that the middle reflection series break at the section filled with brick fragments (right hand side of the section) and the signal coming from the back side of the wall arrives earlier. The reason for this phenomenon is that the speed in the air between the brick fragments is three times higher than in the bricks, so the signal arrives sooner through the fragments than through the masonry.

1st anomaly:

A ½ brick long, 1 brick high, 1 brick thick cavity in the third brick course.

Although the missing brick is visible in *Figure 13*, there are also other signals with similar amplitudes in the section. The greatest reflection is located at the 44th cm of the section in the depth of 12.4 cm. The fact that this has a higher amplitude than that coming from the surveyed anomaly can be considered normal, since the signal attenuates significantly in the wall, therefore the effect of the closer smaller parameter contrast could as well be higher than that of the greater change further away. However, we cannot account for the phenomenon that in the same depth the extent of the reflection located right from the arrow is nearly similar to that of the signal reflected from the part that lacks bricks.

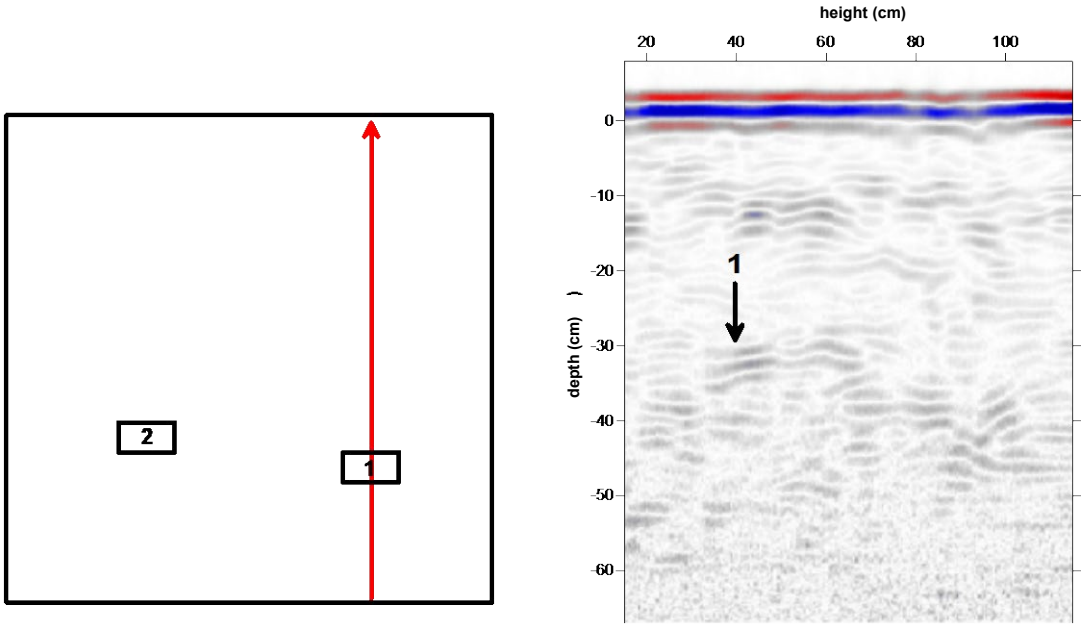

Figure 13. The effect of the 1st anomaly on the radargram of F2 wall

2nd anomaly:

A ½ brick long, 1 brick high, 1 brick thick cavity in the second brick course.

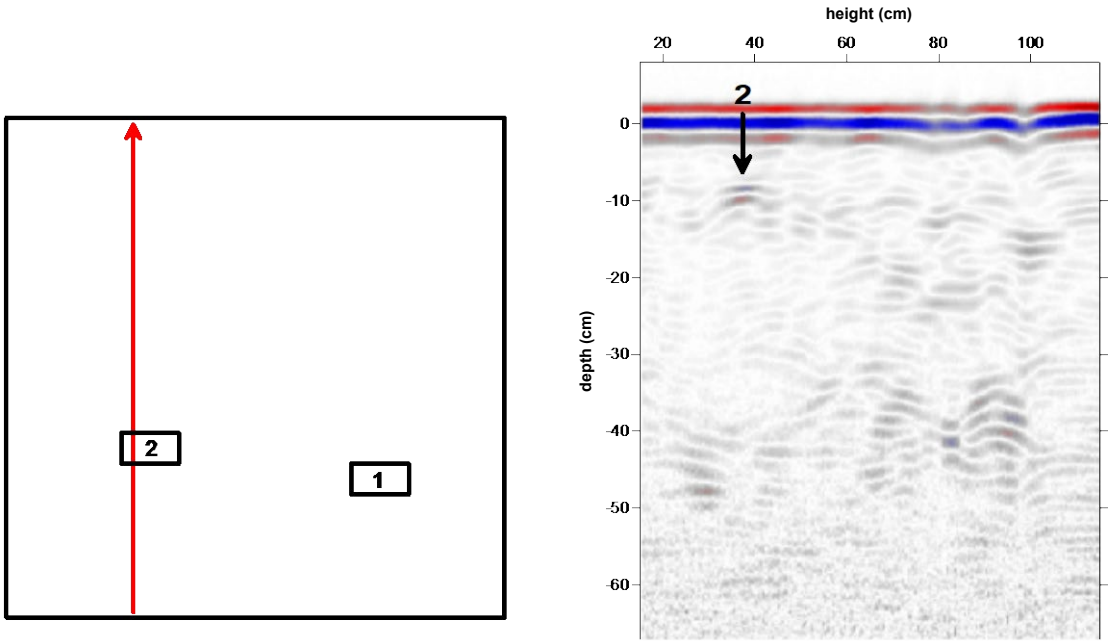

Figure 14. The effect of the 2nd anomaly on the radargram of F2 wall

In *Figure 14* the 2nd anomaly can be seen clearly with high amplitude. Despite the high attenuation in the wall there is a surprisingly strong reflection at the 92.5th cm of the section in a depth of 35 cm. The origin of this is unknown. There are significant reflections in the depth

ranges of 8-15 cm and 18-25 cm, although they are lower than that of the 2nd anomaly. These are not artificial defects, these inhomogeneities created during the building of the wall which result in significant reflections whose amplitudes can be compared to those from the cavity, although they are somewhat lower.

4.3.3 Investigation of the 3rd test wall (F3)

The thickness of the wall is 1 brick course. Hidden anomalies and the construction of the wall are seen in *Figure 15* and *Photo 6*.

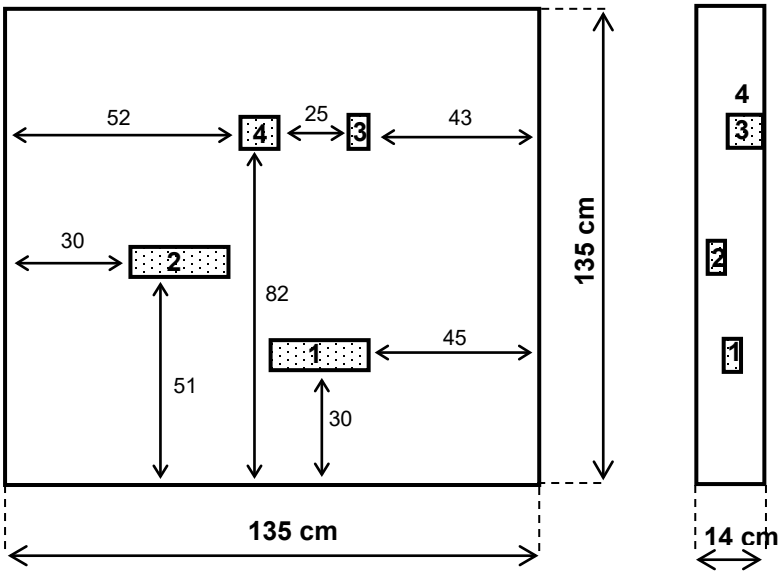

Figure 15. The configuration of the F3 test wall with artificial anomalies

Photo 6. Construction of F3 test wall

Figure 16 shows a section that was recorded on the defect-free part of the 1-brick-thick test wall. A strong reflection arrived at the receiver from the back side of the wall that was marked by a black arrow. The amplitude of the signal is much higher than those that we have seen during the previous measurements due to the high parameter contrast and small thickness of the wall. It is clearly visible that the strength of the reflections changes along the wall, there is an edge effect at the top and bottom edges of the wall, while the lower amplitudes over the middle part are presumably due to moisture.

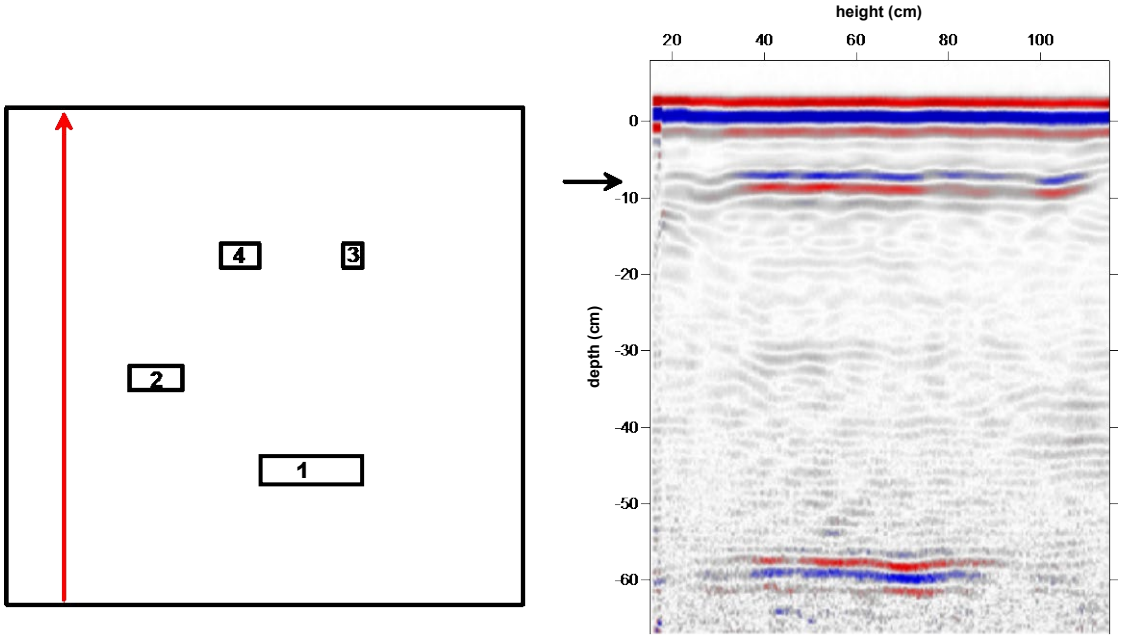

Figure 16. Radargram of the undisturbed part of F3 wall

1st anomaly:

A 1 brick long, 1 brick high, 4 cm thick cavity in the middle of the brick.

3rd anomaly:

A 5 cm long, 1 brick high, ½ brick thick cavity in ½ brick depth.

Both of these anomalies can be seen well in the recorded section shown in *Figure 17*. This is due to the fact that they are located not too deep in the 1-brick-course thick test wall. The 3rd anomaly is so strong that it screens the wall behind it in a bigger area, and the smaller one also covers the air-brick boundary behind it. The reflection coming from the bigger cavity is much stronger than the one coming from the smaller one.

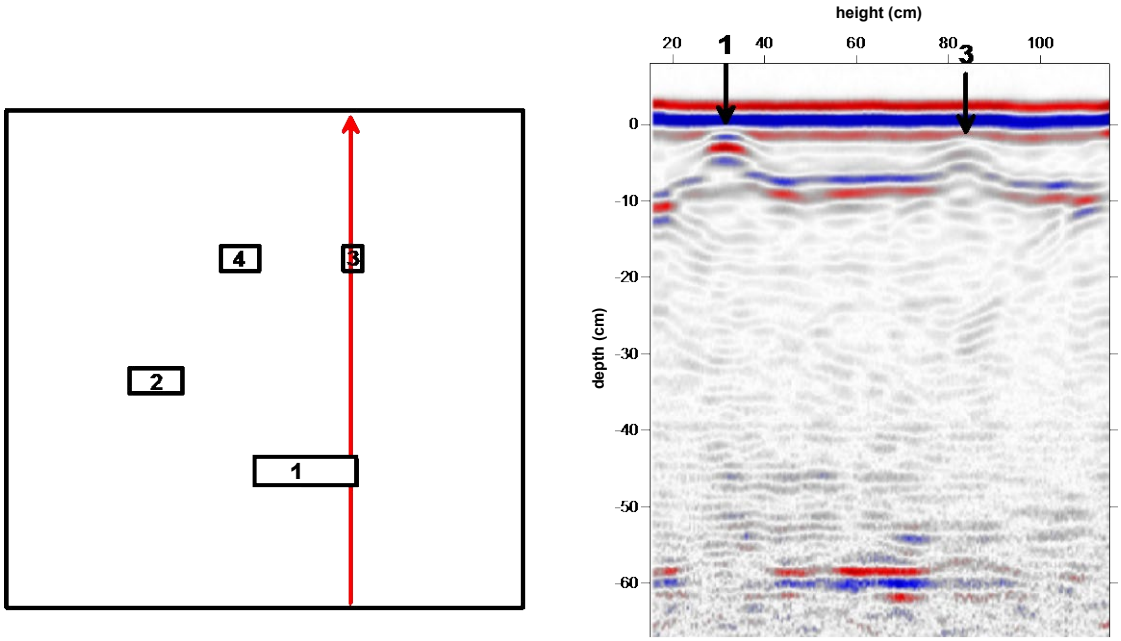

Figure 17. The effect of the 1st and 3rd anomalies on the radargram of F3 wall

2nd anomaly:

A 1 brick long, 1 brick high, 2 cm thick cavity at 2 cm depth.

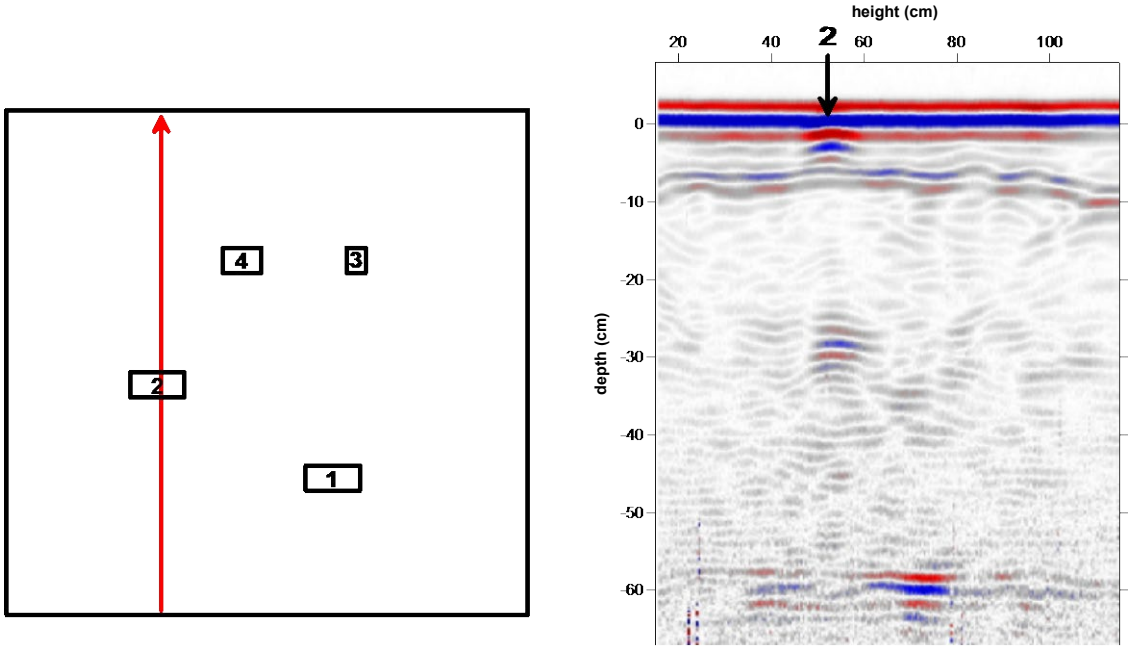

Figure 18. The effect of the 2nd anomaly on the radargram of F3 wall

The 2nd anomaly is clearly visible in *Figure 18*. Due to the small depth, the first phase of the wave interferes with the first arrival, but due to its high amplitude the reflection coming from the cavity is clearly visible. Under this, at the depth of about 26 cm there is another anomaly. This, however, is not coming from the wall, since its thickness is smaller. Most probably, the wave got reflected from another object behind the wall.

4th anomaly:

A 10 cm long, 1 brick high, ½ brick thick cavity in ½ brick depth.

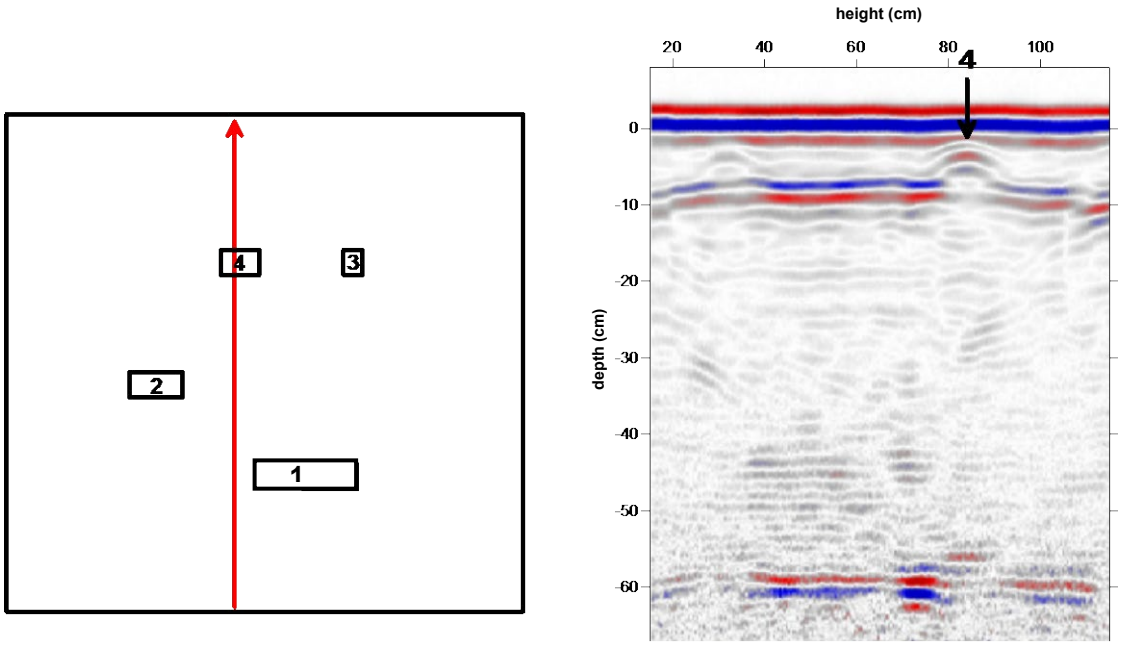

Figure 19. The effect of the 4th anomaly on the radargram of F3 wall

Figure 19 shows the recorded section in which the 4th anomaly can be seen. The reflection of the cavity marked by a black arrow is so strong that it screens the part of the wall behind it. There is another anomaly visible in the recorded section, at the same depth with the 4th anomaly, at the height of about 30 cm. This is weaker than the previous one, but it is clearly visible, with slightly lower amplitudes. The reason for the second reflection is unknown but it is possible that it is due to a natural inhomogeneity produced during construction.

4.3.4 Investigation of the 4th test wall (F4)

The thickness of the wall is three brick courses, at the bottom part of the wall the joints between the courses were well-filled with binding material and a header bond was used, while at the top part the joints in the first two brick courses are well-filled and third course is divided by a 1.5 cm air gap from the first two. There was 1 brick long, 3 bricks high and1 brick thick cavity built inside the wall at 1 brick course depth.
The configuration of the wall and the anomalies are shown in *Figure 20* and *Photo 7*.

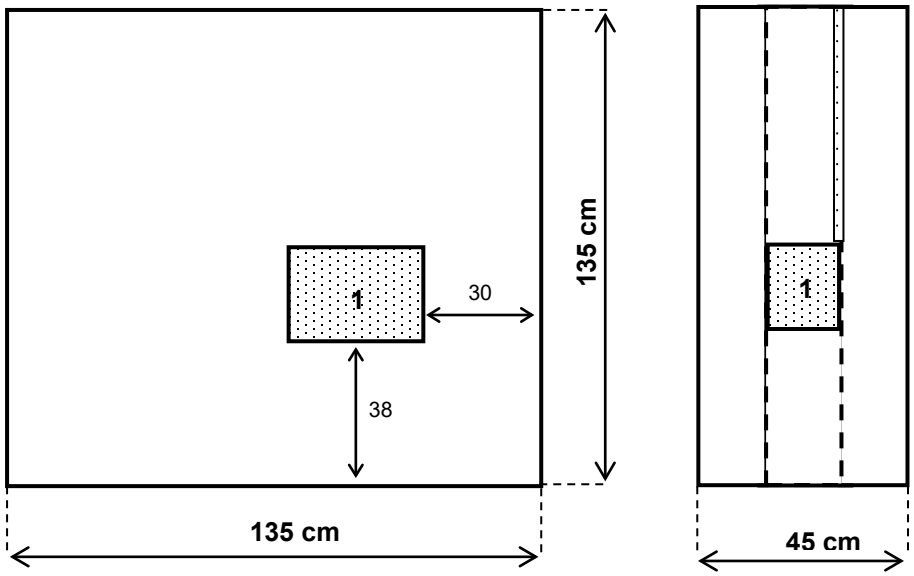

Figure 20. The configuration of the F4 test wall with artificial anomalies

Photo 7. Construction of F4 test wall

In *Figure 21*, the identified brick courses are marked by a black arrow. The effect of the air gap is significant both in terms of amplitude and phase. The amplitudes of the signals coming from the joints filled with binding material are smaller than those of the ones coming from the air gap. In theory the expected reflection from the brick-air boundary is higher by a magnitude order. This, however, is not obvious in the section due to the destructive interference of the signal coming shortly after from the air-brick boundary.

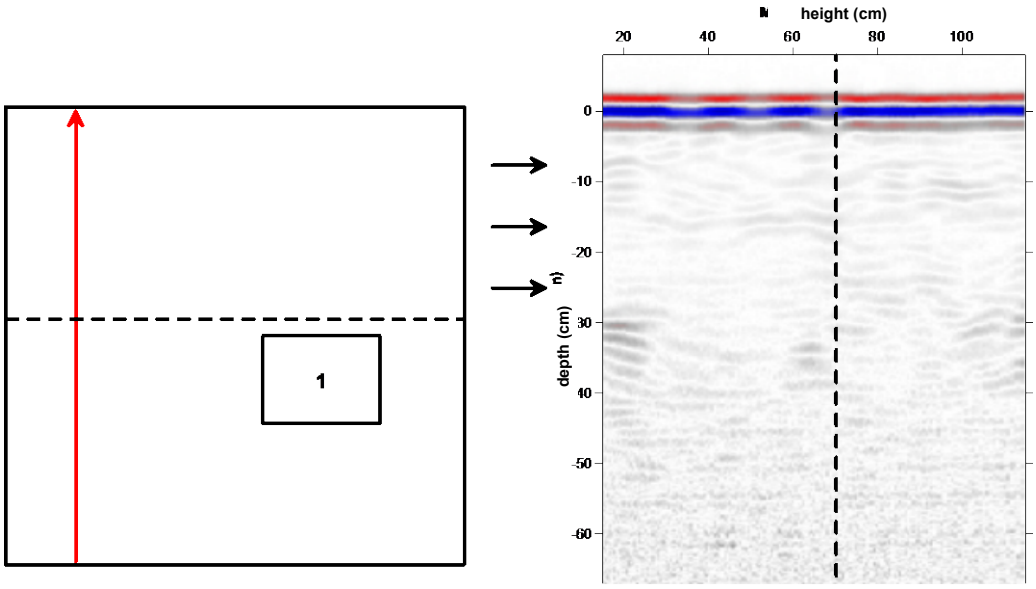

Figure 21. Radargram of the undisturbed part of F4 wall

1st anomaly:

A 1 brick long, 3 bricks high, 1 brick thick cavity in 1 brick course depth.

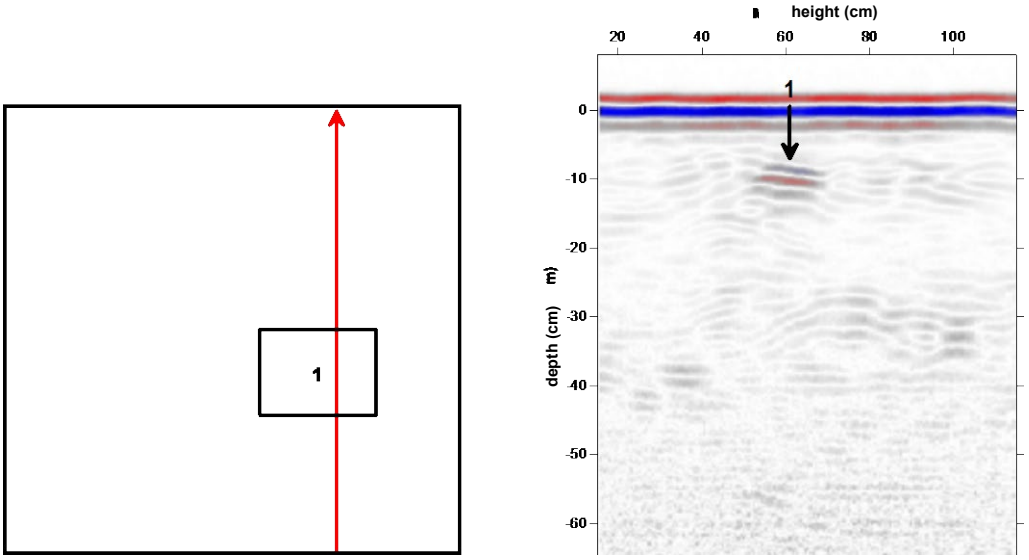

Figure 22. The effect of the 1st anomaly on the radargram of F4 wall

In *Figure 22*, the cavity that is much bigger than the previous ones is marked by a black arrow. The reflection is very strong and clearly visible.

4.4 Natural anomalies

The anomalies shown in *Figures 23-26* are natural anomalies (i.e. anomalies that were accidentally introduced during the construction of the walls or appeared as a result of various environmental effects).

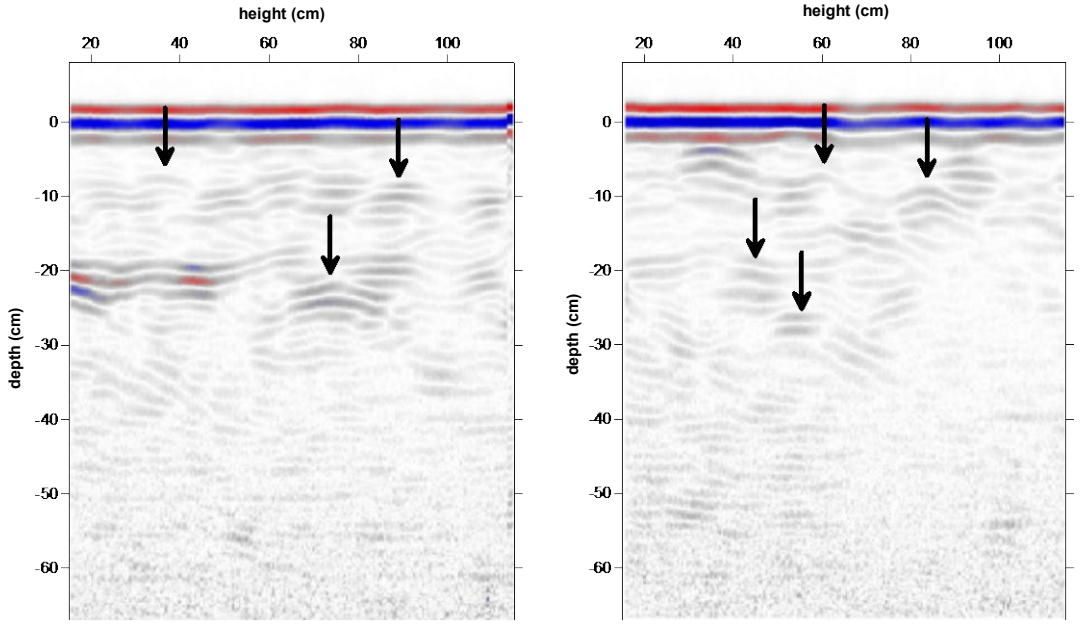

Figure 23. Natural anomalies – Examples l.

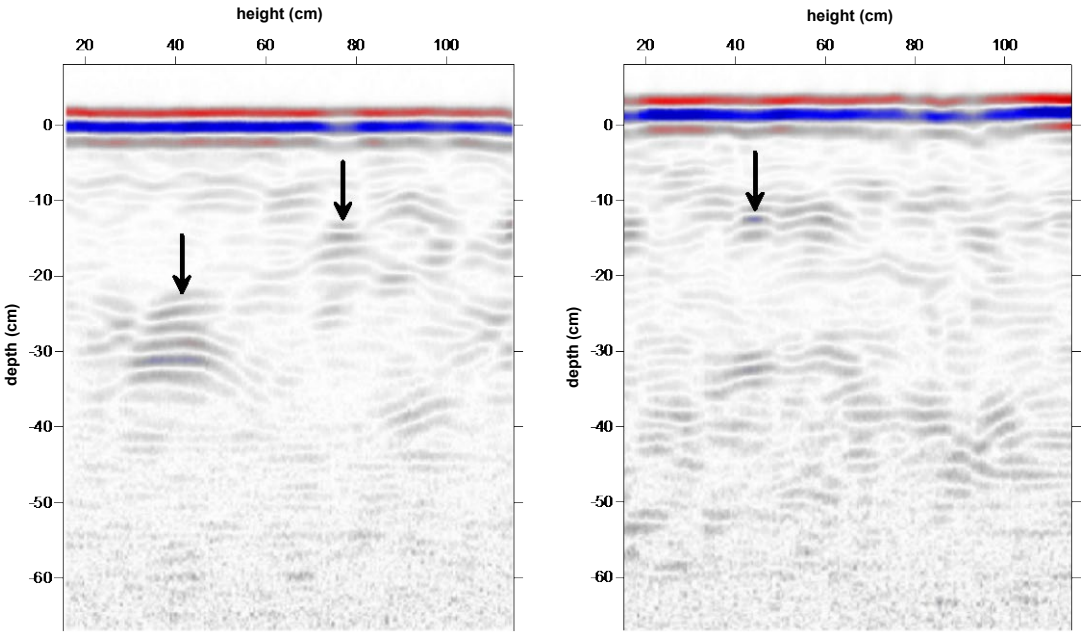

Figure 24. Natural anomalies – Examples ll.

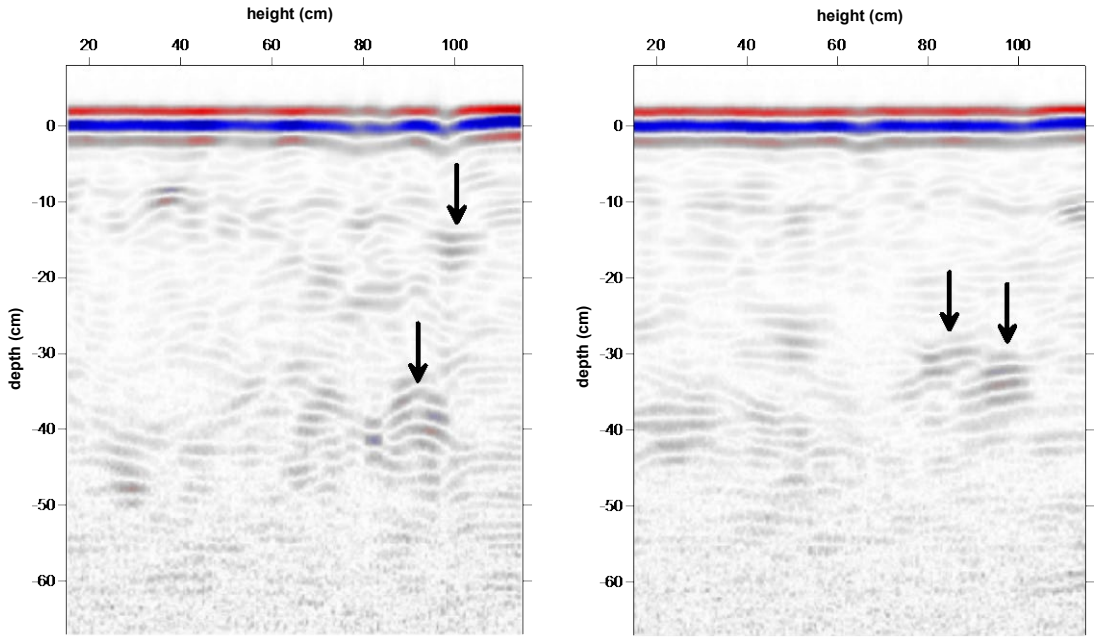

Figure 25. Natural anomalies – Examples III.

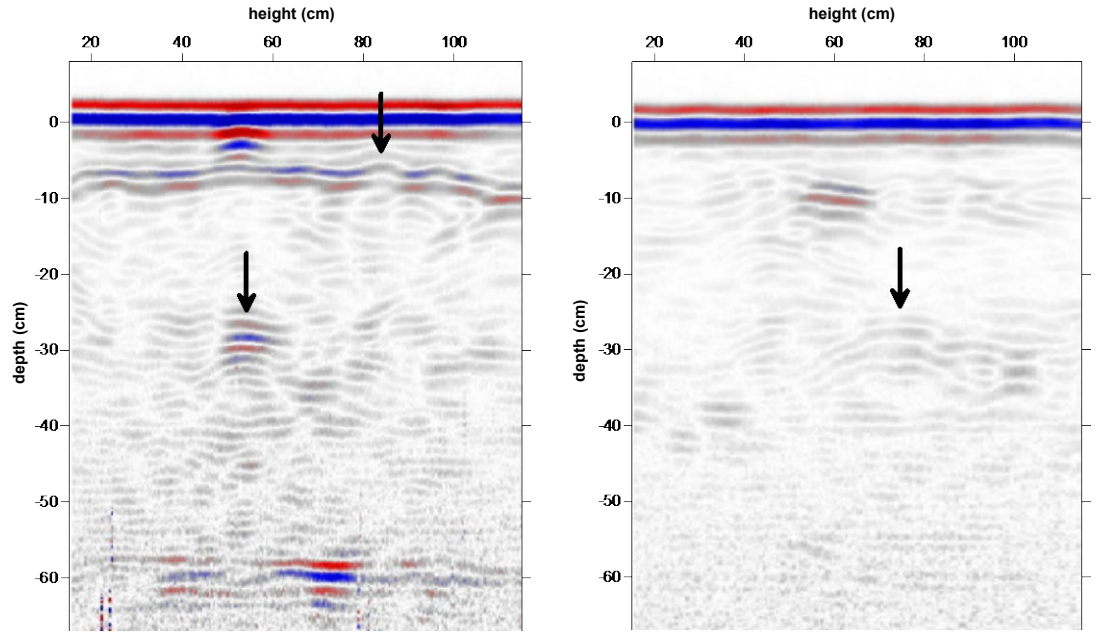

Figure 26. Natural anomalies – Examples lV.

The sources of the phenomena marked by arrows above are not exactly known. All of them provided amplitudes that are comparable to those generated by those of artificial origin, therefore they can be misleading in the interpretation.

4.5 Further experiments

In addition to cavities and gaps in the masonry the effect of dampness and the presence of various filling materials inside the gaps and cavities was also investigated. In this chapter some examples will be shown for the investigation of these effects.

Figure 27 presents the effects of water on the first test wall. The sections were recorded by using the GSSI device with the 1.5 GHz antenna. When the left hand side section was recorded the wall was dry. The section in the middle was recorded after pouring in 5 litre of water into the gap between the courses, while the one on the right was made after pouring 10 litre of water.

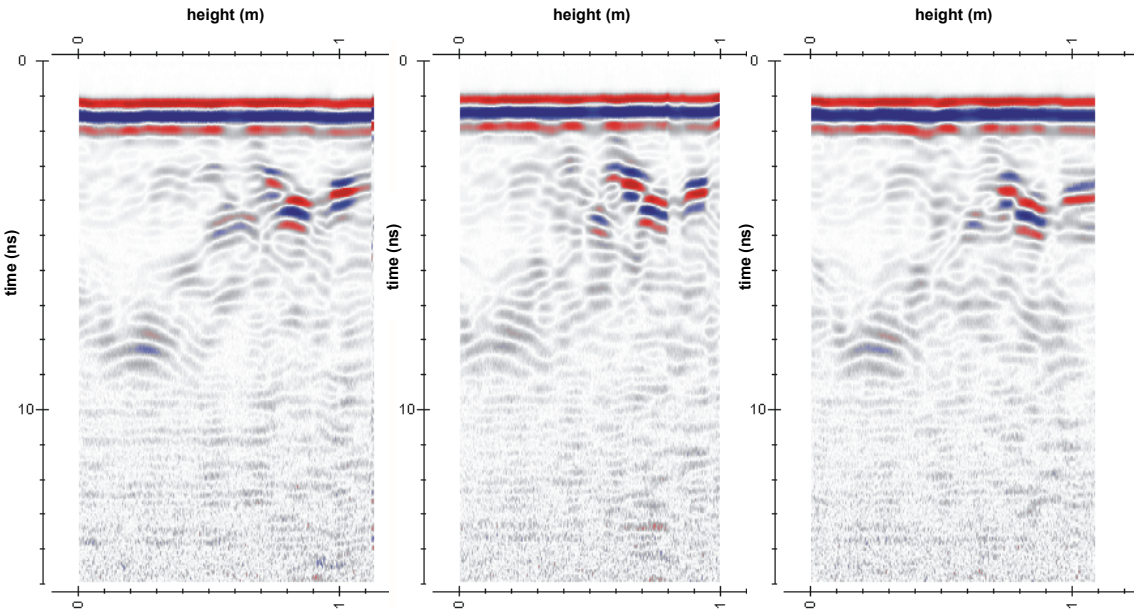

Figure 27. The effect of wettness on the radargrams of F1 wall

The effects of the water appear by changes in the amplitude and by time delay. The reason for the time delay is that the speed of the electromagnetic waves is about one-third of the speed in bricks. The change in amplitude size usually means lower amplitudes due to the electric conductivity of the water. It is clearly visible in the section that a larger amount of water caused stronger attenuation. In walls that are exposed to water for a longer period of time and are totally damp the signals can be significantly absorbed.

On the left hand side of *Figure 28* one can see the original state of the first test wall (F1). In the middle part the gap between the brick courses is filled with dry sand, while on the right the sand had been dampened (*Photo 8*). The original state was recorded earlier and unfortunately the changes can partly be accounted for the fact that the weather conditions were different during the first and the next two measurements. In spite of this it is clearly visible that filling the gap with sand caused significant changes. At the height of 95-110 cm and the depth of about 9 cm the reflections nearly disappear due to the decreased parameter contrast. On the right hand side of the section, the amplitudes are lower due to the higher conductivity in the water.

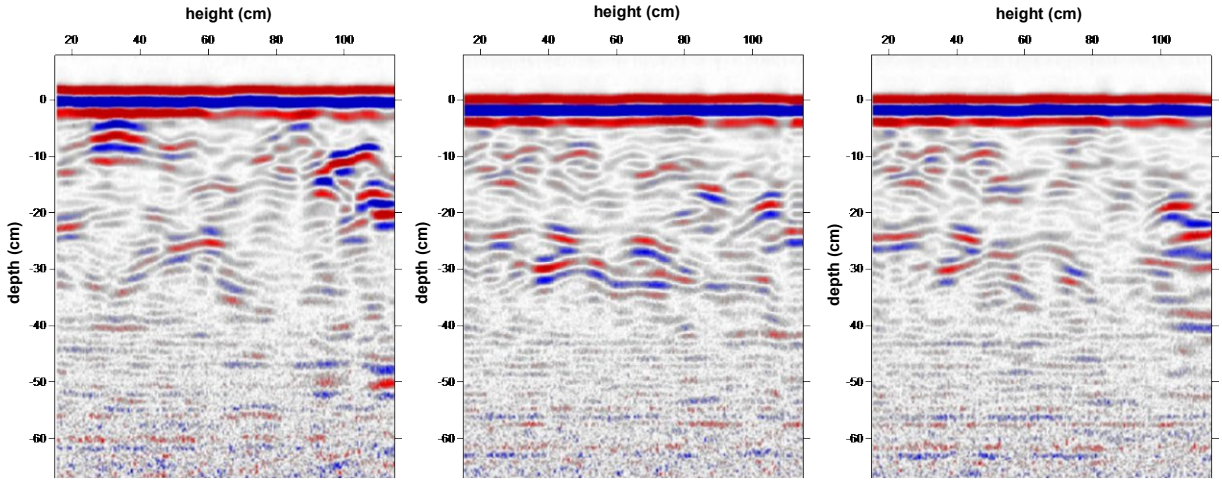

Figure 28. The effect of sand filling and wettness on the radargrams of F1 wall

Photo 8. Left: air gap between the courses of F1 wall.
Middle: the air gap is filled with sand. Right: the sand in the gap is wetted.

In *Figure 29* the effect of varous type of filling can be observed that were filled in the gap between the two outer courses of the upper part of the second wall (F2). The left hand side radargram shows the effect of debris filling, on the middle radargram dry gravel and sand were used, while the gravel and sand filling was wetted on the right hand side radargram (*Photo 9*). The radargrams recorded in the debris and gravel show significant differences, which is possibly caused by the significant amount of air in the debris. Surprisingly, the sections recorded in the dry and wet gravel are more or less similar, although based on previous experiences, a more significant difference was expected.

Further measurements were carried out when the F1 and F3 test walls were pulled next to each other and the gap between them was filled with mixed material. The measurements were conducted on the surface of the F1 test wall. The infill material consisted of two layers of bricks, 30 cm debris on top of the bricks and gravel with sand in the remaining space (*Photo 10*). Due to the thickness of the two walls 900 MHz antennas were used that could penetrate through the whole thickness about 10 ns. On the left hand side of *Figure 30*, the infill material is dry and wet on the right. However there are no significant differences visible between these two sections.

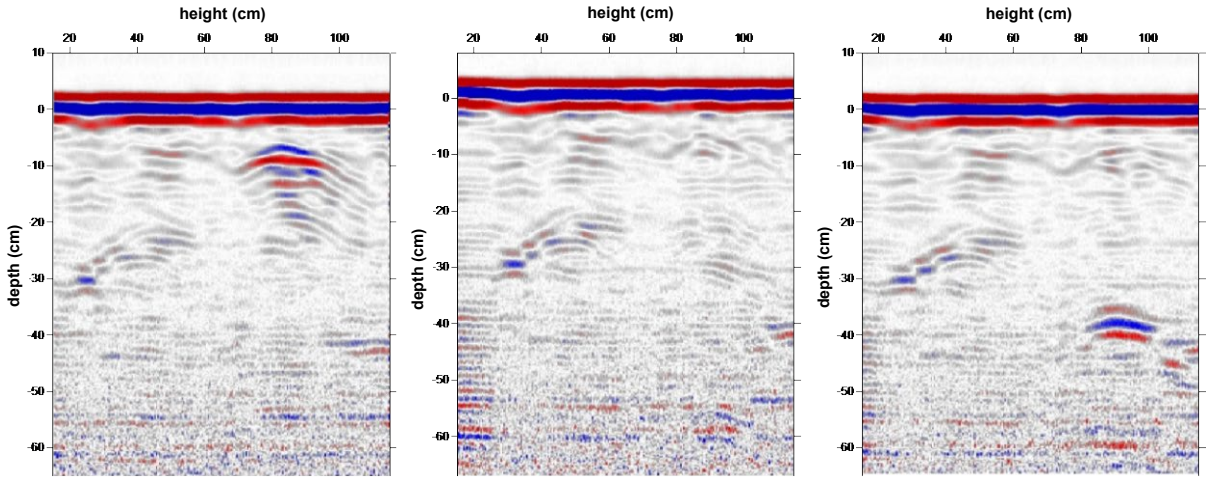

Figure 29. The effect of various type of filling and wettness on the radargrams of F2 wall

Photo 9. Left: the gap between the courses of F2 wall is filled with debris. Middle: the gap is filled with gravel and sand. Right: the sand in the gap is wetted.

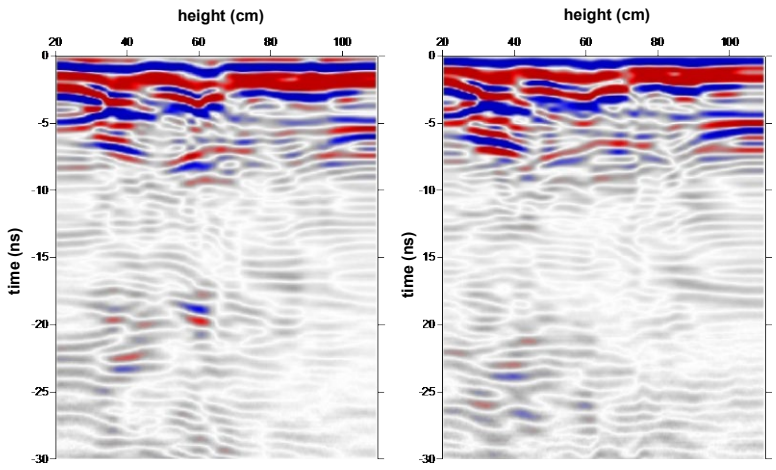

Figure 30. The effect of various type of filling and wettness on the

Photo 10. Filling up the gap between F1 and F3 walls with brick debris, gravel and sand

5. Summary

All the 405 sections have been analysed and evaluated that were recorded in the course of the measurements. Considering the confines of this study it was not possible to show all the sections only those that, for some reason, were more interesting than the others.

The brick walls are strongly inhomogeneous, all the bricks and jointings appear with individual reflections, the recorded sections show their interferences. The defects of the walls should be detected in this environment.

The experiences have shown that it is possible to find almost all the defects in the sections if their location is known. Knowing the original state even the effects of dampness are clearly visible. In reality these conditions are never present when analysing existing structures.

It was possible to identify the boundary of different brick courses (rings) especially when there was a gap between these courses (separation).

Based on the measurements conducted on the test walls it can be concluded that although the radar method is capable to show resolutions of some cm, the evaluation cannot keep pace with this. In this scale the walls are strongly inhomogeneous, therefore the method is mainly suitable for the investigation of the average inhomogeneities in larger areas of walls and the detection of the frequency of the defects and not for the investigation of individual defects. In walls consisting of more brick courses the effects of cavities smaller than one brick are not significant in practice. The characteristics of the entire wall-section can be judged by the measurements and it can be determined whether the brick construction needs repair.

Case Study 2

Radar survey of a single-span stone masonry arch bridge

1. Objectives

The objectives of the non-destructive radar survey was to investigate the internal structure and condition of the bridge. It was expected that the radar survey could point at voided or wet areas and other irregularities inside the masonry structure and in the fill material behind the arch barrel.

Image 1: The view of the Szerencs bridge

2. Description of the structure

The bridge is 10m wide with a span of 2.00m in a semi-circular shape. The height of the abutments is approximately 1.5m. The depth of fill above the arch barrel is approximately 1.2m. Both the arch barrel and the abutments were constructed from rhyolitic tuff ashlars with cement-based mortar. The structure has been extended later with concrete arches and spandrel walls at both sides. The view of the bridge is seen on Image 1.

There was no reliable information available on the thickness of the barrel neither on its variations along transversal and longitudinal profiles. The bed was dry at the time of the measurement but the water level can frequently change according to weather conditions.

The following damages were observed during the visual inspection prior to the measurements:

- Wet and weathered stonework surface due to the lack of proper waterproofing. Considerable wetness was observed on the barrel at some parts of the barrel, especially in the middle of the bridge.

- The masonry surface is covered with moss on the abutment, along a strip above the ground level.
- Hammering of the barrel surface suggests internal voids at some parts.

Image 2: Condition of the structure. Wet spots refer to drainage problems

3. Survey with Ground Penetrating Radar (GPR)

The radar survey was carried out in November 2004, in winter conditions, by means of a GPR system using a pulseEKKO-1000 antenna of the Canadian Sensors & Software Inc. The measurements were primarily made along ten longitudinal lines and three transversal profiles in order to control the data collected from the longitudinal lines (Image 3). The first longitudinal line on each side of the bridge started at 20 cm above the ground level. The distance between the longitudinal lines was 50 cm. About a 1 meter wide strip along the arch soffit was left out form the measurement. The transversal profiles on the intrados for the control tests were taken at 2,5m, 5m and 7,5m measured from the bridge ends.

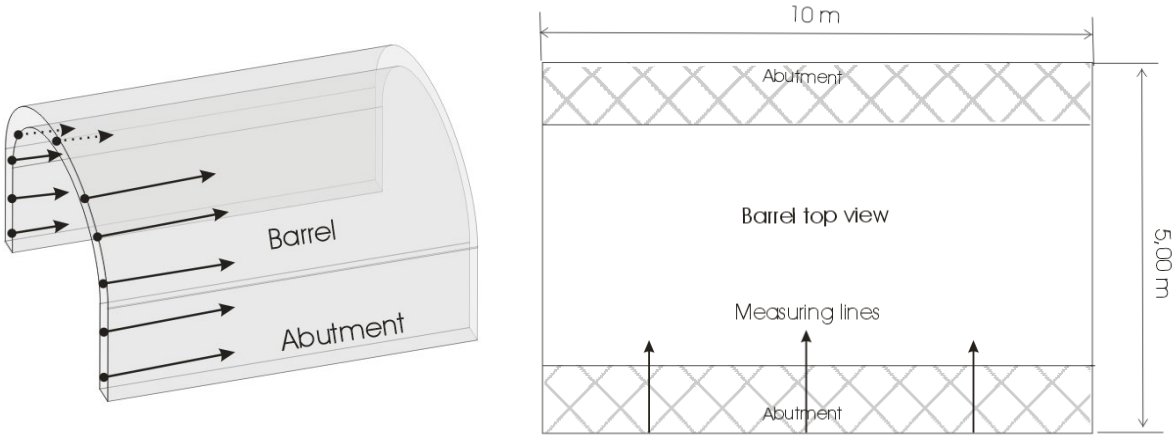

Image 3: Measurement with GPR along longitudinal and transversal lines

The frequencies used during the measurement were 450 MHz, 900 MHz and 1200 MHz. Radargrams with various frequencies recorded along a typical longitudinal profile on the arch barrel are seen on Image 4. The structure is presented with different resolution at various depth levels on the recordings influenced by the different penetration depths that depend on the frequency of the waves. Higher resolution was achieved with the higher frequency antennas but the penetration depth is consequently reduced. On the recordings, the scale of distance can be seen in metres on the top horizontal axle of the charts. The wave propagation time is indicated on the vertical axle.

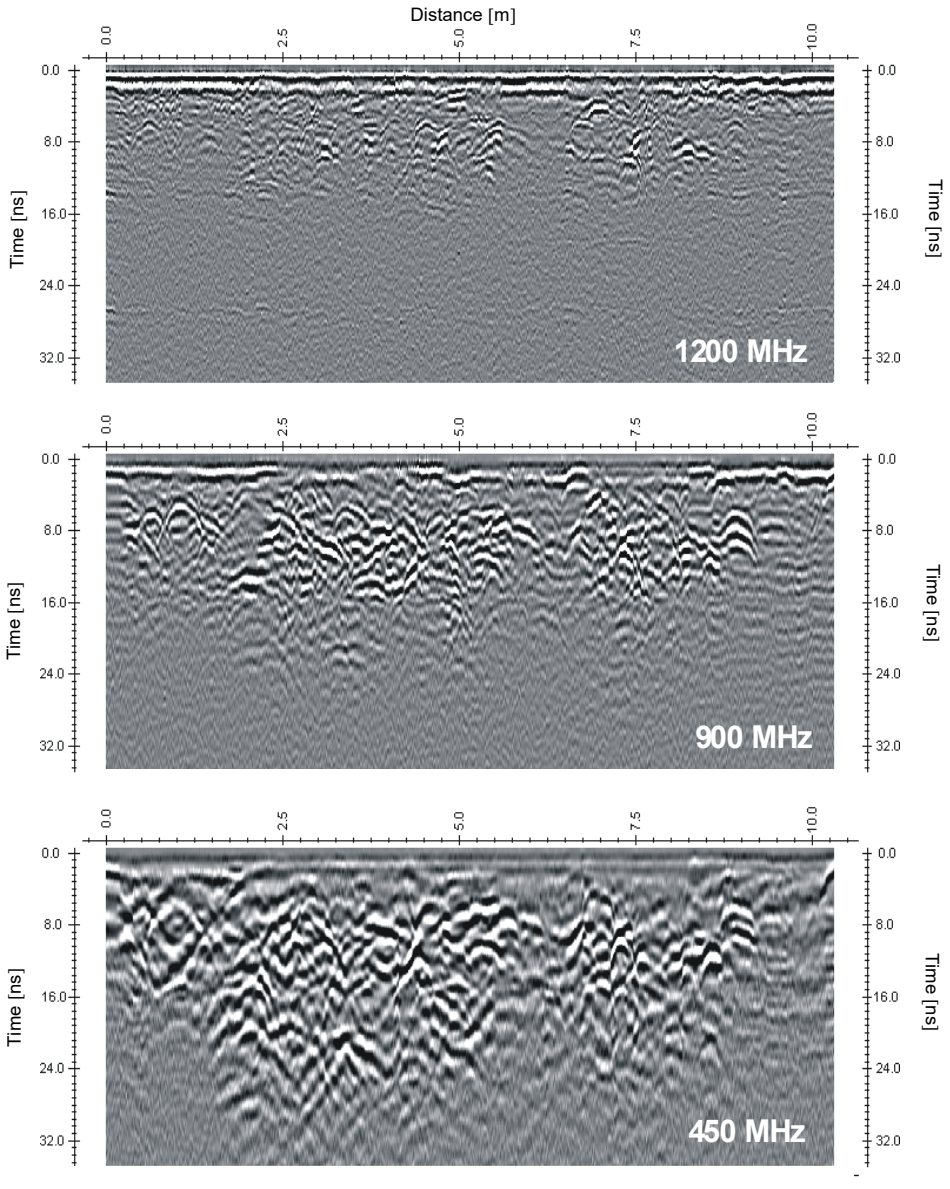

Image 4: Radargrams taken with various frequency antennas on the arch barrel along longitudinal line.

Measurements were also made with 450MHz antennae on track level parallel to the rails. The purpose of this measurement was to check the ability of the system to survey the geometry of the structure from above the arch on track level. Red arrows indicate reflections

received from the extrados of the arch (Image 5). As proper penetration depth could not been achieved with the used antennae the measurement was unable to provide valuable information regarding the dimensions of the structure.

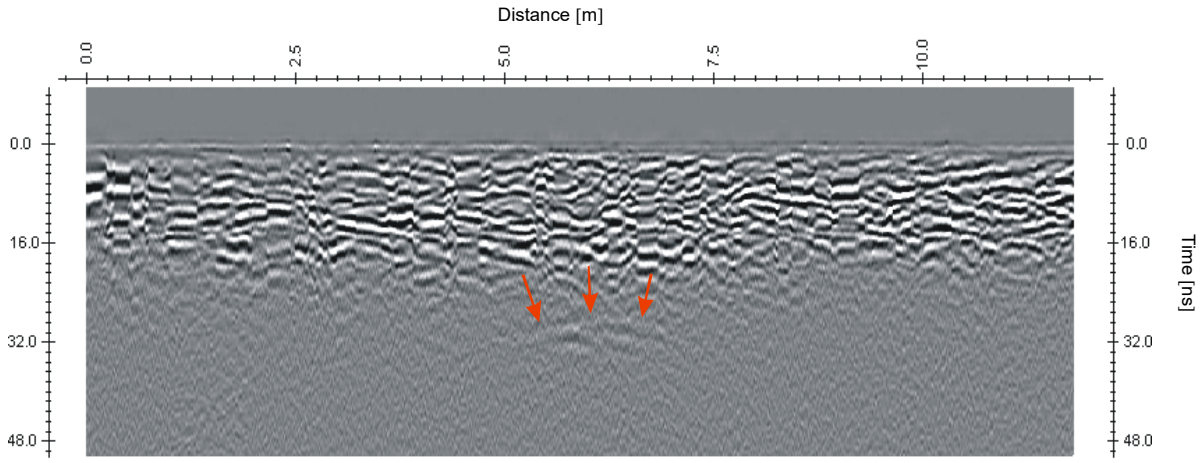

Image 5: Radargram taken parallel to the rails on track level

4. Evaluation

The radar impulses are reflected at interfaces between materials with different dielectric properties. Therefore strong reflections are expected from the boundary of internal voids with a size in the measurable range. By analysing the individual radar recordings there no continuous gap or large size cavity was found behind the stonework.

Many individual diffractions were found however on the radargrams. It is very likely that these diffractions were received from point-like objects. After processing of the recordings anomaly maps were constructed. The anomaly maps show, at a given depth level, the changes in the amplitude values. These anomalies mark the areas from where the electro-magnetic waves are reflected differently. Appendix 1 shows the anomaly maps of the arch measured at three different frequencies (450MHz, 90MHz, 1200MHz) and at five different depth levels (20cm, 40cm, 70cm, 100cm, 150cm) for each frequency. The maps are plotted against the penetration depth of the waves on a flat sheet. As the arch soffit was left out from the measurement this area is represented on the anomaly maps with a 1 meter wide white strip. The higher amplitudes on the maps (seen in reddish colours) refer to cavity or other highly reflecting material, while areas with lower amplitudes (seen in bluish colours) refer to increase in moisture level or to material with smaller compactness.

Highly reflecting areas determined at different frequencies and depth levels are represented on the flat sheets with red spots in Appendix 2. These anomalies have been summarized for each depth level. Darker spots suggest areas where the reflection was perceived consequently at more frequencies. Drawing up all these areas on one single flat sheet we get a cumulative map where all highly reflecting zones (potential location of cavities) are indicated (Appendix 3). Blue markings on this cumulative map refer to points where the most reflection was recorded. These areas are primarily suggested for further survey. Zones with green and yellow markings are also potential areas of cavities but with less likelihood.

5. Summary

The individual radargrams and the anomaly maps suggest that there is no continuous gap or large size cavity is found inside and behind the stonework. The anomaly maps pointed to smaller areas where the reflections are higher than at other parts of he structure, these areas are considered potential zones of cavities.

The recorded data have been represented in a demonstrative form (cumulative anomaly map) that highlights all potential zones of irregularities and helps to appoint areas for further survey.

Appendix 1: Anomaly maps

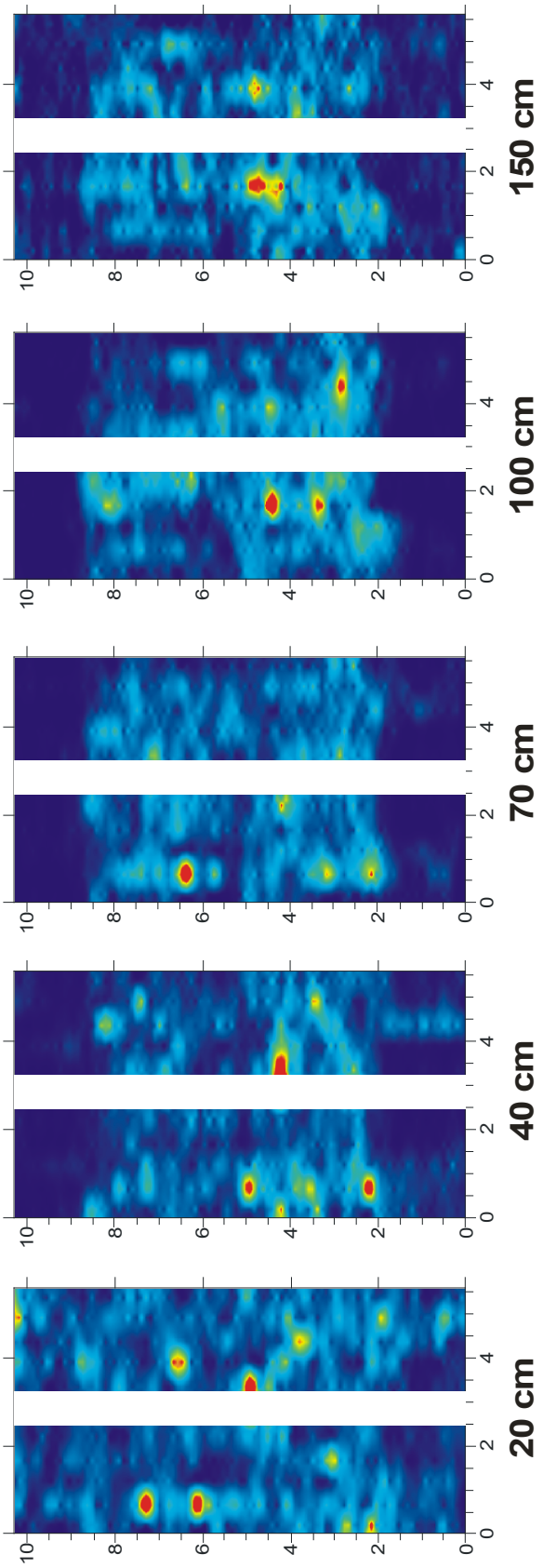

Anomaly maps of the arch (variations in reflectivity) at various depth levels recorded with 450MHz antennae

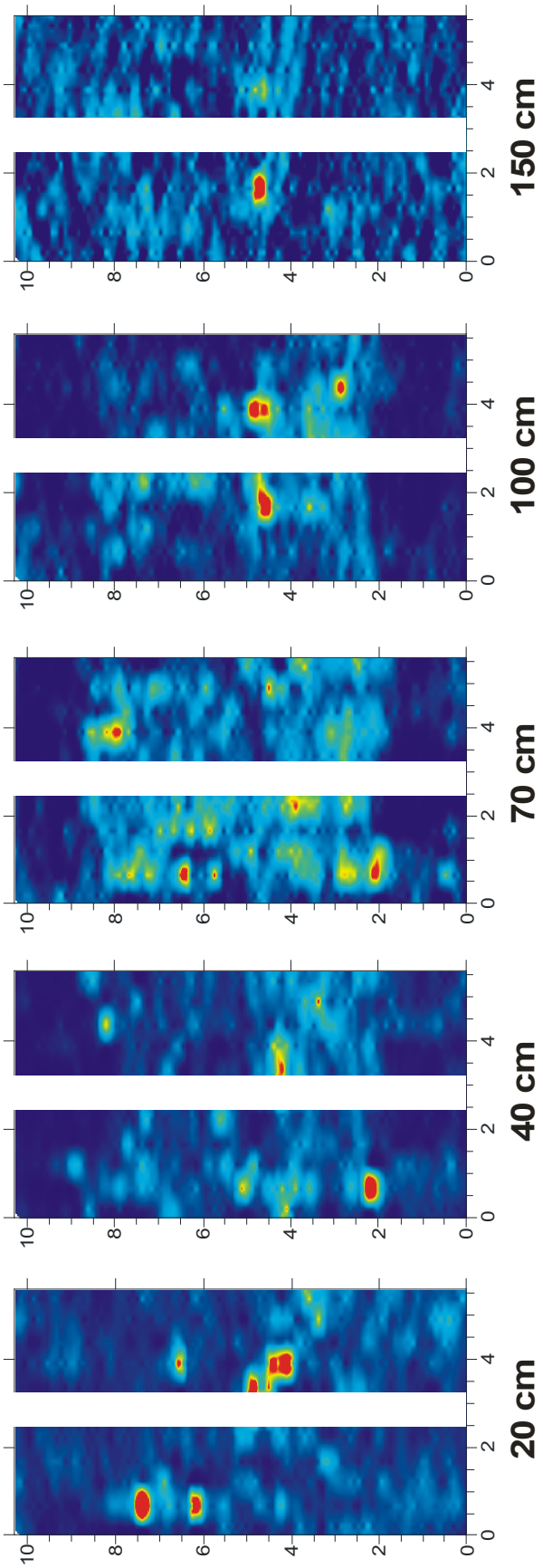

Anomaly maps of the arch (variations in reflectivity) at various depth levels recorded with 900MHz antennae

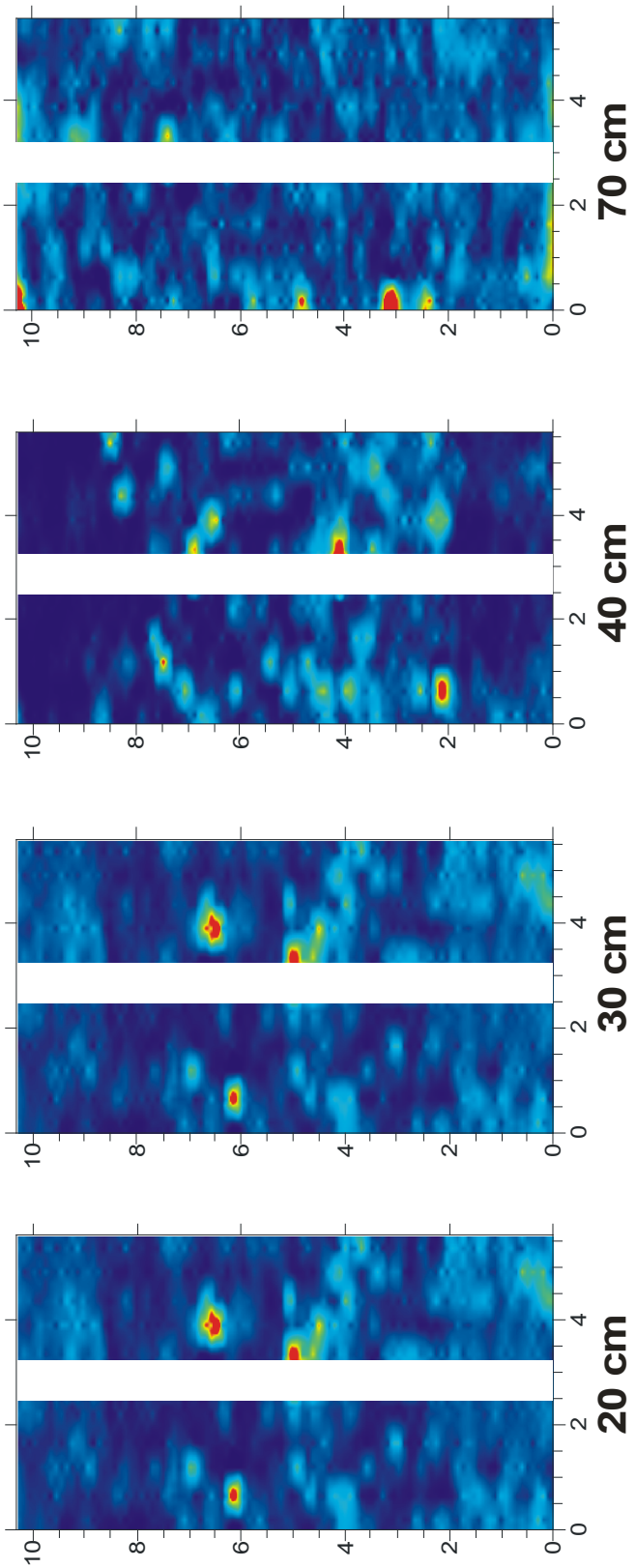

Anomaly maps of the arch (variations in reflectivity) at various depth levels recorded with 1200MHz antennae

Appendix 2: Cumulative anomaly maps at various depth levels

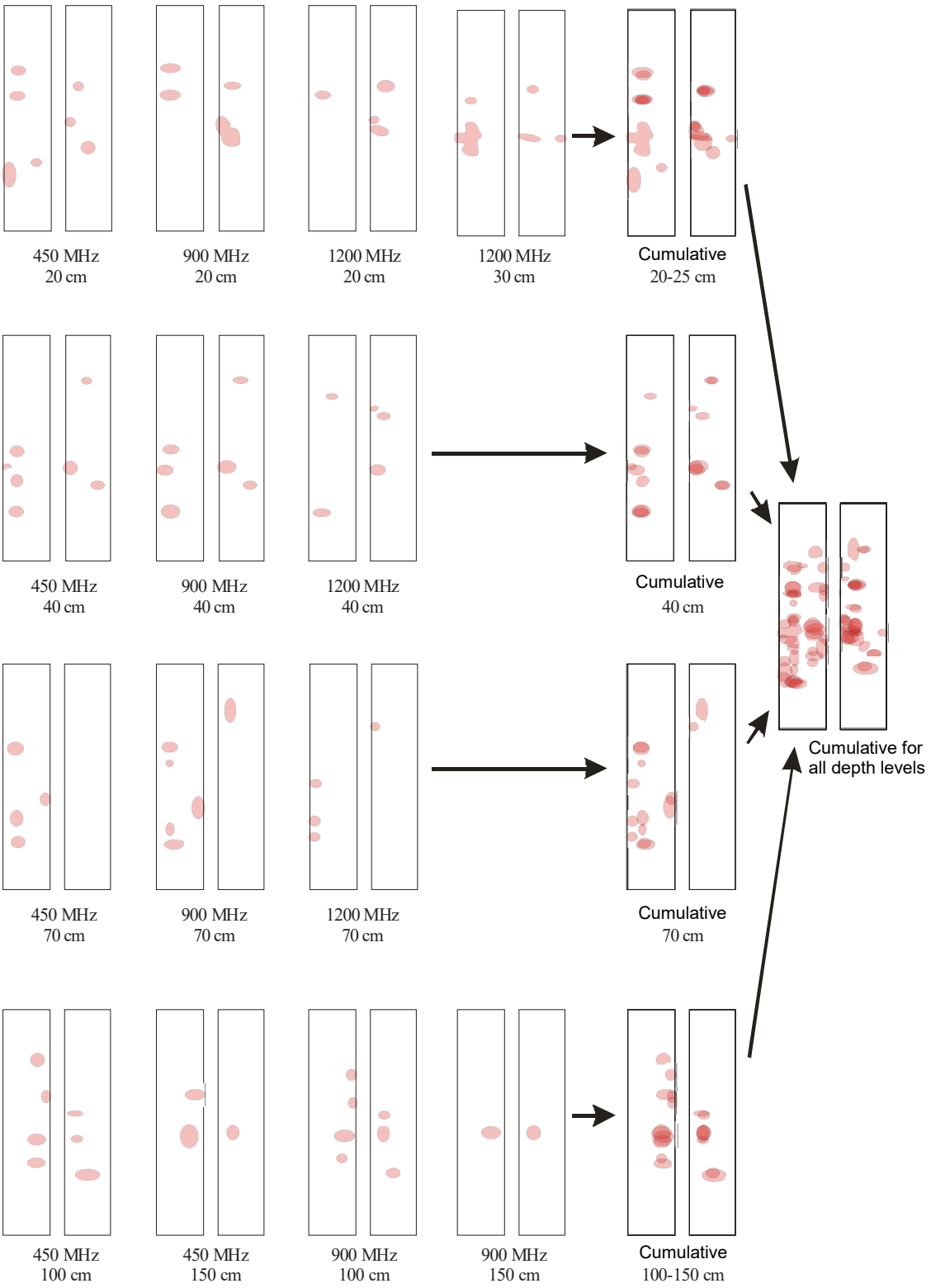

Appendix 3: Cumulative anomaly map for all depth levels

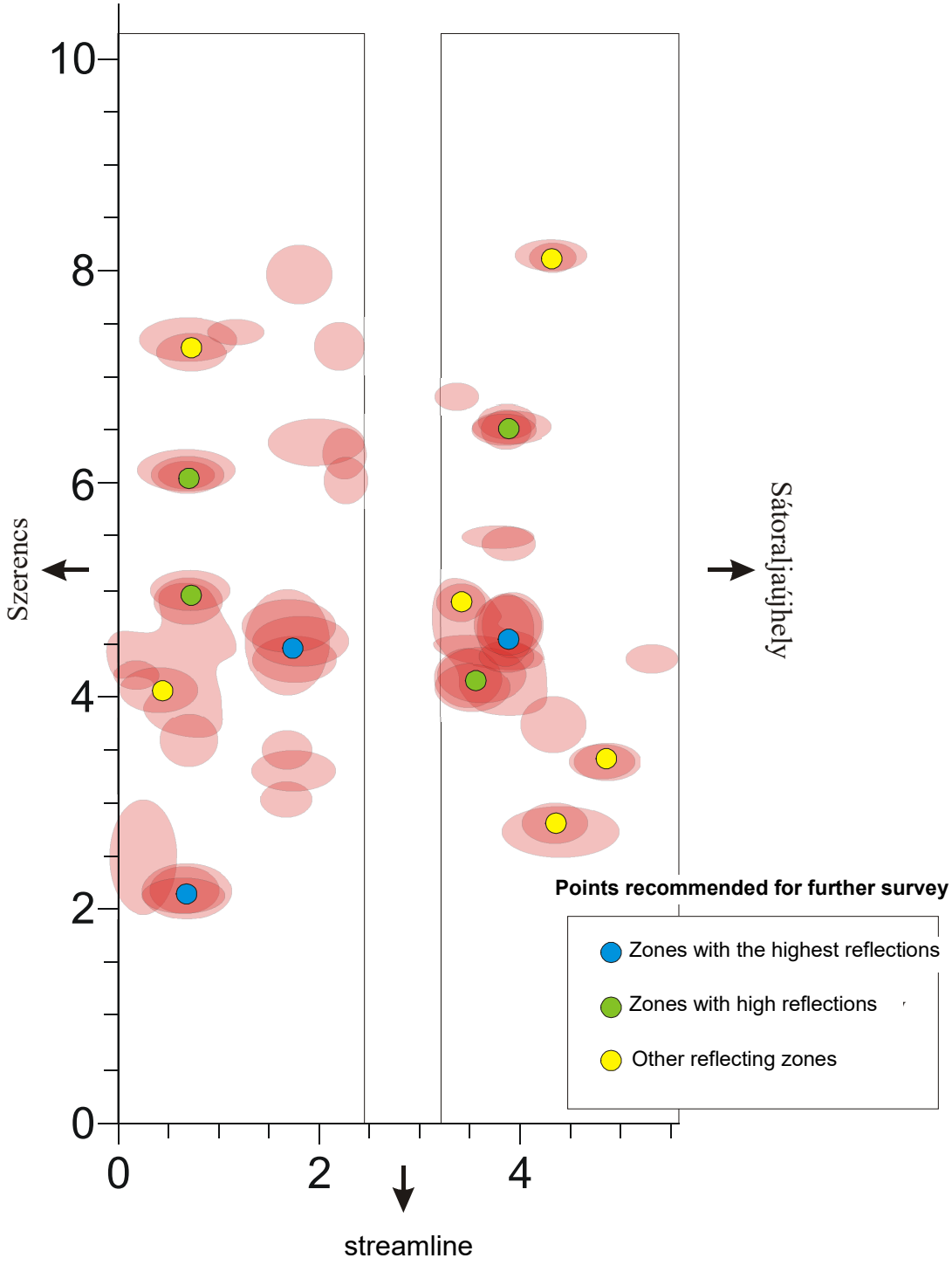

Case Study 3

Non-Destructive Investigation of a single-span brick masonry arch bridge

1. Objectives

The objective of the survey was to conduct a geophysical inspection of the abutment and arch barrel of the bridge and to demonstrate possible ways of processing and representing measured data. The test was aimed to investigate the condition of the brickwork masonry, to point at voids, wet areas and any other irregularities inside and behind the masonry structure and to detect the state of damage by a non-destructive testing method using ground penetrating radar.

The bridge represents a typical small span masonry arch bridge at the Hungarian railway network. Due to the easy accessibility to the whole arch barrel the bridge was an ideal choice for carrying out radar survey without using temporary scaffolding.

2. Description of the structure

The bridge was constructed in 1882. The structure is 10m wide with a span of 2.84m in a semi-circular shape. The height of the abutments is approximately 1.5m but could not be accurately measured due to the thick layer of mud in the bed. The depth of fill above the arch barrel is approximately 2,0m. Both the arch barrel and the abutments were constructed from solid clay brickwork with lime mortar although repointing was made with cement mortar. The structure was extended with a reinforced concrete edge beam in the 1960s.

The barrel consists of two layers of brickwork rings in a header/stretcher bonding type. The barrel thickness is 60cm at the front sides but there was no information available on the thickness changes towards the internal parts of the bridge. The water level in the bed was low at the time of the measurement but frequently changes according to weather conditions.

The following damages were observed during the visual inspection prior to the measurements:

- Wet and weathered masonry surface due to the lack of proper waterproofing. Considerable wetness was observed at the abutments near the ground level and at some parts of the barrel.
- Loss of bricks and joint material due to freeze and wetness.
- Transversal cracks at the arch soffit. These cracks are thin and are not extensive.
- The bed is filled up with mud.

Image 1. demonstrates the condition of the bridge in photos.

3. Site survey with Ground Penetrating Radar (GPR)

The survey was carried out in February 2005 by means of a GPR system using a pulseEKKO-1000 antenna of the Canadian Sensors & Software Inc. Calibratory investigations were made after the GPR survey by the analysis of cores and using boroscopy in order to confirm and interpret data obtained by the radar measurements. The location of the calibratory

measurements were determined by representative points of the radargrams where anomalies were suspected.

3.1 Survey Grid

The data were collected along a series of longitudinal and transversal profiles (Image 2). The mesh contained 5 lines in longitudinal (C1-C5) direction including the abutments and 11 lines in transversal direction (D1-D11) covering the full arch profile starting from the ground level. The frequencies used were 450 MHz, 900 MHz and 1200 MHz. The distance between the lines was approximately 1 meter at both directions, the sampling frequency along the lines was varying between 1 and 3 cm. Marks were inserted onto the raw radar data as the transducer passed the grid points. These marks were used during processing and analysis of the data to ensure accurate relocation.

Image 1: Photos demonstrating the condition of the bridge

3.2 Processing and presentation of data

The raw radar data obtained on site were subject to different processing procedures: positioning, time-correction, amplification, frequency filtering and other filtering. Some samples from these radar data are presented after the processing procedures in Appendix 1. On these radargrams the length scale is given in metres, the double wave propagation time (forward and backward) is given in nanoseconds (ns) and can be seen on the left hand side of the radargrams. The depth scale is on the right hand side of the radargrams indicated in metres. As the penetration depth was calculated with an average wave velocity presumed for

the structural material the depth scale is only approximate. The recorded radargram highlights the constructional anomalies along a given profile plotted against the depth of the measurement. Longitudinal segments measured at three different frequencies along line C2 (corresponds to the barrel of the arch) are shown on Appendix 1. Due to the different frequencies used in the measurements the radargrams have different resolutions at different structural depths.

Further option for processing, when the density of the grid allows, is to plot the amplitude values of the individual radargrams in time and depth sequences to get an anomaly map for various depth levels (slice technique). The anomaly map shows, at a given depth level, the changes in the amplitude values. The resolution of the anomaly map depends on the grid density during the measurement. The anomalies mark the areas from where the electro-magnetic waves are reflected differently. Appendix 2 show three anomaly maps of the arch surface measured at three different frequencies. The maps are plotted against the penetration depth of the waves on flat sheet.

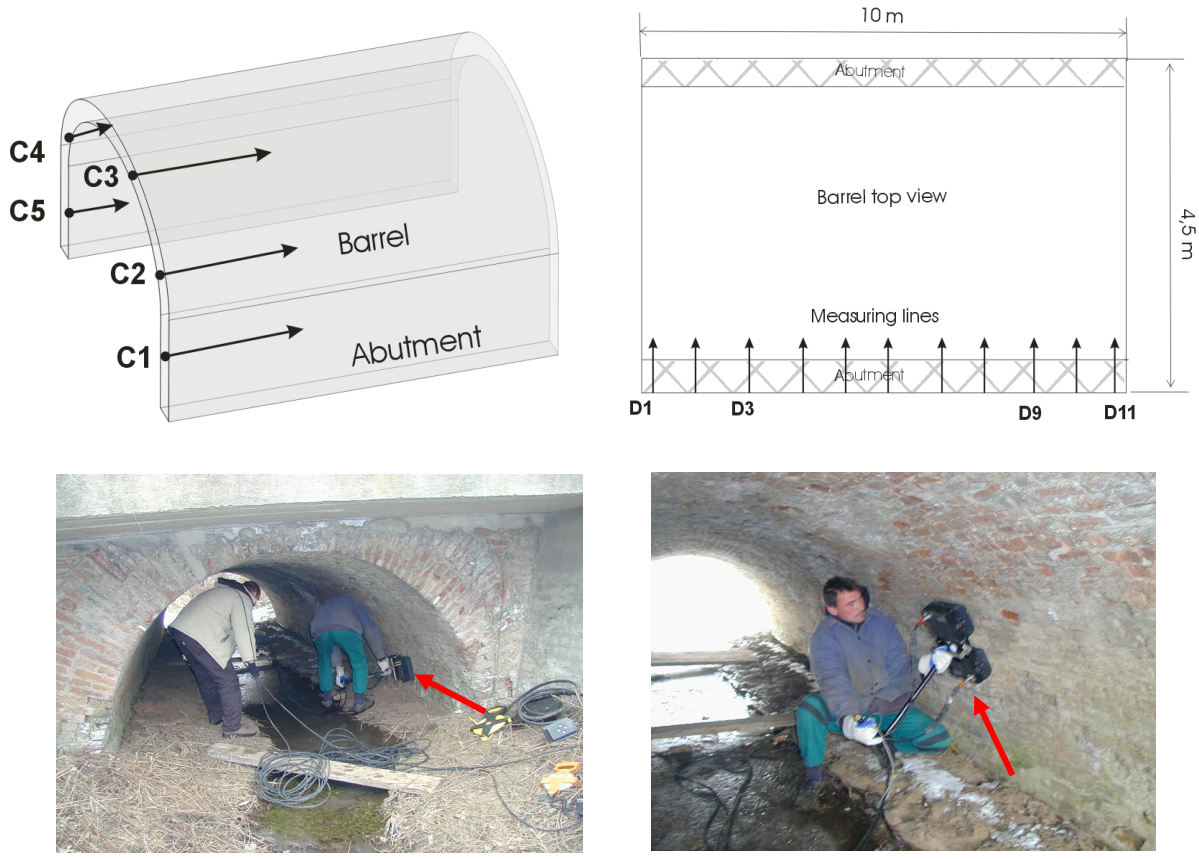

Image 2: Measurement with GPR along longitudinal (C1-C5) and transversal (D1-D11) profiles

3.3 Evaluation of the results

Longitudinal profiles

The radargrams recorded along the longitudinal profiles of the arch were evaluated separately. The three radargrams on Appendix 1 show two distinctive depth levels and a boundary between these levels that characterize the internal structure of the arch. This internal structure is presented with different resolution at various depth levels on the recordings influenced by the different penetration depths that depend on the frequency of the waves. The depth scale of

the radargrams was calculated with an average wave velocity presumed for the masonry material.

The green line on the radargrams indicates a boundary of a relatively homogenous structural layer that can most be seen on the recordings taken with a 900 MHz antennae. This line is at 30-35 cm depth suggesting that it is in fact the boundary between the two brickwork rings. The thickness of the arch barrel decreases at the spandrel walls. Neither the 900 MHz recording nor the 1200 MHz with better resolution show any major inhomogeneity within the brickwork structure. On the other frequencies the boundary between the rings is not even noticeable.

The area behind the brickwork structure until the yellow line shows more reflection (see the 900 MHz and the 450 MHz recordings) that indicates a variation in the construction material and the inhomogeneity of this area. The depth of the yellow boundary is approximately 80 cm from the intrados surface. It is more visible on the 450 MHz recoding. This depth is apparently changes near the spandrel walls.

The material behind the level marked yellow is undoubtedly highly reflecting. It might be concluded from the changes in amplitude along this level that the material is fairly inhomogeneous.

The thickness of the brick layer can be better explored on the 1200 MHz recording. Here, the reflections caused by the spandrel walls are well seen.

Depth segments (anomaly maps)

Appendix 2 shows the anomaly maps in flat sheets of the barrel for the 30, 50, 70 and 100 cm depths, at both three frequencies. Based on experiences higher amplitudes (seen in reddish colours on the map) refer to cavity or other highly reflecting material, e.g. larger blocks of stone). They are numbered and marked by Roman numerals on each map. Lower amplitudes (bluish colour) generally refer to an increase in moisture level or to rocks and soil with smaller compactness (e.g. fill material). These larger spots are marked by capital **N** on the map. The smaller, local anomalies are not described one by one, they may refer to smaller joint gaps, voids, or the presence of harder, highly reflecting material divergent from its environment.

4. Survey with boroscopy

The objective of the survey was to help interpreting the results of the radar survey.

The following zones were recommended for exploitation: the critical points of the structure investigated by radar measurement, the positive anomalies occurring and correlating at different depths and/or different frequencies and the zones with smaller resistance (N) which are detectable on several anomaly maps.

The survey was carried out with a boroscopy camera that was inserted into boreholes drilled in assigned parts of the structure. Digital recordings were made during the operation that allowed a detailed study of the internal parts of the structure.

4.1 Documentation

The locations of the boreholes and the recorded boroscopy images are summarised in Appendix 5. The collection demonstrates the most representative images recorded at each borehole.

4.2 Findings of the survey

The boroscopy survey has provided localised information on the internal structure of the brickwork. The survey has lead to the following conclusions:

- The boroscopy survey has confirmed the presence of the boundary between the two arch rings. This boundary is a mortar layer which has varying compactness. Photos taken from Borehole 1 suggest a narrow gap between the two layers, while in Borehole 2 this gap if totally filled with mortar.

- According to the boroscopy images the arch has solid brickwork backing. The backing cannot be distinguished from the brickwork of the barrel, although some recordings show that this area is less filled with mortar.

- The area behind the backing is varying. Recordings from Borehole 2 suggest a dense clayey medium while a less compacted dry material on recording from Borehole 1 and 4.

- There were no large cavities found in the brickwork although the quality of mortar fill is varying.

5. Summary

Both the radar and boroscopy survey have confirmed the multiring nature of the barrel. This could be best seen on the radar recordings with the 900 MHz antennae.

The depth scale of the radargrams was calculated with an average wave velocity presumed for the masonry material. To achieve better accuracy in the detected dimensions, this scale has to be recalculated according to data gained by boroscopy measurements or coring.

High frequency areas on the radargrams and anomaly maps have been confirmed to be localised anomalies in the masonry structure. Areas with poor mortar infiltration or gaps seem be noticeable on the radar recordings. It has to be mentioned however that not all anomalies indicated on the radar images have been confirmed by the boroscopy survey. This might be attributed to the erroneous assignation of the location of the boreholes and its failure to find very localised anomalies.

Wet areas suspected by the radar anomaly maps have not been confirmed by the boroscopy survey.

Variations in the fill properties may cause different reflections that can be seen on the radar images. However it is clear that boroscopy confirmation is indispensable for the successful interpretation of the radar images.

Appendix 1: Radargram samples

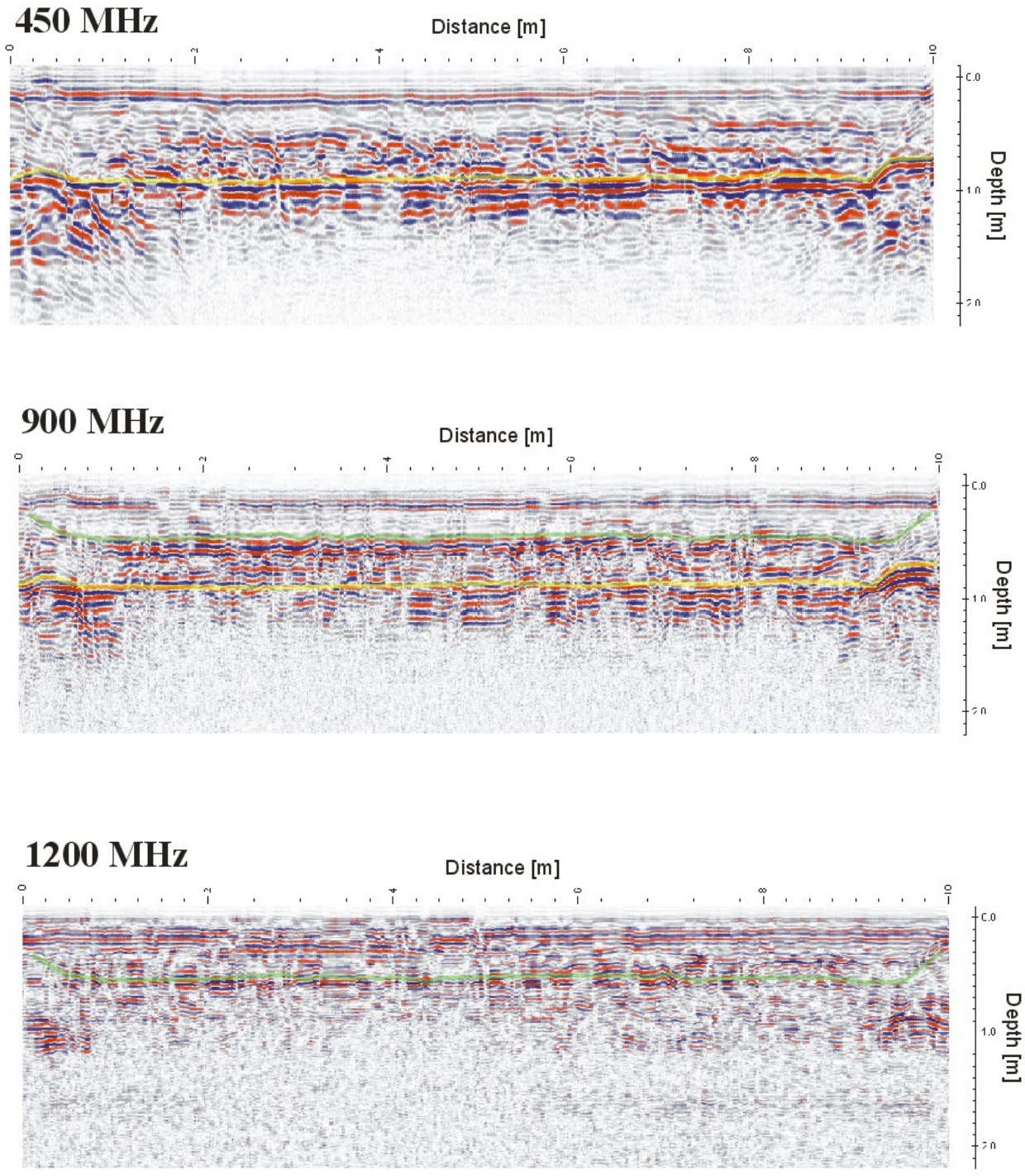

Radargrams taken with various frequency antennas along longitudinal line (C2) on the arch barrel.

Appendix 2: Depth segments (anomaly maps) of the radar survey

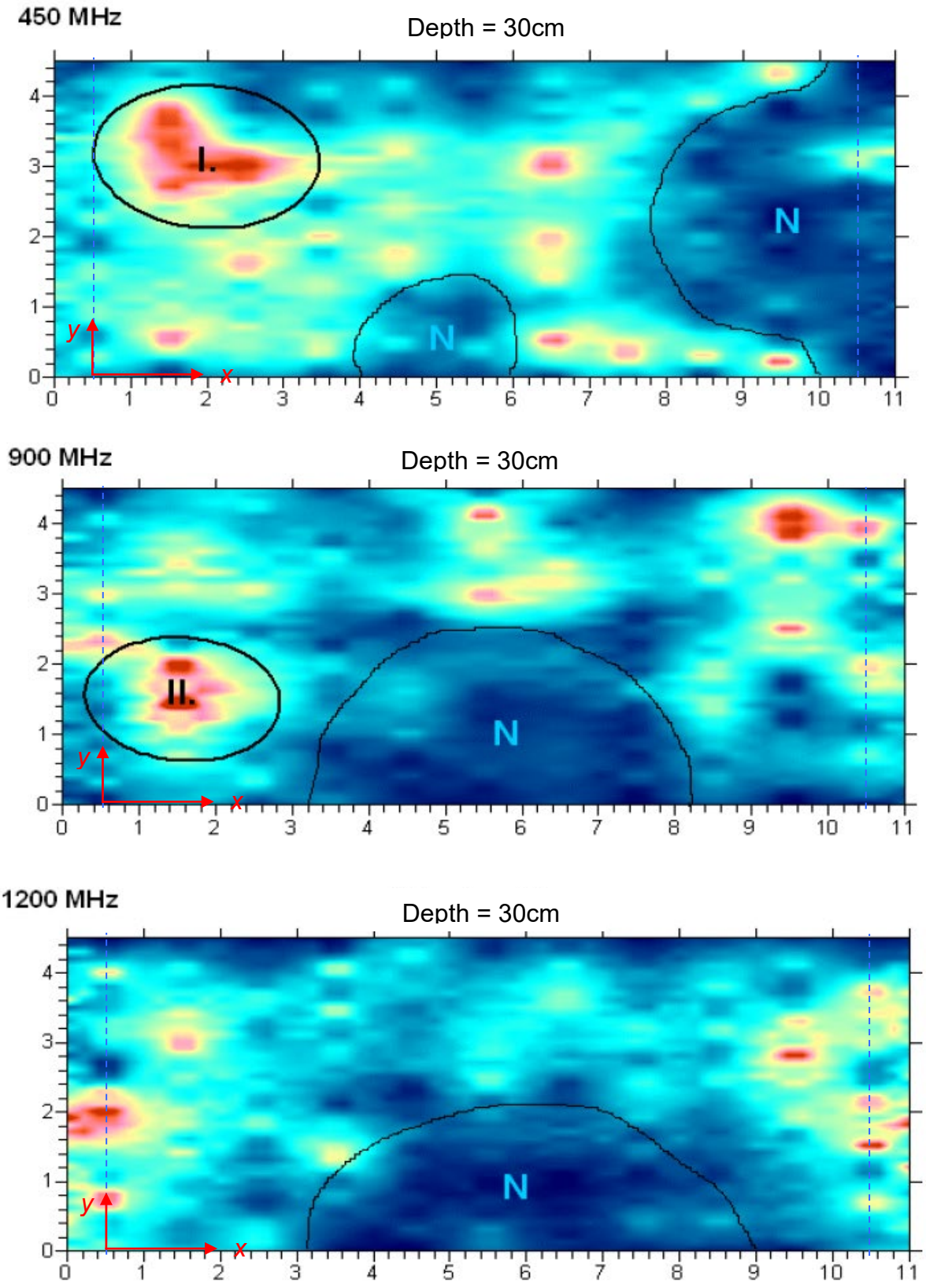

Anomaly maps of the arch barrel with various frequencies at 30cm depth segment, represented on flat sheets (horizontal: longitudinal profiles, vertical: transversal profiles)

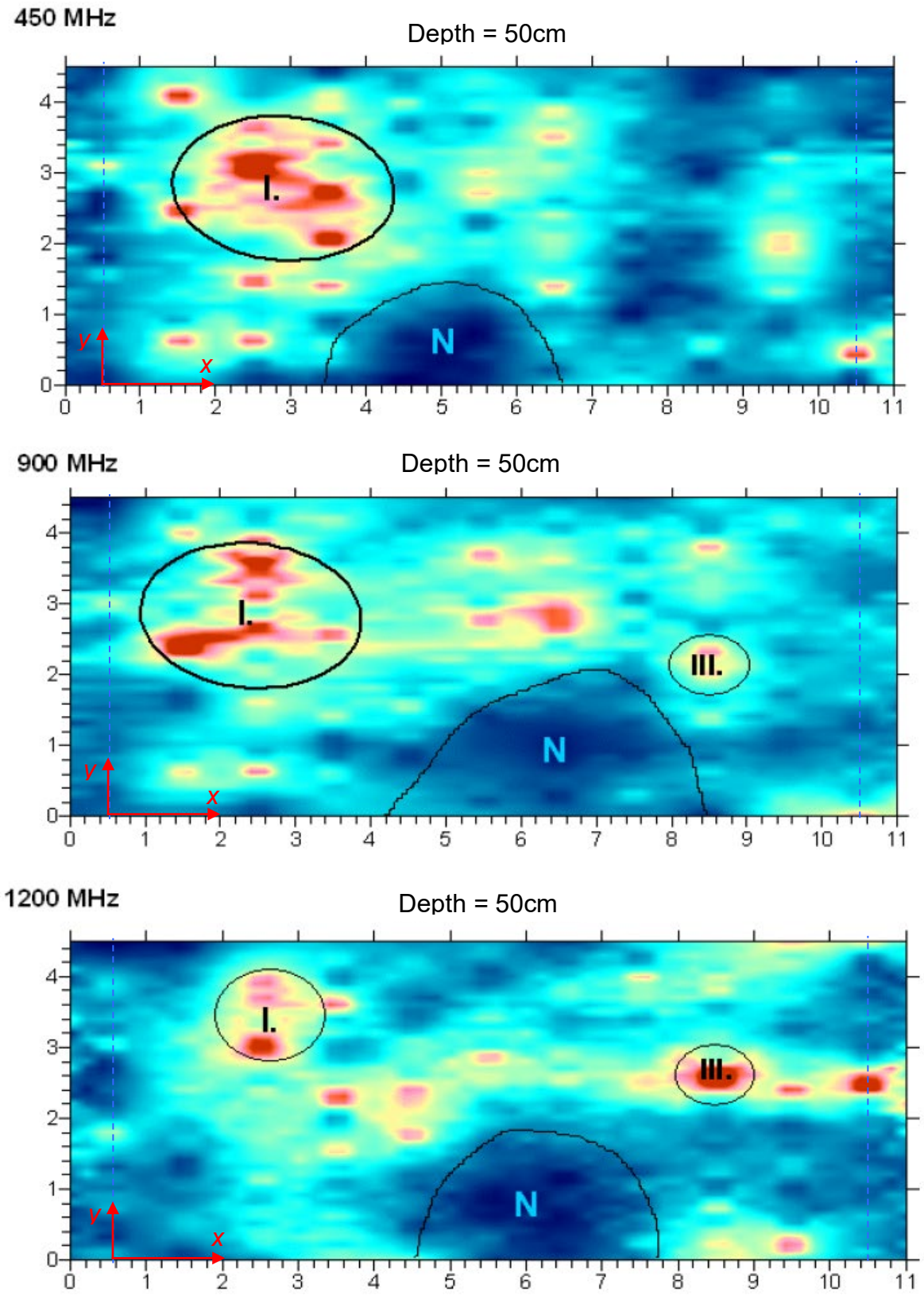

Anomaly maps of the arch barrel with various frequencies at 50cm depth segment, represented on flat sheets (horizontal: longitudinal profiles, vertical: transversal profiles)

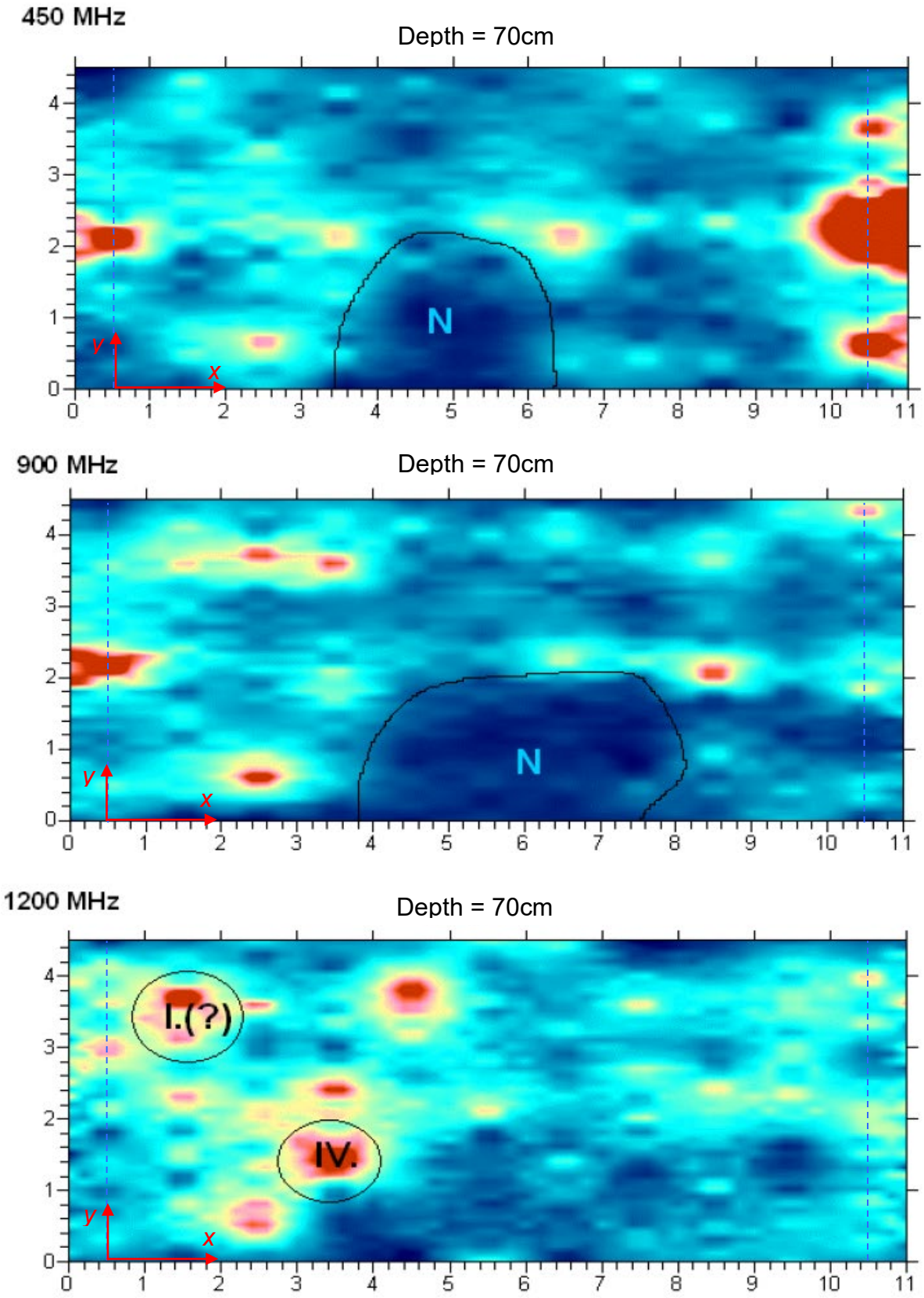

Anomaly maps of the arch barrel with various frequencies at 70cm depth segment, represented on flat sheets (horizontal: longitudinal profiles, vertical: transversal profiles)

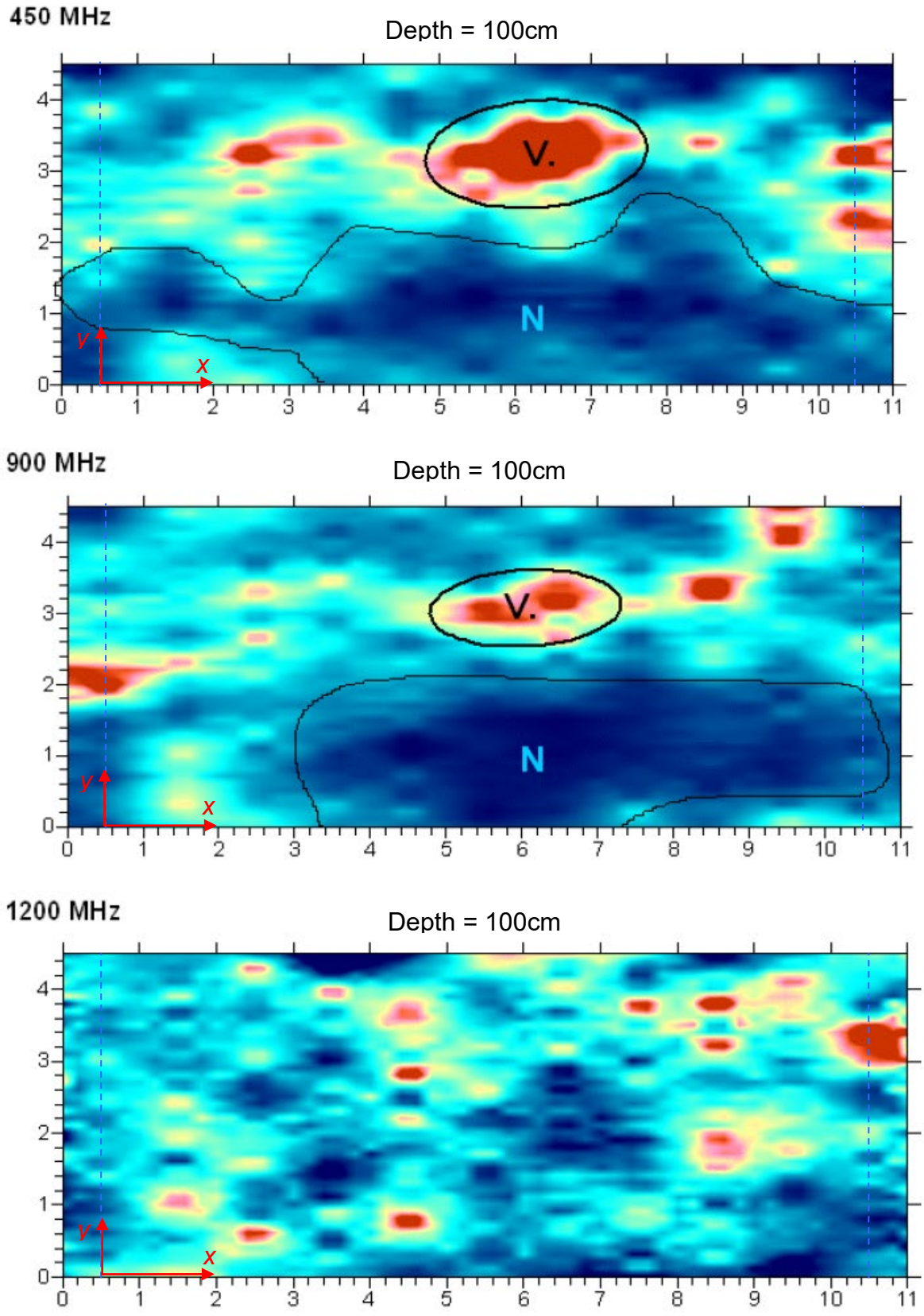

Anomaly maps of the arch barrel with various frequencies at 100cm depth segment, represented on flat sheets (horizontal: longitudinal profiles, vertical: transversal profiles)

Appendix 3: Boroscopy images

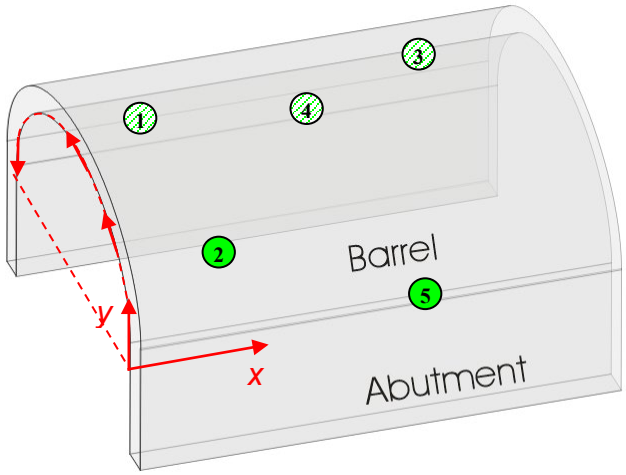

Borehole Number	Location of the borehole in longitudinal direction, *x* (m)	Location of the borehole on transversal profile, *y* (m)	Sign of suspected anomaly	Length of borehole (cm)	Diameter of borehole (mm)
1.	1,75	3,30	I.	75	50
2.	1,75	1,20	II.	88	50
3.	8,00	2,90	III.	57	50
4.	6,00	3,50	V.	110	50
5.	6,00	0,80	N	112	50

Borehole	Location
1.	Arch barrel quarter point /left/

Depth = 28cm	Depth = 55cm	Depth = 72cm

Borehole	Location
2.	Arch barrel quarter point /right/

		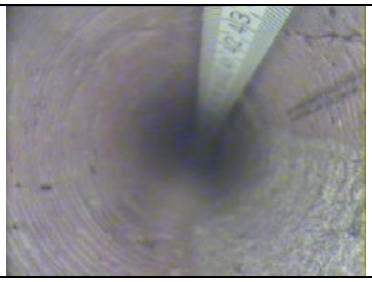
Depth = 10cm	Depth = 30cm	Depth = 44cm
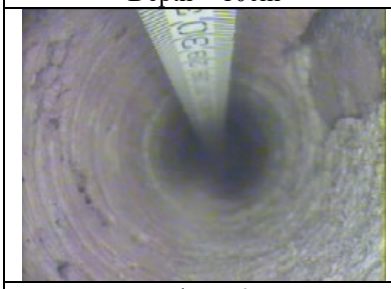	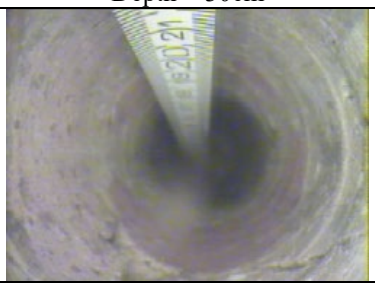	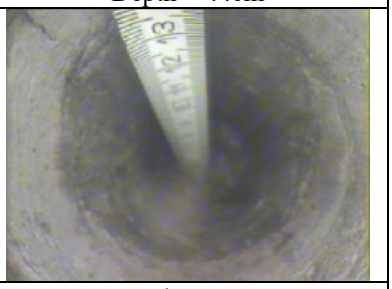
Depth = 56cm	Depth = 67cm	Depth = 75cm

Borehole	Location
3.	Arch barrel quarter point /left/

		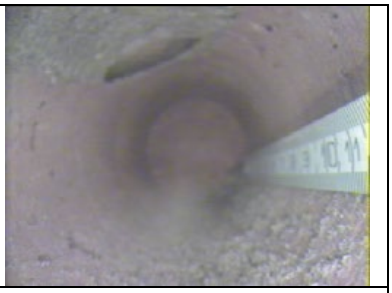
Depth = 25cm	Depth = 30cm	Depth = 45cm

Borehole	Location
4.	Abutment /left/

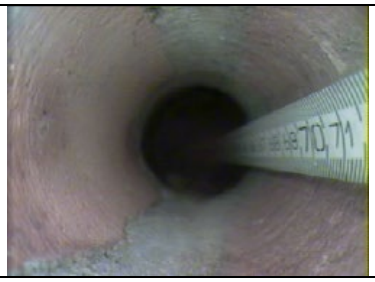

Depth = 40cm

Depth = 57cm

Depth = 62cm

Depth = 89cm

Depth = 100cm

Depth = 105cm

Borehole	Location
5.	Abutment /right/

Depth = 15cm

Depth = 37cm

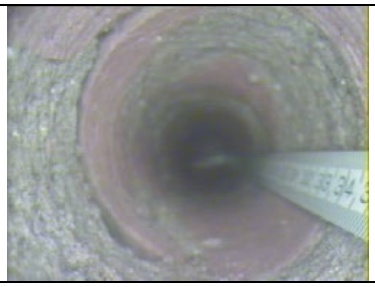

Depth = 77cm

Case Study 4

Testing masonry arch bridges with infrared thermographic remote sensing method

1. Background and objectives

The aim of the survey was to explore the application possibilities of infrared thermographic remote sensing method in non-destructive testing of railway masonry arch bridges. Four bridges were selected for the survey from the bridge stock of MÁV Hungarian Railways. The selection was considered representative for both the variety of typology, construction materials used and current condition of these bridges. The ultimate objective of the research was to determine how this testing method could be integrated into a more complex frame of analysis of masonry structures and to point out the currently conceivable directions of further research.

The significance of research is confirmed by the fact that during the periodical inspection of masonry arch bridges, especially those with difficult or costly access, more and more importance must be given to remote sensing methods besides destructive tests or other testing procedures carried out from a touching distance.

The main task of periodical damage identification procedures based on 'in situ' remote sensing methods is to gain technical information by means of striking concomitant signs of possible damages which justify the necessity of further detailed investigation of the given structural area or section.

2. Description of the survey

The site tests on the four selected masonry arch railway bridges were carried out in May 2005. The bridges have been selected for the tests from the same area, very close to each other, in order provide similar circumstances for the measurement at each bridge. To achieve better confidence in interpretation the tests have been repeated in October 2005.

This report outlines the general results and experiences of the survey and in Appendix 1 shows some of the characteristic thermal distribution images followed by short evaluating comments.

2.1 Instrumentation

The following instrumentation was used during the measurements:

- ThermaCAM® PM695 thermovision camera (see Image).
  The camera has a 0.08 ºC sensitivity within the recorded range of temperatures. The thermal distribution images were recorded using lenses of 24-40º with surface and lens distances of 2-30 meters. Images were recorded on memory cards, processing and analysis was made by ThermaCAM Reporter 2000 software. Each thermal image was

accompanied by a conventional digital photo that shows the visual representation of the surface.

- TESTO 400 thermometer and hygrometer.

- Wind speed recorder.

Thermovision camera used for the survey

2.2 First survey

A few days before the first survey significant amount of precipitation occurred on the site, and on the external surfaces of the structures, therefore the different constituent building materials of these surfaces, such as various stones, bricks, concrete, joint mortar, repair mortar and the surrounding soil were exposed to wetness to a different extent.

Before and during the survey the weather was only slightly windy. Therefore depending on the position and the quality of materials and the location of the bridges, it produced diverse drying effects on the surfaces. The weather conditions of the measurements are described in Appendix 1 for each bridge.

2.3 Repeated survey

The survey was preceded by a dry period without notable amount of rain. Before and during the survey the weather was a bit more windy than at the first test. There was a discontinuous sunshine occurred on the site before and during the measurement which may have had considerable effect on some of the results. The weather conditions of the repeated measurements are described in Appendix 1 for each bridge.

2.4 Evaluation

The surface temperatures are represented on the thermal images by colours where lighter colours refer to higher temperature while darker colours refer to colder temperature. The collection of thermal images recorded during the measurement is found in Appendix 1.

After a comprehensive evaluation of the thermal images the following observations could be made:

- Infrared thermography was able to identify some of the characteristics of the masonry structure and to differentiate between the basic construction materials such as stones, bricks and mortars. Locations of patch repairs where materials different from the existing ones were used could also be seen on some of the thermal images.

- Anomalies have been recognised at some of the thermal images such as wet regions, cracks, weathered stones or bricks and remarkable mortar loss in the joints. In may cases these anomalies, referring to damages, were not perceivable by the human eye from the same distance as the measurement was made.

- Areas were also clearly detected, where undesirable plants and roots were incorporated into the structure, which later on could cause damages due to frost or expansion.

- It could also be concluded that similar thermal distribution images were recorded at the examined bridges, which implies that the method could be systematised if a comprehensive research work is carried out. This kind of diagnostic may have the significant advantage that it can detect damaging factors by means of remote sensing and can determine the direction of their progress at an initial stage when they cannot be perceived by the human eye.

On the other hand:

- Interpretation of the temperature variations on the images is sometimes fraught with difficulties due to the boundary effects caused by direct solar radiation or air motion.

- The procedure was less effective in the repeated survey, when the measurement was not preceded by a rainy period. In addition to that, due to the larger air motion in that case, the structures was almost in a thermal equilibrium. It seems that the 0.08ºC sensitivity of the measurement was incapable to detect some of the anomalies that were clearly perceivable during the first survey.

- It has to mentioned that the weather condition during the measurements were not absolutely ideal for an infrared thermographic survey. It is therefore recommended to repeat the measurement under more ideal ambient circumstances.

2.5 Conclusions

Based on the results of the performed survey it can be concluded that infrared thermography can effectively be applied for some inspection purposes of masonry bridges. It should however be noted that this method cannot be used by itself, but together with other inspection methods that help interpreting the results and calibrating the measurements.

On the other hand it was found necessary to complete an expansive research programme in order to elaborate proper methodology and evaluation system.

3. Proposed directions of further research

In order to develop and systematize infrared thermographic remote sensing method for masonry arches the following main tasks should be clarified:

- Definition of the effect of boundary conditions, such as:

  - interfering radiation, solar radiation,
  - maximum allowable wind velocity,
  - ambient temperature,
  - temporal changes in ambient temperature during the survey,
  - effects of rain – beating rain,
  - moving object between the camera of the measuring device and the surface tested,
  - elimination of reflecting secondary radiation,
  - humidity of air.

- Determination of the optimal distance between the measuring device and the object under survey.

- Selection of the optimal viewing angle for the lens applicable with the measuring device.

- Clarification of interpretation questions, such as:

  Determination of the causes of thermal anomalies with the help of other inspection methods, such as:
  - radar survey,
  - sonic and ultrasonic methods,
  - boroscopy,
  - hardness and penetration tests,
  - site explorations,
  - determination of emissivity coefficient of the materials,
  - visual investigation of samples taken from the structure,
  - physical and chemical tests on samples to identify the type of materials and determine their physical properties,
  - destructive tests on samples to determine mechanical properties.

- Optimisation of test arrangement.

- Elaboration of conditions of time-basis surveys.

  All conditions should be determined under which the proper evaluation of the time-basis surveys can be performed.

- Recording the results of the surveys, content and formal requirements of reports.

- Technical conditions for the operation of the applied measuring device.

Appendix 1: Representation and interpretation of thermal images

Bridge 1:

Description of the bridge:

Span: 6m, length: 12m, barrel: sandstone, abutment: sandstone, shape: semi-circular.
Damages: waterproofing damage (only local and not serious)

Measurement conditions:

Time of measurement: 2005.05.24. $9^{10} – 9^{33}$
Air temperature: 18.2 – 18.9 °C
Relative humidity: 60%
Other: There was a light wind and no sunshine prior and during the measurement. There was a considerable amount of rainfall a few days before the measurement was made.

Image	Location
B1-01	Spandrel wall and arch barrel – northern side
Comments: No inhomogeneity was found on the stonework. Vegetation and moss on the surface can clearly be identified. Minor local anomalies can be observed on the thermal image at wet areas.	

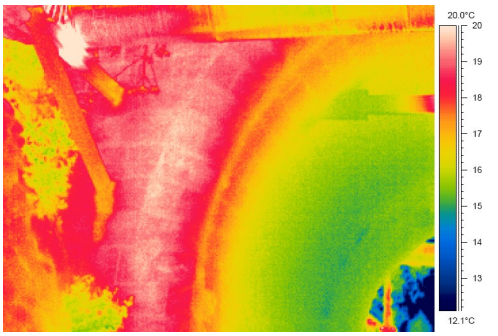

Image	Location
B1-02	Eastern abutment at ground level
Comments: No inhomogeneity was found on the stonework. Different construction materials can be identified (stone, mortar). A colder band is seen on the stone surface near the ground.	

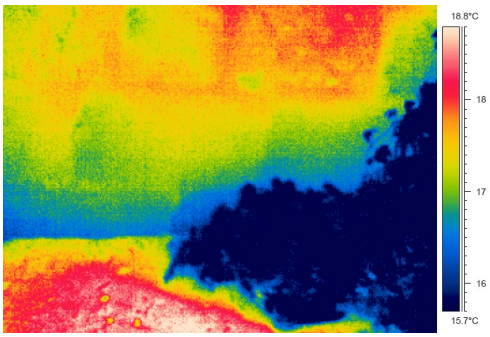

Image	Location
B1-03	Eastern abutment at midlle level
Comments: No inhomogeneity was found on the stonework. Different construction materials can be identified (stone, mortar). The right side of the surveyed area is warmer due to the side effect.	

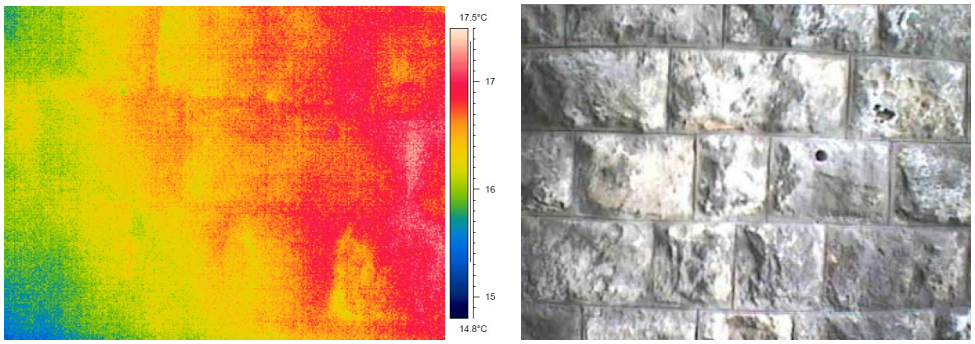

No inhomogeneity was found on other images.

Repeated measurement

Measurement conditions:

Time of measurement: 2005.10.17. $9^{45} – 10^{12}$
Air temperature: 10.4 – 11.2 °C
Relative humidity: 47%
Wind speed: 2,5-3.8 m/s (northern)
Other: There was a discontinous sunshine before and during the measurement. The southern side of the bridge was subjected to direct sunshine before the measurement. There was no rainfall in two weks time before the measurement was made.

Image	Location
B1-04	Bridge front view (northern side)
Comments: No inhomogeneity was found on the stonework. The structural parts (barrel and spandrel wall) and the different structural material cannot be distinguished. The hot parts on the thermal image are originated from the effect of the heat pipe and the direct solar radiation on the surface.	

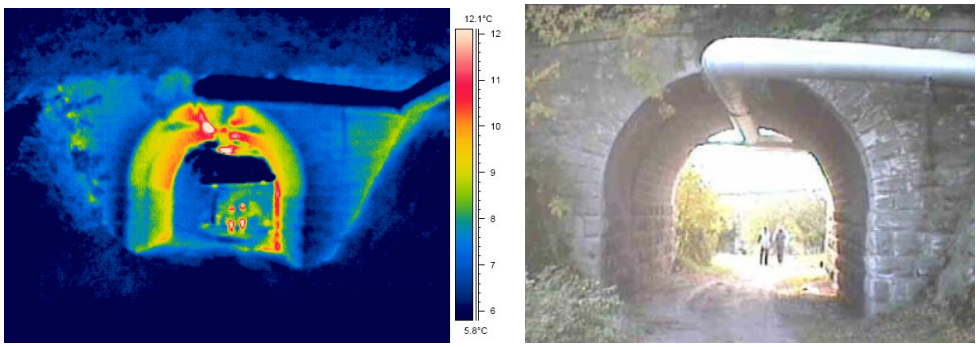

Image	Location
B1-05	Eastern abutment at ground level
Comments: No inhomogeneity was found on the stonework. Different construction materials can be identified (stone, mortar). Moss on the surface can be identified on the thermal image. A warmer band is seen on the stone surface near the ground. The surface is more or less in thermal equilibrium.	

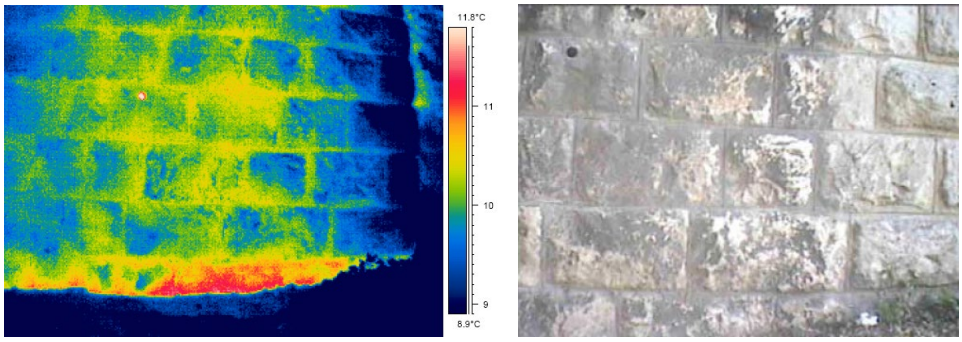

Image	Location
B1-06	Arch barrel (middle of the bridge)
Comments: No inhomogeneity was found on the stonework. Different construction materials can hardly be identified (stone, mortar). The hot spot in the middle of the image is a borehole. The surface is more or less in thermal equilibrium.	

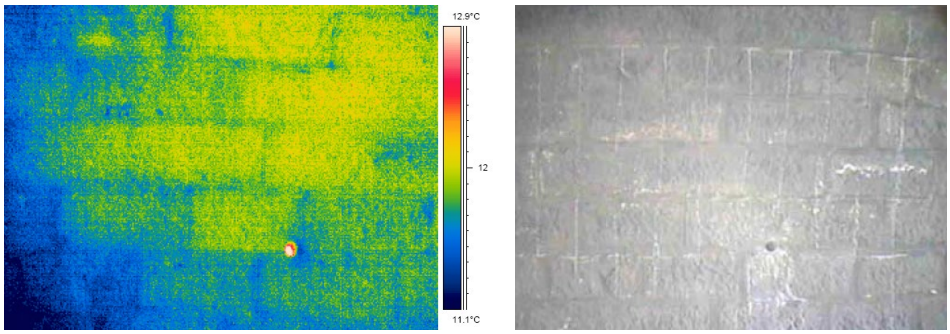

Image	Location
B1-07	Abutment and arch barrel –(eastern side, middle of the bridge)
Comments: No inhomogeneity is seen on the surface. Different construction materials can hardly be identified (stone, mortar). The surface is more or less in thermal equilibrium. Separation between the two bridge segments is clearly be seen on the thermal image.	

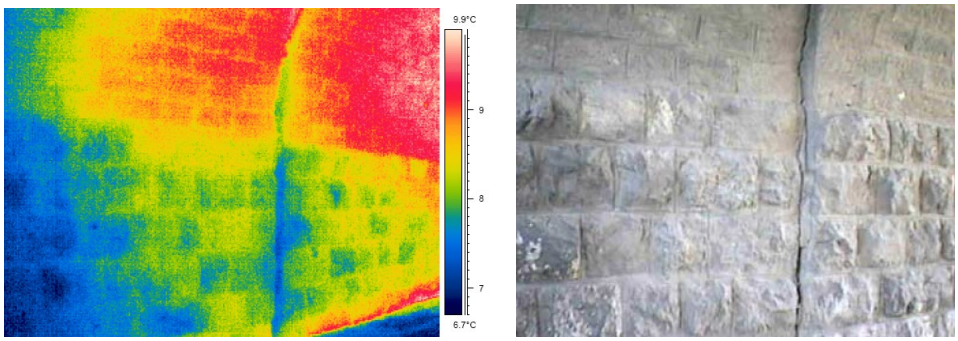

Bridge 2:

Description of the bridge:

Span: 3m, length: 10m, barrel: brick, abutment: rubble-stone, wing wall: rubble-stone, shape of arch: semi-circular.

Damages: waterproofing damage and water ingress (serious), weathered stones, delamination of mortar cover, loss of mortar, strong invasion of vegetation.

Measurement conditions:

Time of measurement: 2005.05.24. $9^{45} – 10^{15}$

Air temperature: 18.5 – 19.2 °C

Relative humidity: 55%

Other: There was only a very small air motion during the measurement. Some parts of the structure were subjected to solar radiation for a few minutes period before the measurement. There was a cosiderable amount of rainfall a few days before the measurement was made.

Image	Location
B2-01	Front view of the bridge (south-west)
Comments: The left side of the spandrel wall was subjected to sunshine for a few minutes prior to the measurement. This surface is therefore warmer than the other side with approximately 2°C. Presence of vegetation can be identified at both parts of the structure.	

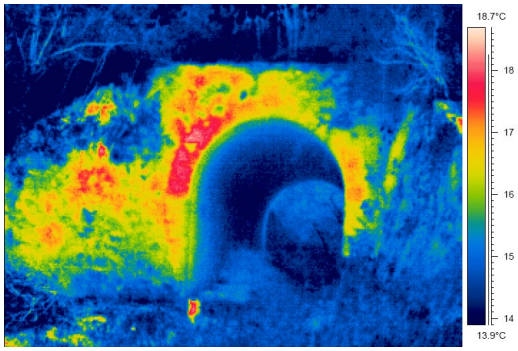

Image	Location
B2-02	Front view of the bridge (left side of the barrel near springing)
Comments: The barrel can be distinguished from the spandrel wall (i.e. brick surface from stone surface). Presence of vegetation is more striking on the thermal image than on the photo. Parts with loss of material (brick or mortar) can be identified on the thermal image.	

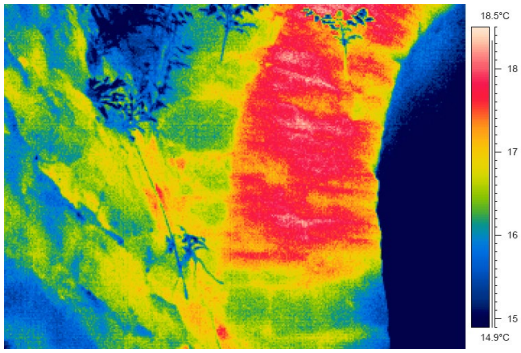

Image	Location
B2-03	Wing wall
Comments: Different type of stones can be identified on the thermal image by using the same emissivity coefficient (□). Temperatures of selected points (SP1, SP2, SP3) are given in Table (the temperature values were calculated with □=0.8). The temperature variation along horizontal and vertical segments can be followed on the given charts.	

	SP1	SP2	SP3
hőm. (°C)	15.3°C	13.4°C	14.6°C

Thermal distribution along vertical segment (L01)

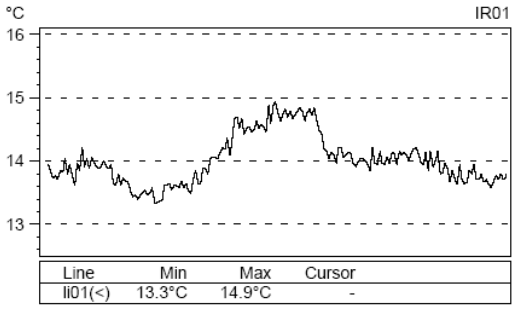

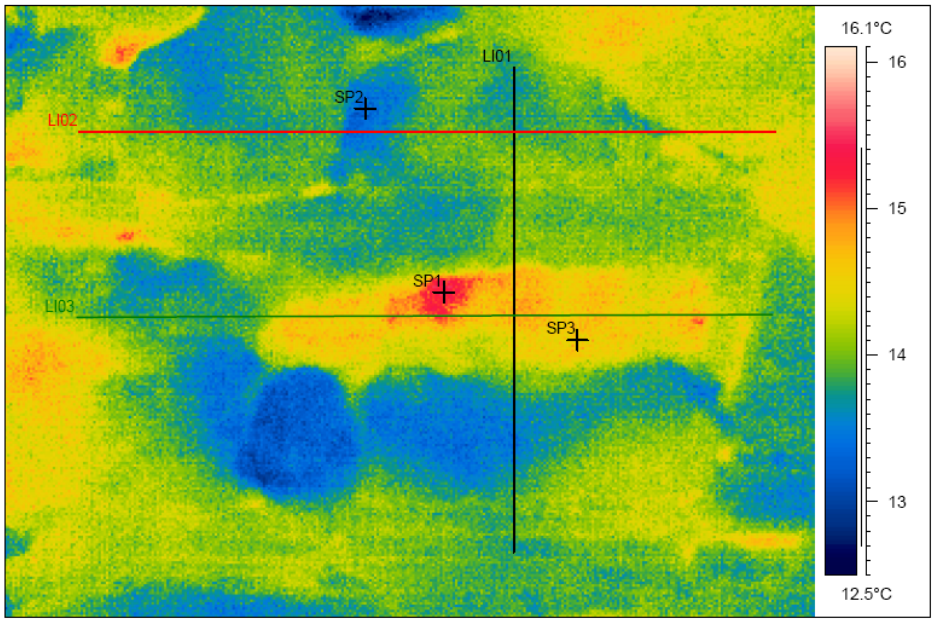

Thermal distribution along horizontal segments (L02, L02)

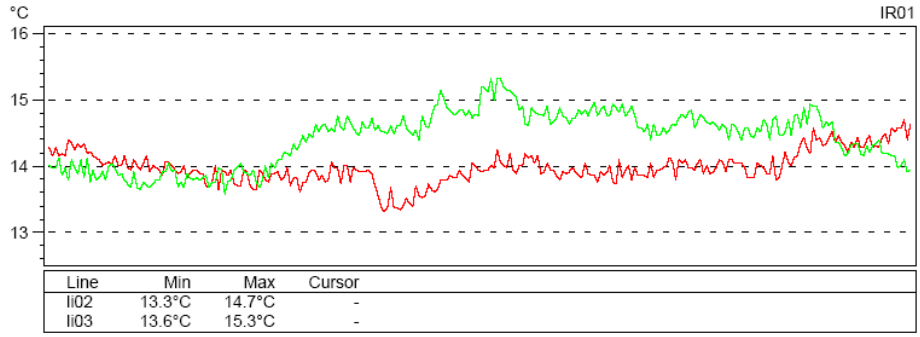

Image	Location
B2-04	Arch barrel (at the middle of the bridge)
Comments: Areas covered with cement mortar (as a result of an improper repair) can be distinguished from others. Delaminated mortar cover from the surface and weathered bricks can clearly be seen on the thermal image. Temperatures of selected points (SP1, SP2, SP3) are given in Table (the temperature values were calculated with □=0.8). The temperature variation along horizontal and vertical segments can be followed on the given charts.	

	SP1	SP2	SP3
hőm. (°C)	15.0°C	14.5°C	14.9°C

Thermal distribution along vertical segment (L01)

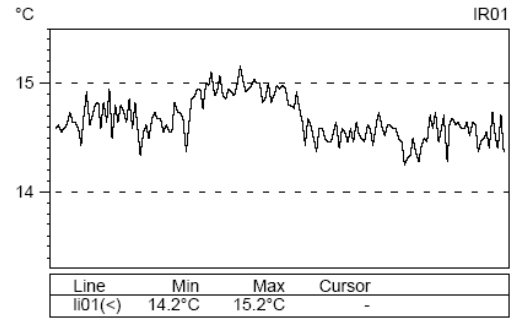

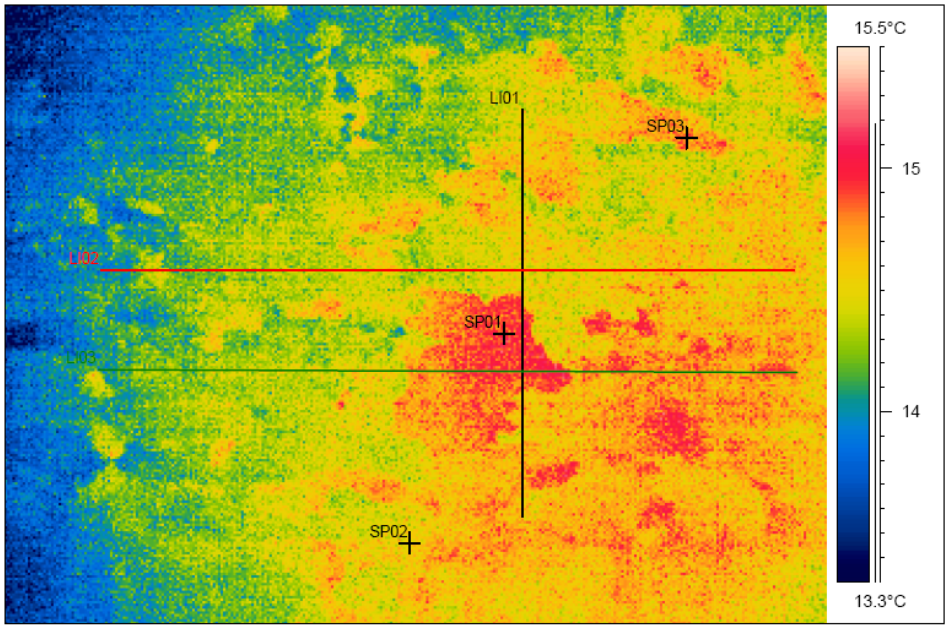

Thermal distribution along horizontal segments (L02, L02)

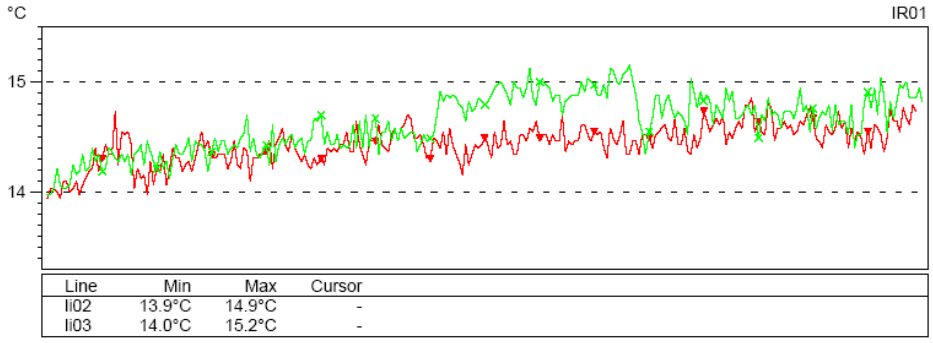

Image	Location
B2-05	Arch barrel (at the middle of the bridge)
Comments: Extensive temperature variations can be observed both on the thermal image and the segments. These refer to largely weathered brick surface and loss of material. Temperatures of selected points (SP1, SP2, SP3) are given in Table (the temperature values were calculated with □=0.8). The temperature variation along horizontal and vertical segments can be followed on the given charts.	

	SP1	SP2	SP3
hőm. (°C)	14.4°C	14.7°C	14.1°C

Thermal distribution along vertical segment (L01)

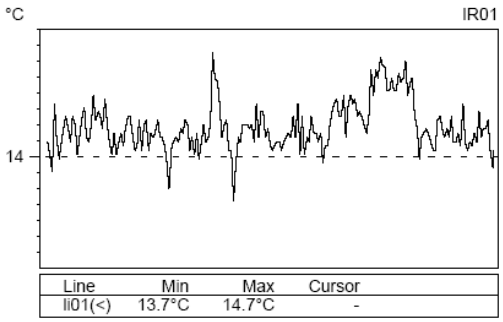

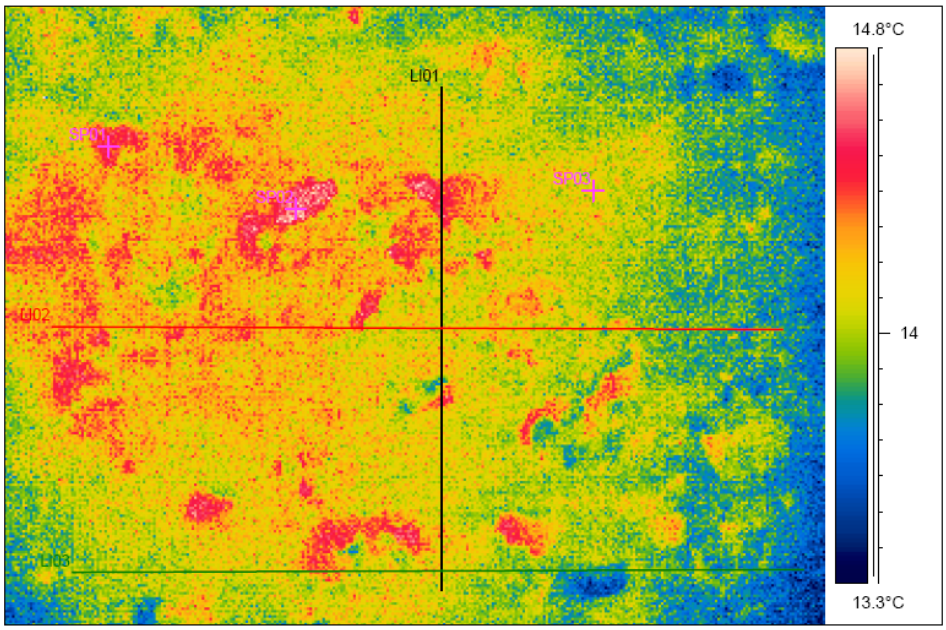

Thermal distribution along horizontal segments (L02, L03)

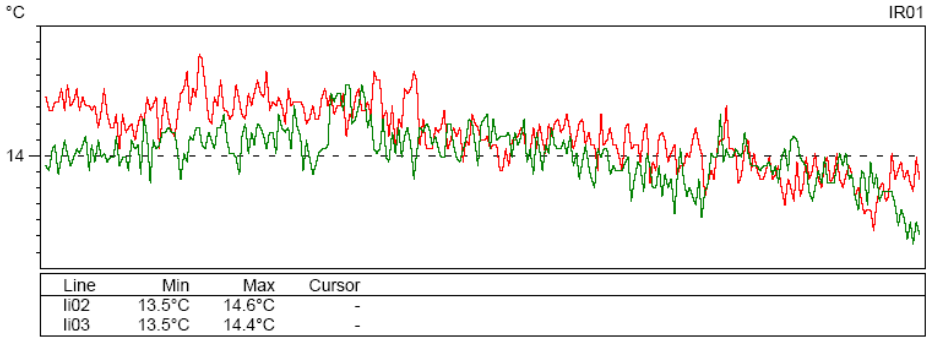

Repeated measurement

Measurement conditions:

Time of measurement: 2005.10.17. $10^{50} – 11^{20}$
Air temperature: 11.5 – 12.1 °C
Relative humidity: 35%
Wind speed: 0,9 m/s
Other: There was a discontinuous sunshine before and during the measurement. There was no rainfall in two weeks time before the measurement was made.

Image	Location
B2-06	Front view of the bridge (south-west)
Comments: The left wing wall was subjected to direct sunshine prior to the measurement. This surface is therefore warmer than other parts. The spandrel wall and the arch barrel was virtually in thermal equilibrium, the range of surface temperature differences is very narrow. Even the basic construction materials can hardly be distinguished. The presence of vegetation can easily be identified.	

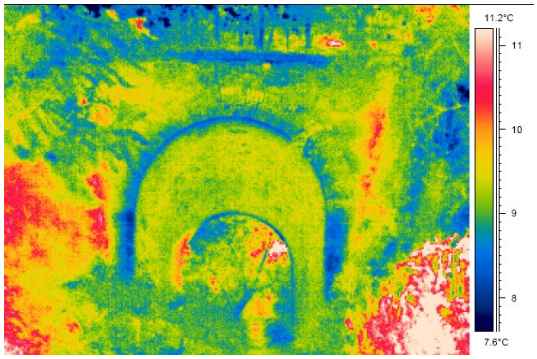

Image	Location
B2-07	Front view of the bridge (left side of the barrel near springing)
Comments: The exposed surface of the spandrel wall and the wing wall was subjected to direct sunshine before the measurement (hot region). The barrel cannot even be distinguished from the spandrel wall on the thermal image. Vegetation can clearly be seen. Other anomalies and damages on the brickwork surface cannot be identified on the thermal image, although they are noticeable on the photo.	

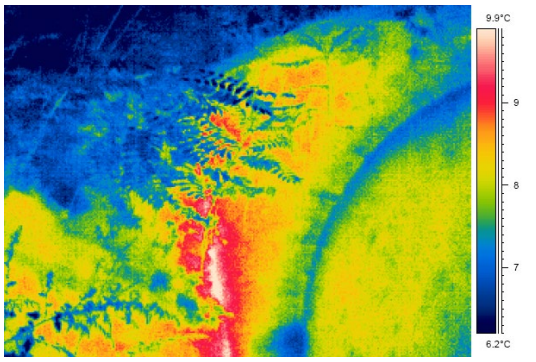

Image	Location
B2-08	Wing wall

Comments: The surface was subjected to direct sunshine before the measurement. Different type of stones can be identified on the thermal image, even with a small range of temperature variations, by using the same emissivity coefficient (□). Temperatures of selected points (SP1, SP2, SP3) are given in Table (the temperature values were calculated with □=0.9). The temperature variation along horizontal and vertical segments can be followed on the provided charts. Vegetation can clearly be seen on the thermal image.

	SP1	SP2	SP3
hőm. (°C)	9.3°C	10.3°C	10.2°C

Thermal distribution along vertical segments (L01)

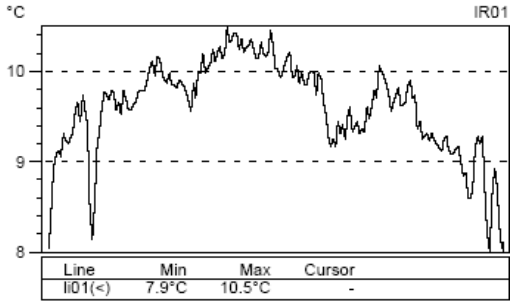

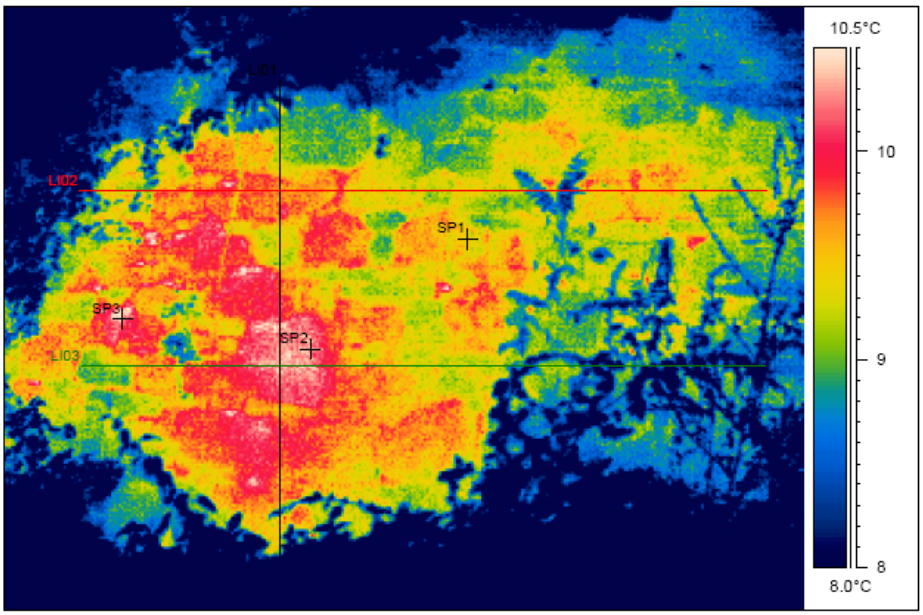

Thermal distribution along horizontal segments (L02, L03)

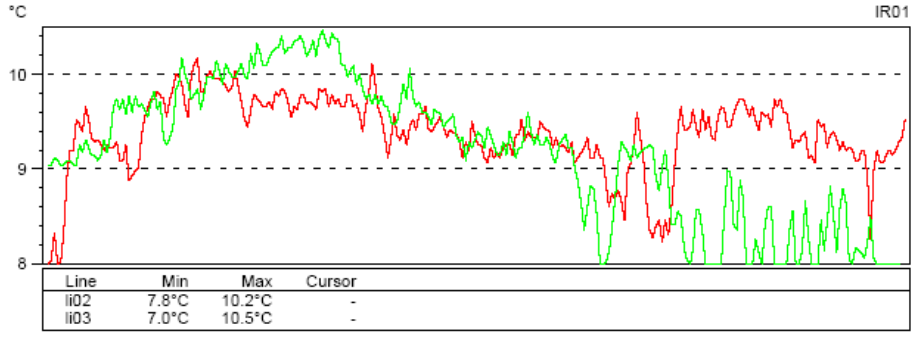

Image	Location
B2-09	Arch barrel (middle of the bridge)

Comments: The same are was surveyed as at Image B2-05. This area has weathered brick surface and suffers loss of brick material.
Temperatures of selected points (SP1, SP2, SP3) are given in Table. The temperature variation along horizontal and vertical segments can be followed on the provided charts. The thermal image suggests the variation in quality of the masonry surface but the range of temperature changes is much less that that of the previous measurement (see Image B2-05 and the corresponding thermal distribution charts). The thermal distribution of the surface is rather uniform as such the detection of surface anomalies is less effective.

	SP1	SP2	SP3
hőm. (°C)	10.0°C	9.8°C	9.4°C

Thermal distribution along vertical segments (L01)

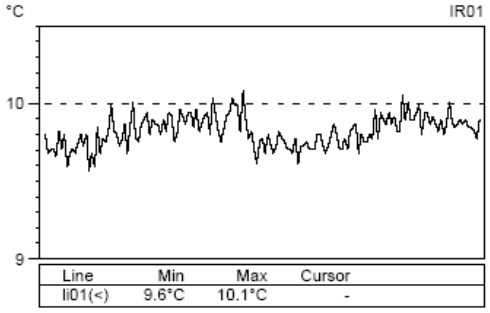

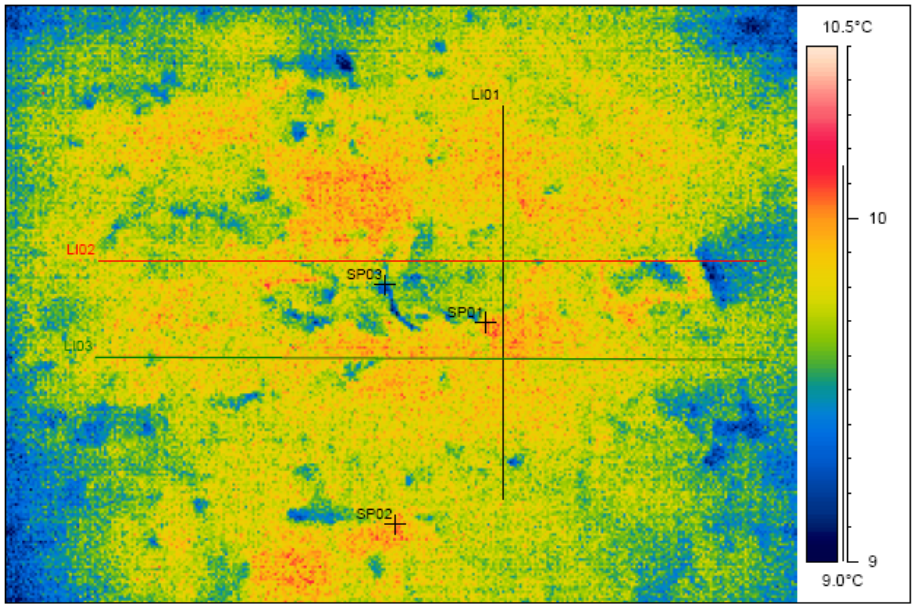

Thermal distribution along horizontal segments (L02, L03)

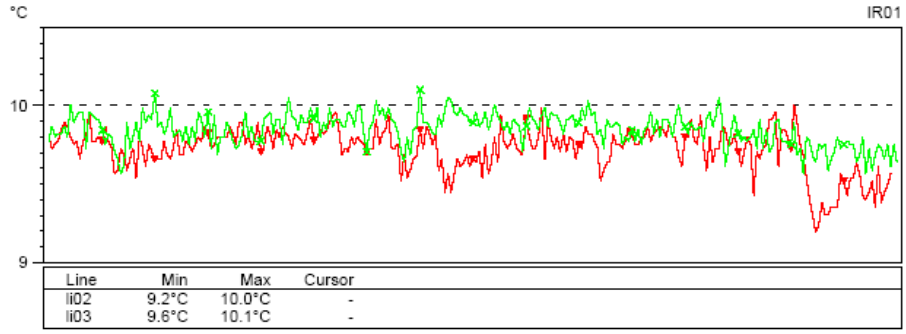

Image	Location
B2-10	Front view of the bridge (north-east)

Comments: The right part of the spandrel wall was subjected to diffused sunshine prior to the measurement. This surface is therefore warmer than other parts. Areas affected by the invasion of vegetation can be identified.

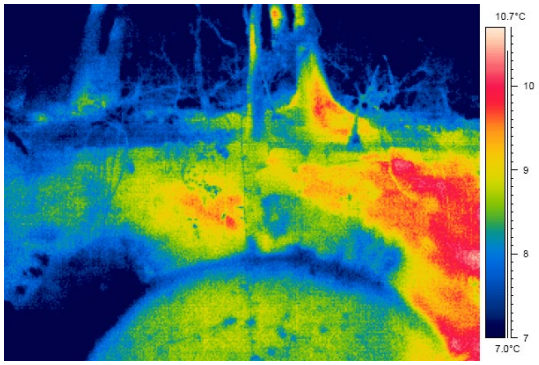

Bridge 3:

Description of the bridge:

Span: 5,70m, length: 20m, barrel: brick, abutment and spandrel walls: quarry stone, wing wall: rubble-stone, shape of arch: semi-circular.

Damages: waterproofing damage and water ingress (not serious), weathered brickwork surface, delamination of mortar cover, cracks at the barrel.

Measurement conditions:

Time of measurement: 2005.05.24. 10^{28} – 10^{55}

Air temperature: 18.5 – 19.5 °C

Relative humidity: 50%

Other: There was only a very small air motion during the measurement. Some parts of the structure were subjected to solar radiation for a few minutes period before the measurement. There was a cosiderable amount of rainfall a few days before the measurement was made.

Image	Location
B3-01	Bridge front view (western side)
Comments: The front side of the bridge was subjected to sunshine for a few minutes prior to the measurement. The upper side of this surface is warmer than the lower parts because it received more solar radiation. The barrel (brick material) can be distinguished from the spandrel wall (quarry stone) on the thermal image. Spots with lower temperatures on the thermal image of the barrel refer to locations of patch repairs.	

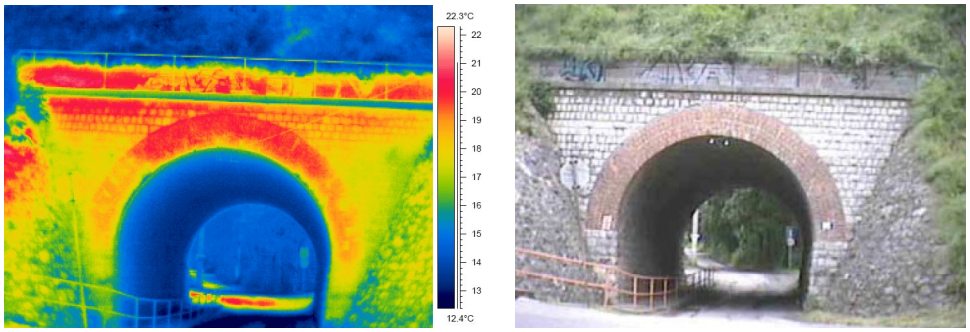

Image	Location
B3-02	Bridge front view (eastern side)
Comments: The front side of the bridge was not subjected to sunshine before and during the measurement but difference between the temperatures at the upper side and lower side can be observed. The barrel (brick material) can be distinguished from the spandrel wall (quarry stone) on the thermal image. Spots with lower temperatures on the thermal image of the barrel refer to locations of patch repairs. The area with lower temperature (deep blue spots) on the barrel and the abutment refers to the presence of wetness around a crack. This anomaly can be observed even at a distance of 15m.	

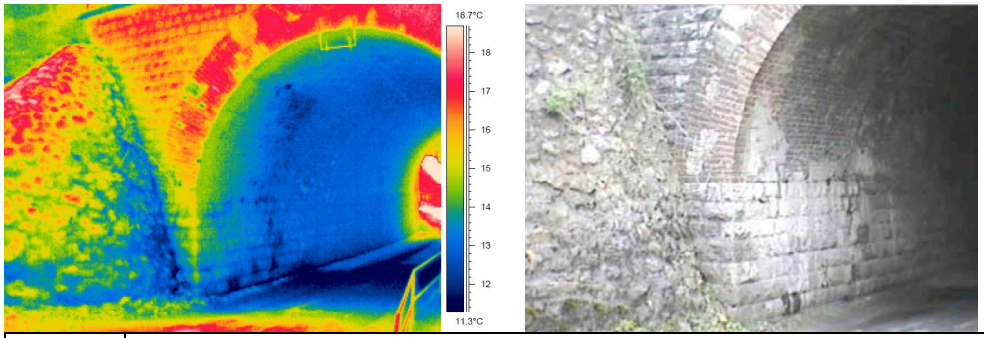

Image	Location
B3-03	Abutment (3m from the eastern end)

Comments: The cold parts on the thermal image refer to a vertical crack on the abutment stonework. More moisture is found near the crack therefore the surface here is colder than elsewhere. The moisture distribution around the crack cannot be seen by pure visual observation. The blue strip above the ground level may also refer to stones with a higher moisture content. Mortar joints can also be distinguished from stones especially in the wet area as the moisture content of mortar differ from that of the stone material. The extent of the moisturised zone can be more accurately determined on the charts showing the thermal distribution along horizontal and vertical segments.

	SP1	SP2	SP3
hőm. (°C)	11.9°C	13.0°C	11.6°C

Thermal distribution along vertical segments (L04, L05, L06)

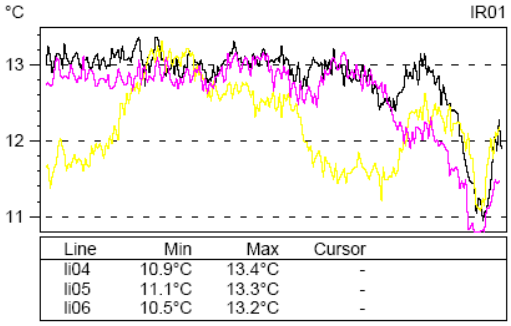

Line	Min	Max	Cursor
li04	10.9°C	13.4°C	-
li05	11.1°C	13.3°C	-
li06	10.5°C	13.2°C	-

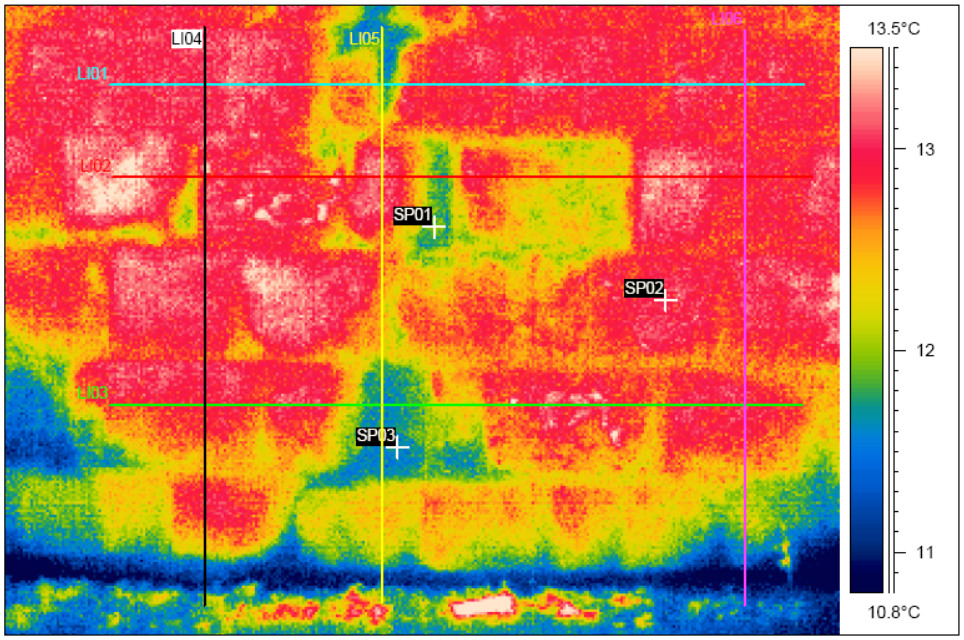

Thermal distribution along horizontal segments (L01, L02, L03)

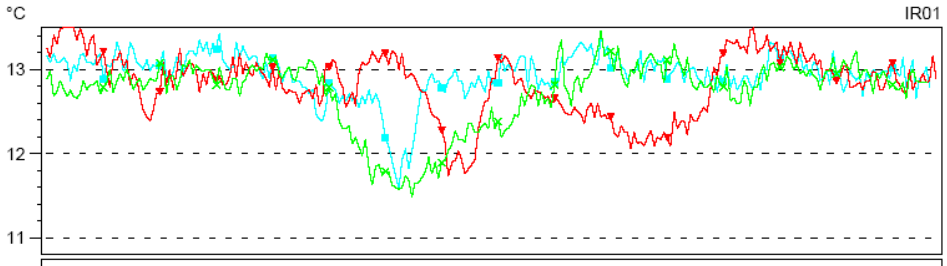

Line	Min	Max	Cursor
li01	11.6°C	13.4°C	-
li02	11.7°C	13.7°C	-
li03	11.5°C	13.5°C	-

Image	Location
B3-04	Arch barrel (middle of the bridge)

Comments: The middle part of the analysed area is covered by moss. It is assumed that this area is more wet than its surrounding resulting in lower surface temperature. Temperatures of selected points (SP1, SP2, SP3) are given in Table. The temperature variation along horizontal and vertical segments can be followed on the given charts.

	SP1	SP2	SP3
hőm. (°C)	13.5°C	14.2°C	12.6°C

Thermal distribution along vertical segments (L04, L05, L06)

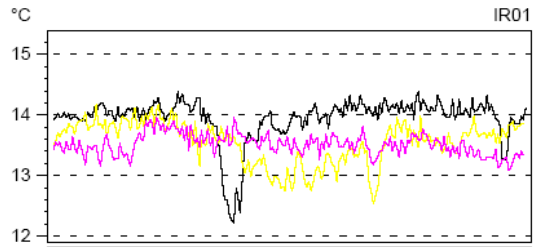

Line	Min	Max	Cursor
li04	12.2°C	14.4°C	-
li05	12.5°C	14.2°C	-
li06	13.1°C	14.0°C	-

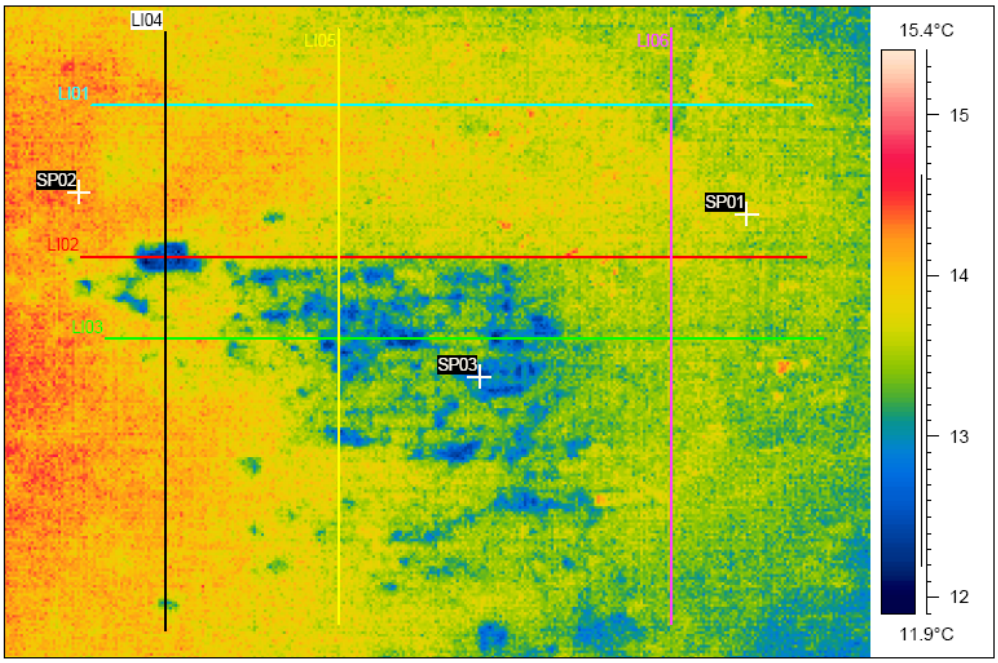

Thermal distribution along horizontal segments (L01, L02, L03)

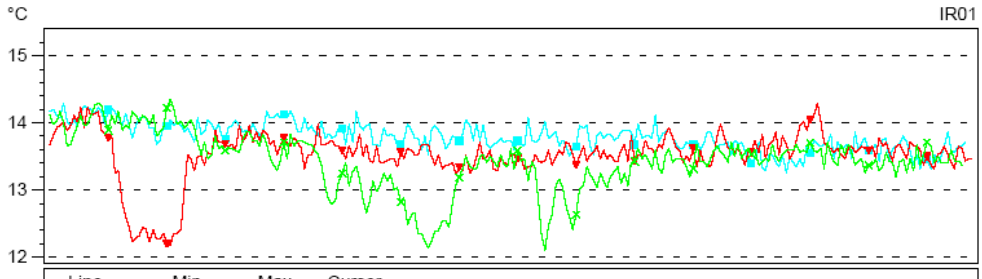

Line	Min	Max	Cursor
li01	13.3°C	14.3°C	-
li02	12.2°C	14.3°C	-
li03	12.1°C	14.4°C	-

Repeated measurement

Measurement conditions:

Time of measurement: 2005.10.17. $11^{30} – 12^{05}$
Air temperature: 11.9 – 12.5 °C
Relative humidity: 41%
Wind speed: 0,7-1.5 m/s
Other: There was a discontinous sunshine before and during the measurement. There was no rainfall in two weks time before the measurement was made.

Image	**Location**
B3-05	Bridge front view (western side)
Comments: The left wing wall was subjected to diffused sunshine prior to the measurement therefore this area is much warmer than the other parts. The various structural parts and materials can hardly be distinguished from each other. The large surface temperature difference between the left wing wall and the other parts prevents observing less striking anomalies.	

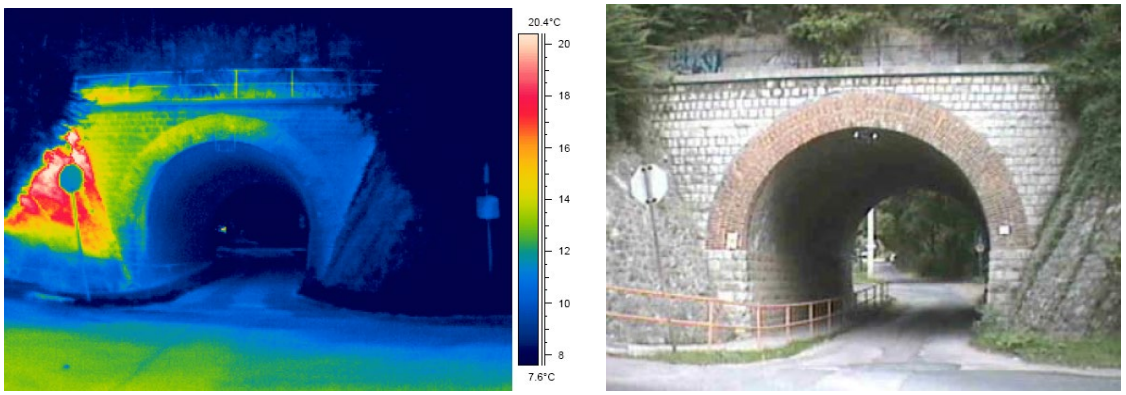

Image	**Location**
B3-06	Bridge front view and arch barrel (eastern side)
Comments: The front side of the bridge and the arch surface were almost in thermal equilibrium during the measurement. No anomaly can be observed on the thermal image. The wet area around a longitudinal crack, that was well seen on Image B3-02 (recorded at the previous measurement), is still noticeable, although the measurement was preceded by a long dry period.	

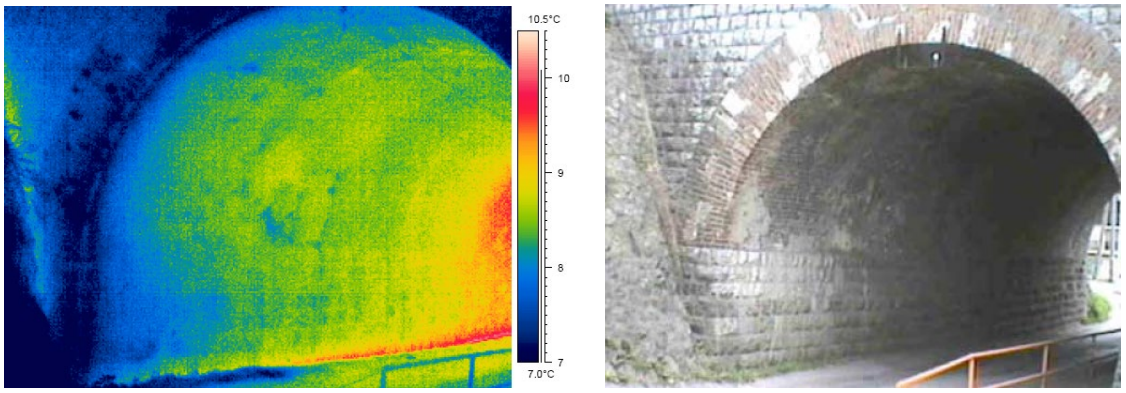

Image	**Location**
B3-07	Abutment and arch barrel (3m from the eastern end)

Comments: The image shows a closer view from the longitudinal crack. Now the thermal distribution of the surface is rather uniform (the temperature variation along the segments is in the range of only 0.3 °C) as such the identification of the crack is rather difficult.

	SP1	SP2	SP3
hőm. (°C)	9.0°C	9.5°C	9.0°C

Thermal distribution along vertical segments (L04, L05, L06)

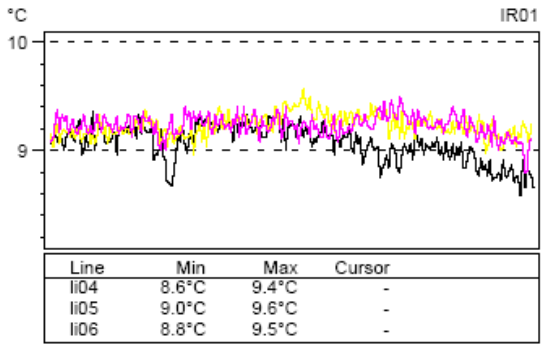

Line	Min	Max	Cursor
li04	8.6°C	9.4°C	-
li05	9.0°C	9.6°C	-
li06	8.8°C	9.5°C	-

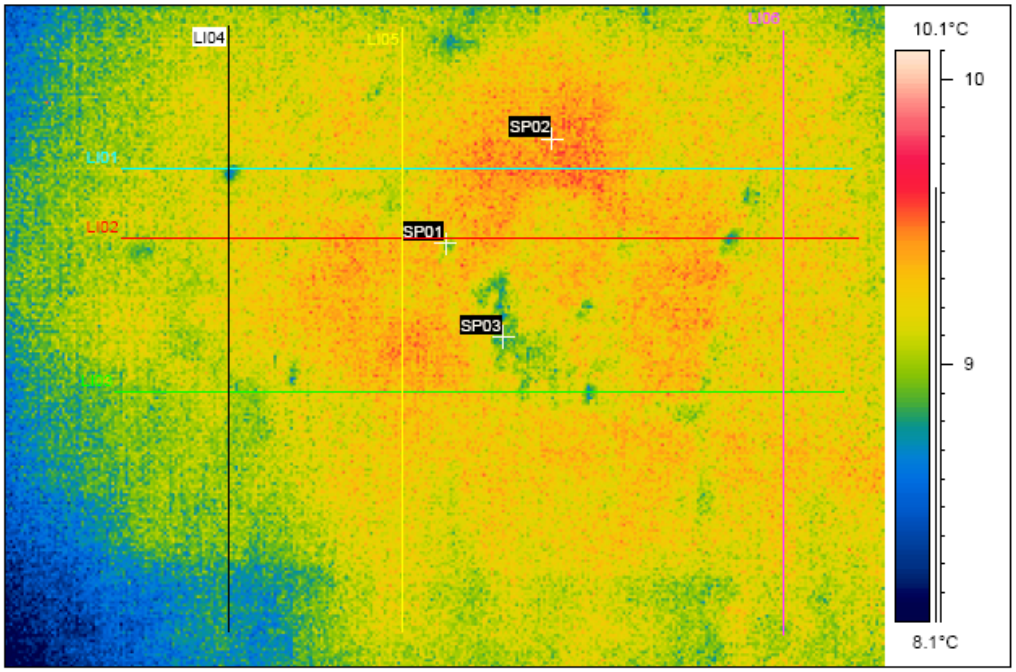

Thermal distribution along horizontal segments (L01, L02, L03)

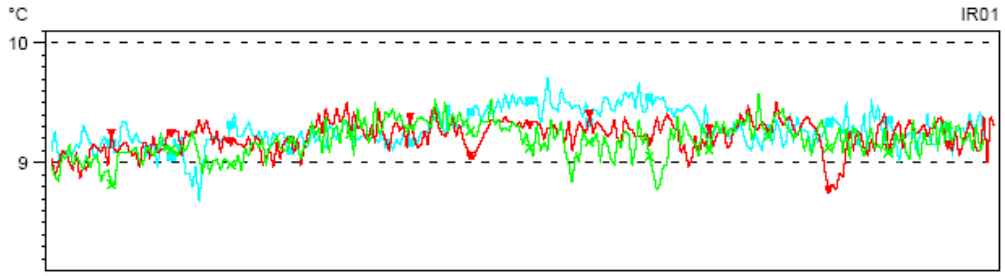

Line	Min	Max	Cursor
li01	8.7°C	9.7°C	-
li02	8.8°C	9.5°C	-
li03	8.8°C	9.6°C	-

Image	Location
B3-08	Arch barrel (middle of the bridge)

Comments: The image shows a closer view from another longitudinal crack in the middle of the bridge. The thermal distribution of the surface is uniform (the temperature variation along the segments is in the range of only 0.3 °C) as such the identification of the crack is rather difficult even on the segments.

	SP1	SP2	SP3
hőm. (°C)	9.5°C	9.5°C	8.8°C

Thermal distribution along vertical segments (L04, L05, L06)

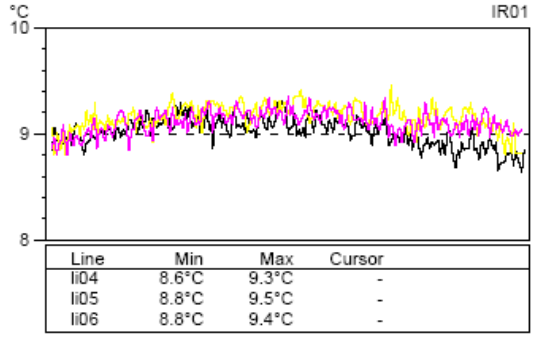

Line	Min	Max	Cursor
li04	8.6°C	9.3°C	-
li05	8.8°C	9.5°C	-
li06	8.8°C	9.4°C	-

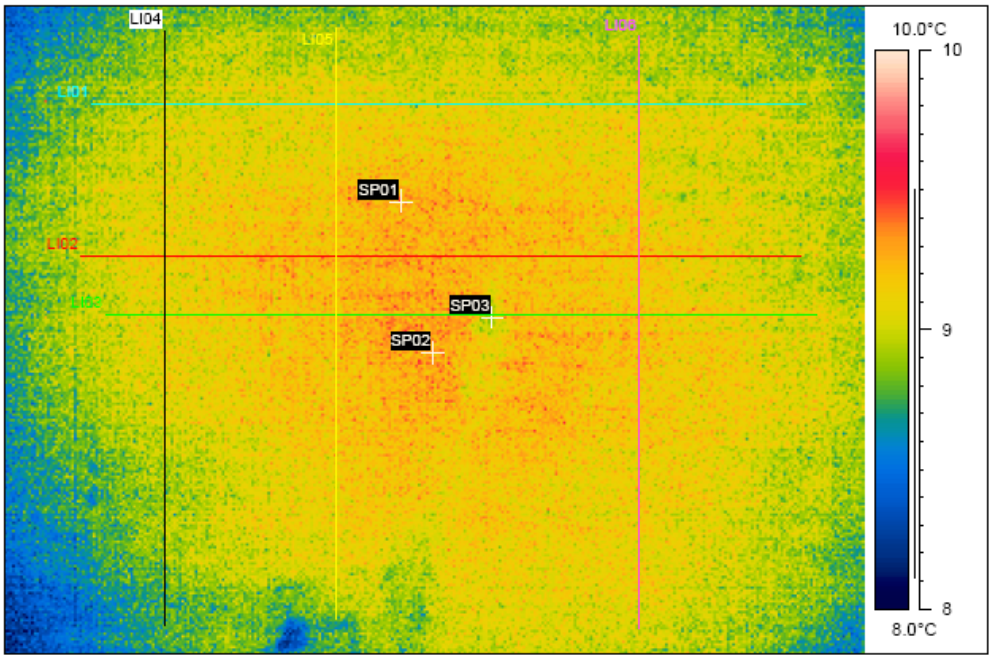

Thermal distribution along horizontal segments (L01, L02, L03)

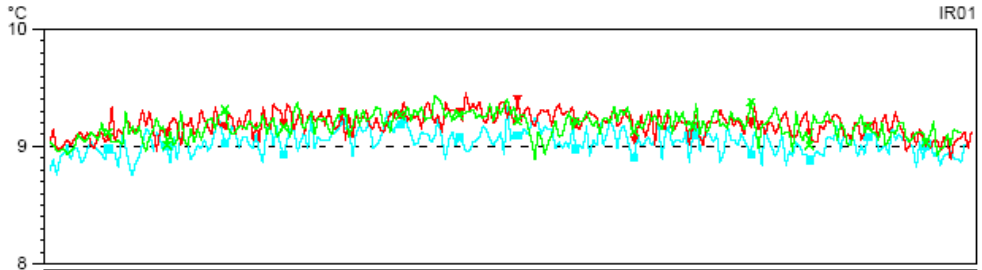

Line	Min	Max	Cursor
li01	8.7°C	9.3°C	-
li02	8.9°C	9.5°C	-
li03	8.9°C	9.4°C	-

Bridge 4:

Description of the bridge:

Span: 6,50m, length: 15m, barrel: brick, abutment and spandrel walls: quarry stone, wing wall: rubble-stone, shape of arch: segmental

Damages: waterproofing damage and water ingress (serious), weathered brickwork surface, delamination of mortar cover, loss of mortar and bricks, cracks at the barrel.

Measurement conditions:

Time of measurement: 2005.05.24. $11^{12} – 11^{26}$

Air temperature: 21.5 – 22.5 °C

Relative humidity: 45%

Other: There was only a very small air motion during the measurement. Some parts of the structure were subjected to solar radiation for a few minutes period before the measurement. There was a cosiderable amount of rainfall a few days before the measurement was made.

Image	Location
B4-01	Bridge front view (south-western side)
Comments: The front side of the bridge was not subjected to direct sunshine before and during the measurement but difference between the temperatures at the upper side and lower side can be observed. The barrel (brick material) can be distinguished from the spandrel wall (quarry stone) on the thermal image. Spots with lower temperatures on the thermal image of the barrel refer to locations of brick losses or delaminating material. Colder parts below the edge beam are due to presence of vegetation.	

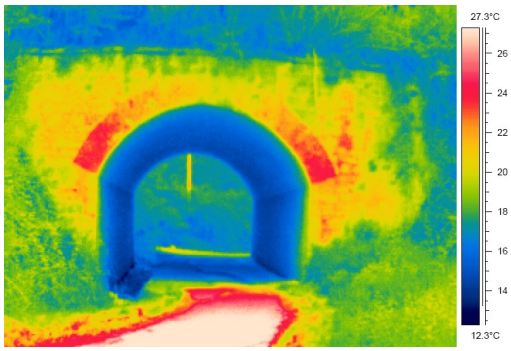

Image	Location
B4-02	Arch barrel (eastern side, at the extension of the bridge)
Comments: Longitudinal crack at the barrel can be identified at the thermal image.	

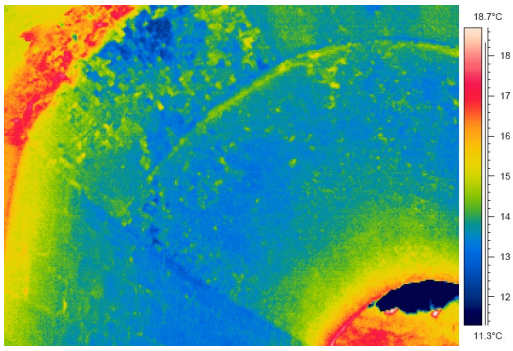

Image	Location

B4-03	Arch barrel (middle of the bridge)
Comments: Longitudinal crack at the barrel can be seen at the thermal image. Areas where delamination has started can be identified. Loss of bricks and weathered surface can also be seen on the thermal image.	

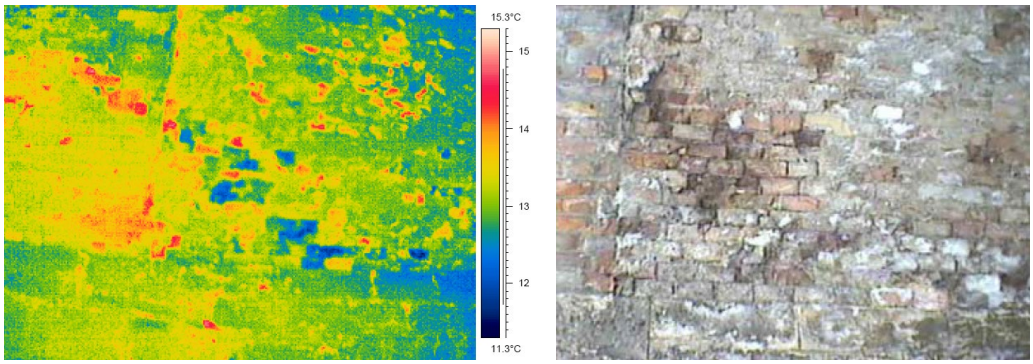

Image	**Location**
B4-04	Abutment (at the extension of the bridge)
Comments: The right part of the surveyed area on the image is covered by plaster while the left part is a stonework masonry with a highly weathered surface. The difference between the two parts can clearly be seen on the thermal image and the various construction materials can be identified. The lower part of the surface is wet that is seen on the thermal image.	

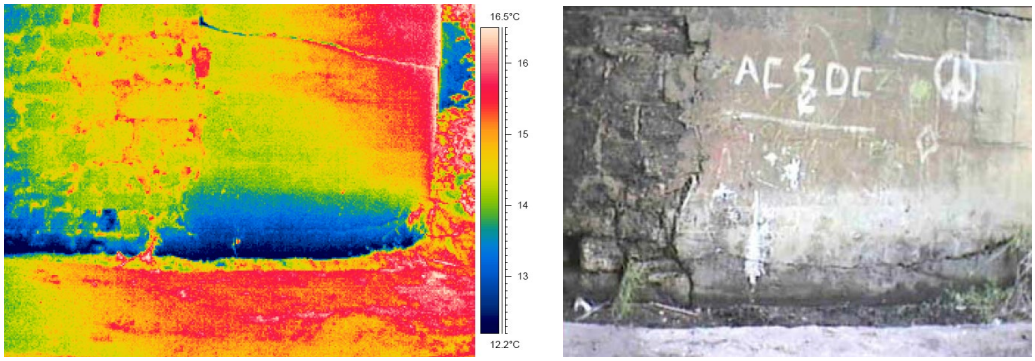

Repeated measurement

Measurement conditions:

Time of measurement: 2005.10.17. $12^{10} – 12^{45}$
Air temperature: 11.5 – 12.3 °C
Relative humidity: 43%
Wind speed: 1,1-1.5 m/s
Other: There was a discontinous sunshine before and during the measurement. There was no rainfall in two weks time before the measurement was made.

Image	Location
B4-05	Bridge front view (south-western side)
Comments: The front side of the bridge was subjected to direct sunshine before the measurement. The barrel (brick material) can be distinguished from the spandrel wall (quarry stone) on the thermal image. Spots with lower temperatures on the thermal image of the barrel refer to locations of brick losses or presence of vegetation. Colder parts below the edge beam are due to presence of vegetation and the shadow effect.	

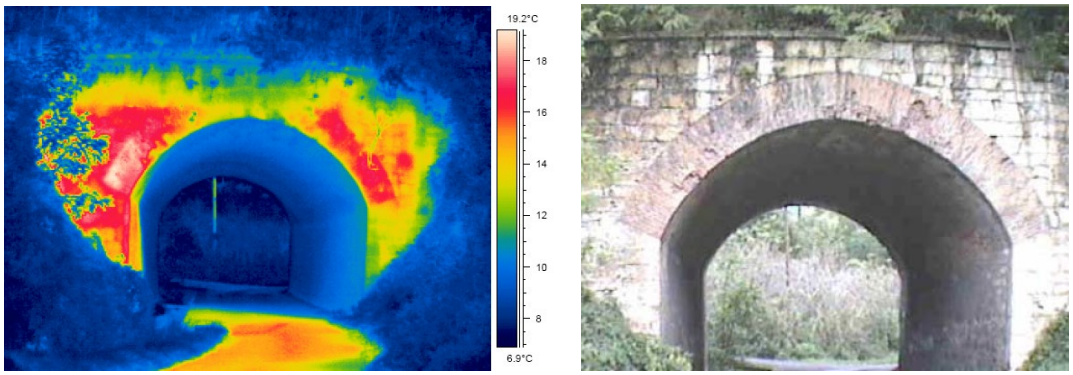

Image	Location
B4-06	Arch barrel (at the extension of the bridge)
Comments: Longitudinal crack (separation at the extension) at the barrel can be seen on the thermal image. The right part of the surveyed area on the image is covered by plaster while the left part is brickwork masonry with a highly weathered surface. However this difference between the two parts cannot be identified on the thermal image. No other anomaly can be identified.	

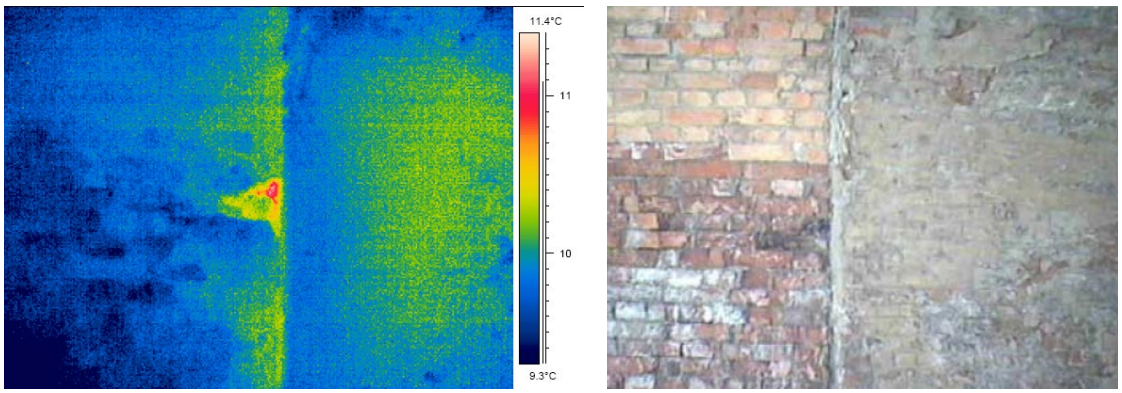

Image	Location

B4-07	Abutment (at the extension of the bridge)
Comments: The right part of the surveyed area on the image is covered by plaster while the left part is a stonework masonry with a highly weathered surface. However this difference between the two parts can hardly be identified on the thermal image. No other anomaly can be identified.	

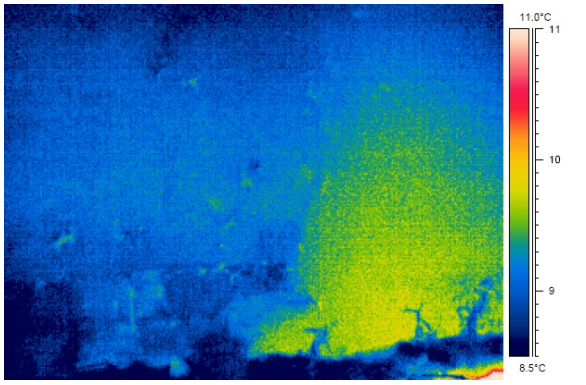

Case Study 5

Non-Destructive Investigation of the masonry abutments of a railway viaduct

1. Objectives

The objective of the non-destructive investigation was to determine the internal structure of the masonry abutment of the viaduct and to survey the condition of the stonework structure and the area behind the outer stone layer.

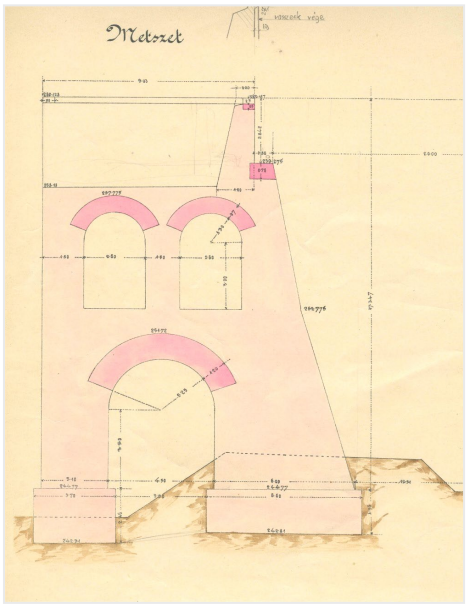

Image 1. Original drawing from the abutment

Image 2. The view of the viaduct

2. Description of the structure

The viaduct was constructed in 1896 and consists of wrought iron truss superstructure with stone masonry abutments. The viaduct is still in service but its reconstruction in the near future is considered necessary.

The view of the viaduct can be seen on Image 2. The original construction plan of the structure was available. (Image 1). The abutments are approx. 15 m high and 5 m wide. Originally, both abutments contained three internal arches from which only one arch at each abutment have remained visible. The others cannot be observed from outside the structure because they are fully covered by earth. According to the drawing the internal arch at the bottom of the abutment is 4,50m wide while those at the top are 2,40m wide. The abutments were constructed from large size stone blocks. There was no information on the internal structure of the abutments although it was presumed that there were loose rubble stones behind the outer stone layer.

The structure is exempt from serious defects. Only the following damages were observed during the visual inspection:

- Cracks at some of the stone blocks. These cracks are thin and are not extensive.
- Waterproofing damage and wet surface at the internal arches.
- Loss of joint material. This defect concentrates mainly at those regions where the surface is wet.
- Weathered stones. Found especially at regions of wetness.

3. Site survey with NDT methods

Non-destructive tests were carried out on the masonry abutments using ground penetrating radar (GPR), seismic method and infrared thermography. Calibratory investigations were made with boroscopy in order to confirm and interpret data obtained by the NDT measurements.

3.1 Radar survey

A pulseEKKO-1000 system by Sensors & Software Inc. from Canada was used for the radar tests. The survey was carried out at 450 MHz along horizontal lines at four different heights on the front wall of each abutment (Image 3-4) and on the entire surface of one of the exposed internal arches with frequent horizontal profiling (Image 5-6).

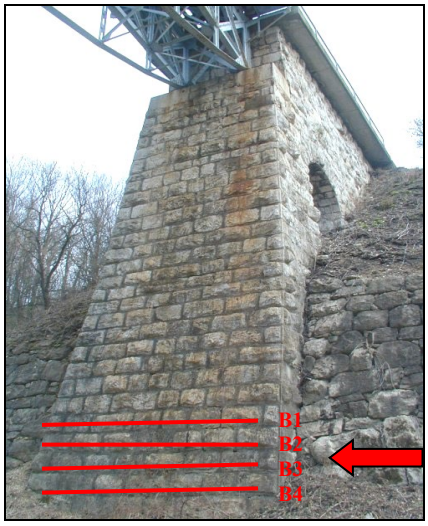

Image 3-4. Location of the GPR survey at the front wall of the left side abutment (B1-B4)

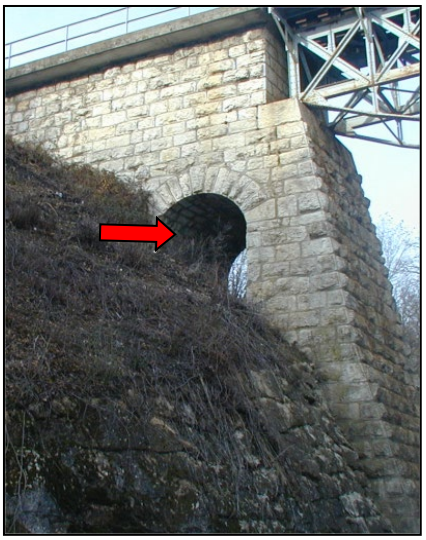

Image 5-6. Location of the GPR survey at the internal arch of the abutment

3.1.1 Processing and presentation of the measured data

The raw data gathered on-site cannot be evaluated directly. First the data have to undergo various processing procedures (positioning, time-correction, amplification, frequency filtering and other filtering) before they are presented (Appendix 1). On the GPR recordings, the scale of distance can be seen in metres on the top horizontal axle of the charts. The depth, calculated by the double of the wave propagation time given in nanoseconds (forward and backward) and by an average wave velocity (approx. 0.1 m/ns), can be seen on the vertical axle.

With the recordings from the internal arch, the amplitude values of the separately recorded profiles were combined in relation to time and depth into a single chart (anomaly map). The anomalies on the chart represent the areas where the electromagnetic waves hit materials with different reflectivity (Appendix 3).

Apart from the simple presentation of the GPR data in a time and depth chart, the data can further be processed to highlight some of the more specific characteristics of the recordings. One of the processing methods is the ***coherence analysis***. The coherence analysis presents the rate of dissimilarity of the data in the recordings that were taken side by side. Although the test is mathematically well defined, the physical interpretation of the results is not always straightforward. The rate of dissimilarity plotted onto the time chart can be found in Appendix 4. The vertical darker lines indicate a horizontal alteration in material within the surveyed area.

3.1.2 Test results

Survey of the the abutment

The front walls of the abutments were surveyed at four different heights. The results of the survey are presented in Appendix 1 in increasing order from top to bottom. The profiles taken on the same height from each abutment were placed side by side (profiles B1-B4 for the left abutment and J1-J4 for the right abutment). The different heights of the recordings were 180 cm, 140 cm, 100 cm and 50 cm measured from the bottom of the abutment.

The first parts of the profiles are exempt from anomalies except for the waves travelling directly from the transmitter to receiver. These waves were ignored in the evaluation. Until the yellow zone no significant reflections were perceivable within the outer part of the stone wall, which means that the outer stone layer is more or less homogenous. The thickness of this layer is about 50 cm but varies from stone to stone. Distinctively, the first and the last row of the rubble stone layer were constructed from thicker stones (see the ends of the profiles at B1 and J4 radargrams). The thickness variation of the abutment wall can clearly be seen on the radargrams, but individual stones cannot be distinguished with the given resolution.

The yellow zone represents the area behind the outer stone layer where strong reflections can be observed. The reflection from the boundary means that this area was built of a different material. The reflections within the area mean that this building material is highly inhomogeneous. There are profiles where the anomalies are more significant at the same depth than on other profiles. This suggests that the area behind the outer stone layer was filled with loose gravel stones rather than being a standard masonry. At the end of the yellow band, around a depth of 2 m, every profile shows a weak anomaly. Beyond the yellow band, no significant reflections could be recorded.

Chances were very small to detect the other end of the abutment, which is about 5 m deep, even with lower frequencies because the debris layer was absorbing the waves to a great extent.

Neither the GPR recordings nor the coherence analysis showed any significant inhomogeneity.

Survey of the internal arch

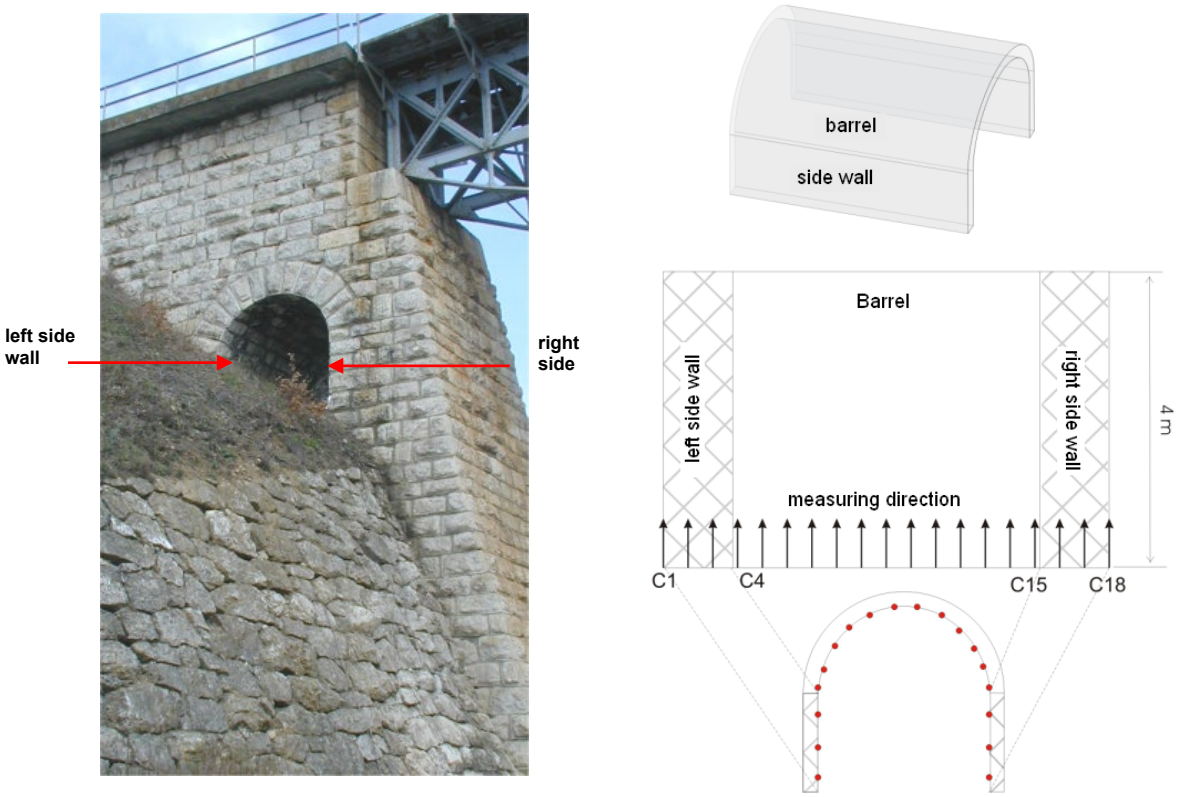

Image 7. Profiles recorded on the surface of the internal arch (demonstration on flat sheet)

Figure 3 shows the location of the GPR recordings on the internal arch. The horizontal profiles are 4 m long and are spaced approximately 30 cm from each other. The numbering of the profiles starts at the left side wall, go along the arch and end at the bottom of the right side wall. The entire surface of the arch and the side walls is 400 cm x 520 cm. The recorded radargrams are shown in Appendix 2, showing side by side the profiles symmetrically facing each other. Profiles C1-C4 were recorded on the left side wall, while profiles C18-C15 were recorded on the right side wall, followed by the profiles recorded on the arch barrel.

The blue line on the radargrams (see Appendix 2) marks the end of the outer stone layer which is about 50 cm thick. No observable reflections could be observed within this layer. The first and the last block of stones in this stone layer are thicker than others, and this is clearly noticeable on some of the profiles.

The reflections recorded within the zone marked on the radargrams with yellow band suggest that this area consists of loose gravel stones similarly to that have been observed from the recordings on the abutment. On profiles C1-C4 and C18-C15, the ulterior boundary of the yellow band implies weak reflections. Behind this boundary, there is an approximately 0.5 m thick area that shows no reflections indicating a homogeneous material. The reflections measured on the left side wall received from the wall of a buried internal arch and the reflections on the right side wall received from the front wall of the abutment were marked by

green line. The end of the radargrams of the right side wall contains strong reflections at around 2.5 m depth, indicating the outer surface of the abutment. Obviously there were no reflections received beyond this surface.

From about 3.5 - 4 m depth in the left side wall, a bunch of weak reflections, marked by a yellow dotted line, was recorded. These reflections are best observable on profile C3 where they are present along the entire profile. The reflections suggest the presence of the second internal arch that is filled up with soil. On the profiles C5-C8 and C14-C11, there are reflections beyond the outer stone layer which is an indication of a change in the wall properties. These reflections were marked on C6, C7 and C13, too.

Knowing the construction details of the abutment, the other reflections marked on the profiles can be well identified.

After analysing the profiles one by one, there have not been found any reflection that could refer to signs of large cavity or severe moisture in the masonry. From the individual radar profiles it was possible to construct the amplitude maps of the barrel. These maps show the electromagnetic reflectivity of the material with a relative deep accuracy (from 20cm to -1m). The maps do not show any sharp inhomogeneity neither in the outer stone layer nor in the area behind it. The only anomaly is a relatively stronger reflection on the surface of the internal arch detected at about 3.2 m length. This reflection has effect on the map only up to 40-50 cm depth. Since this reflection is only slightly stronger than the presumable level of the measuring error, no significant conclusions could be drawn from its presence on the anomaly map. This anomaly might be explained as a gap in the stone joints or a layer of stones with different properties.

Appendix 4 shows the results of the coherence analysis. The coherence analysis emphasizes anomalies if there is a significant alteration in the circumstances of the propagation of waves between the adjacent channels. These anomalies are indicated by vertical grey lines. The test highlights the horizontal variations in the signals, which are due to anomalies in the vertical elements (such as the break in the reflection, phase jump of the radar waves, location of diffractions, etc.).

The variations (signal density) are minimal when the material is homogenous, while the variations are frequent when the material is fragmentary. These variations cannot be quantified at this point, but it is very striking that more variations were observed at the right side wall, which could refer to a more inhomogeneous material.

3.2 Seismic test

The seismic measurements were made on the front wall of the left abutment along a straight line at 150 cm height. An ESS 03-48 type computer-controlled seismic measuring system was used, that was developed by ELGI. The distance between the geophones was 20 cm, and a hammer was used as a signal source (Image 8).

As a result of multi-channel recording option and the varying propagation velocity, the evaluation of the seismic data is more complex than that of the GPR data. The presentation of the recordings is similar with the exception that the double propagation time is given in milliseconds (ms).

Image 9 shows the recordings of seismic reflections. The resolution of the seismic reflections from the area behind the rubble stone layer is not so good as the GPR reflections but the penetration is deeper. The image shows two distinctive anomalies. The first anomaly, a lack of signals at the first reflection between 0-5 ms (see the yellow arrow), could either be caused by a measuring error or by the uneven joints of the rubble stones. The “second anomaly” (brown arrow) was possibly caused by the reflection from the other end of the wall. This anomaly, however, cannot be seen on the first part of the profile, but no serious

conclusion should be drawn because the events of interference are very complex in this system and the actual velocity of the seismic waves is not known. (It should be noted here that the propagation velocity of the seismic waves is more difficult to assess than that of the GPR. In the analysed case, calculating with 1000-1500 m/s, the other side of the abutment wall could be at 4-6 m depth.)

In practice, to achieve better resolution the seismic method has to be carried out at higher frequencies that may, however, increase the coupling problem. Due to the presumable difficulties in interpretation the seismic test has not been carried out on the entire surface of the structure.

Image 8. Test configuration for the seismic investigation

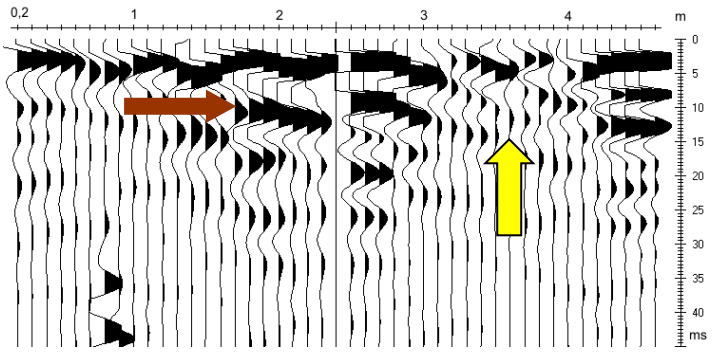

Image 9. Seismic recording on the left side abutment front wall (profile B2)

3.3 Survey with infrared thermography

The objectives of the survey was to point at anomalies in the construction material that are invisible or hardly visible to the human eye, wet areas, defects near the surface and presence of vegetation.

The survey was carried out in winter when the thermal condition of the structure was more or less stabilized. There was no air motion during the measurements therefore the cooling effect of wind has been ignored in the evaluation. Some parts of the masonry structure were subjected to solar radiation for a limited period before the measurements.

3.3.1 Instrumentation

The thermal images were recorded with an AGEMA 470 THV type thermovision camera (Image 10-11) which had a measuring range of -20.0°C - +500.0°C and a 0.1°C sensitivity. The recorded data were stored on floppy discs in a digital format and have been processed by a computer software before presentation.

Image 10-11. Measurement with infrared camera

3.3.2 Documentation of the results

As the thermography measurement is relatively quick and requires no direct access to the surface of the structure the entire masonry structure has been investigated. Although all recorded thermal images have been stored only those images have been processed where the presence of surface anomaly was presumable. Each thermal image was accompanied by a conventional digital photo that shows the visual representation of the surface. The current report contains only a selected range of thermal images, mainly those where the presence of an anomaly is apparent. The documentation of the results is found in Appendix 4. The surface temperatures are represented on the thermal images by colours where lighter colours refer to higher temperature while darker colours refer to colder temperature.

3.3.3 Conclusions

The following conclusions can be drawn from the results of the survey:

- Surface temperature anomalies identified may point at areas of wetness, potential delamination, weathered stones, joints with mortar loss or presence of vegetation.

- Wet areas could be identified at some of the images (see images T02, T04, T11, T12, T16, T17, T20, T22). The measurement was carried out under cold temperature conditions but some parts of the structure was subjected to direct sunshine prior to the measurement. The heating up process of the wet areas happened differently from the surrounding dry surfaces therefore it is possible to see these areas on the thermal images as 'cold spots' (in bluish). On other thermal images the presence of wetness is less striking.

- Weathered stones appear in different colour on the thermal images than other parts because of their altered emissivity (T09, T12, T16, T17, T19, T20, T21).

- The presence of vegetation is easily observable on the images. Generally they appear as 'hot spots' on the images (e.g. T13). Conversely, some areas covered with moss have lower temperature than their surroundings, probably because they grow at wet surfaces. When the surface was subjected to direct sunshine prior the measurement areas covered by vegetation may appear colder than others (T02, T04, T13, T14, T15).

- Generally joints can be distinguished from the stone blocks on the images as the mortar used for the construction has different thermal emissivity (T05, T06, T17, T19). Areas with mortar loss or those repointed with a different type of mortar are also discoverable on the images (T16, T17, T19, T20, T21). However, temperature variations in the joints can strongly be affected by their moisture distribution.

- Due to the strong boundary effects the infrared camera was unable to identify any anomalies on surfaces that were subjected to direct sunshine during the measurement. Here the temperature anomalies may lead to erroneous interpretation (T08, T09, T10, T13, T15).

- Most parts of the structure were in thermal equilibrium during the measurements. This is not an ideal condition for an infrared thermographic survey.

- The observations from the thermal survey of the abutments have concluded that the structure has no significant anomalies that would affect the thermal emissivity of the surface on wide areas. Only local anomalies were identified. Relatively wet parts, weathered stones and remarkable mortar loss in the joints were observed at the internal arches of the abutment.

3.4 Boroscopy survey

The survey was carried out with a boroscopy camera that was inserted into boreholes drilled in representative parts of the abutment. Digital recordings were made during the operation that allowed a detailed study of the internal parts of the structure in the the boreholes.

The objective of the survey was to help interpreting the results of the non-destructive measurements. The cores taken out from the drillings were utilised for testing the physical and mechanical properties of the stonework.

3.4.1 Documentation

The location of the boreholes with the recorded boroscopy images is summarised in Appendix 5. The collection demonstrates the most representative images recorded at each borehole.

Image 12. Boroscopy measurement at the internal arch barrel

3.4.2 Conclusions

The boroscopy survey has provided localised information on the internal structure of the stonework. The depth of the survey was limited to 60-80 cm therefore the outer stone layer and the area closely behind this layer was investigated. The boroscopy images provided a clear view on these areas. The survey has lead to the following conclusions:

- The findings of the radar survey regarding the structure of the stonework has been confirmed by the boroscopy images: the outer stone layer is more or less homogeneous and the area behind this layer consists of loose gravel stones. The outer stone layer is about 50cm thick both at the abutment front wall and at the internal arch. More loose material was found behind the stone layer of the abutment front walls. Gravels behind the internal arch barrel are well embedded in mortar. These observations are in line with the range of reflections perceived by the radar survey.

- There were no large cavities or cracks found within the outer stonework.

- Weathered stones have only a few mm deep damaged region near the surface.

3.5 Other tests

The cores drilled out from the structure were further analysed. The following characteristics have been established by these tests:

- The stone blocks were made from dolomite. The stones are more porous at the internal arches where substantial wetting was observed. The average compressive strength of the stones taken form the abutment front walls was 38,8 N/mm^2 while only 22,1 N/mm^2 for stones taken from the internal arches.

- The mortar between the blocks consists of dolomite and quartzite aggregates having a maximum grain size of approximately 8-10mm and cement with calcium-aluminate and calcium-aluminate-ferrite content. The mortar has an average compressive strength of 1,4 N/mm^2. Conventional cement mortar was used for repointing the joints.

4. Summary

Non-destructive investigation was carried out on the masonry abutment of the viaduct using GPR, seismic method and infrared thermography. Radar and seismic data were collected from the front wall of the abutment and only radar data from the internal arch of the abutment. The infrared thermography was applied on the entire surface of the structure due to the ability of the method to quick and remote data acquisition. Some findings by the radar survey have been confirmed by boroscopy tests.

The radar survey was able to identify some internal geometrical features of the abutment. It has been recognised that the outer layer of the structure is a more or less homogeneous stonework and the area behind this layer, both at the front wall and at the internal arch of the abutment, was filled with loose gravel stones rather than being a standard masonry. This observation has been confirmed by the boroscopy tests. However the radar test was unable to provide more information on the characteristics of the stonework and the gravel fill.

The constructional details of the abutment could be identified until the depth of approximately 2-2.5 m using a 450 MHz antennae in the radar survey. Deeper penetration, to identify the other end of the abutment, would not be possible even with lower frequencies. However, the received seismic data might have been more meaningful if the resolution had been increased by applying higher frequency.

On the GPR results recorded from the internal arch, the buried constructional details were more or less recognisable. Deeper penetration was achieved here than on the abutment front wall with the same 450 MHz antennae. This suggests that there were fewer wave-absorbing materials (e.g. clay) in this area.

The depth scale of the radargrams was calculated with an average wave velocity presumed for the masonry material. To achieve better accuracy in the detected dimensions, this scale has to be recalculated according to data gained by boroscopy measurements or coring.

The thickness variation of the abutment wall can clearly be seen on the radargrams, but individual stones cannot be distinguished with the 450 MHz resolution.

In order to achieve better resolution or more information on the structure, it is recommended to continue the radar investigations: by surveying the outer stone layer and its surrounding area with a 900 MHz or 1200 MHz antennae, and surveying the remote internal constructional details of the abutment with a 225 MHz antennae.

Infrared thermography was able to identify some of the characteristics of the masonry structure and to differentiate between the basic construction materials such as stones and mortars. Local anomalies have been recognised at some of the thermal images such as wet regions, weathered stones and remarkable mortar loss in the joints. However interpretation of the temperature variations on the images is fraught with difficulties due to the boundary effects. Unfortunately most parts of the structure were in thermal equilibrium during the measurements that hindered effective recognition of the anomalies.

Appendix 1: Radargrams

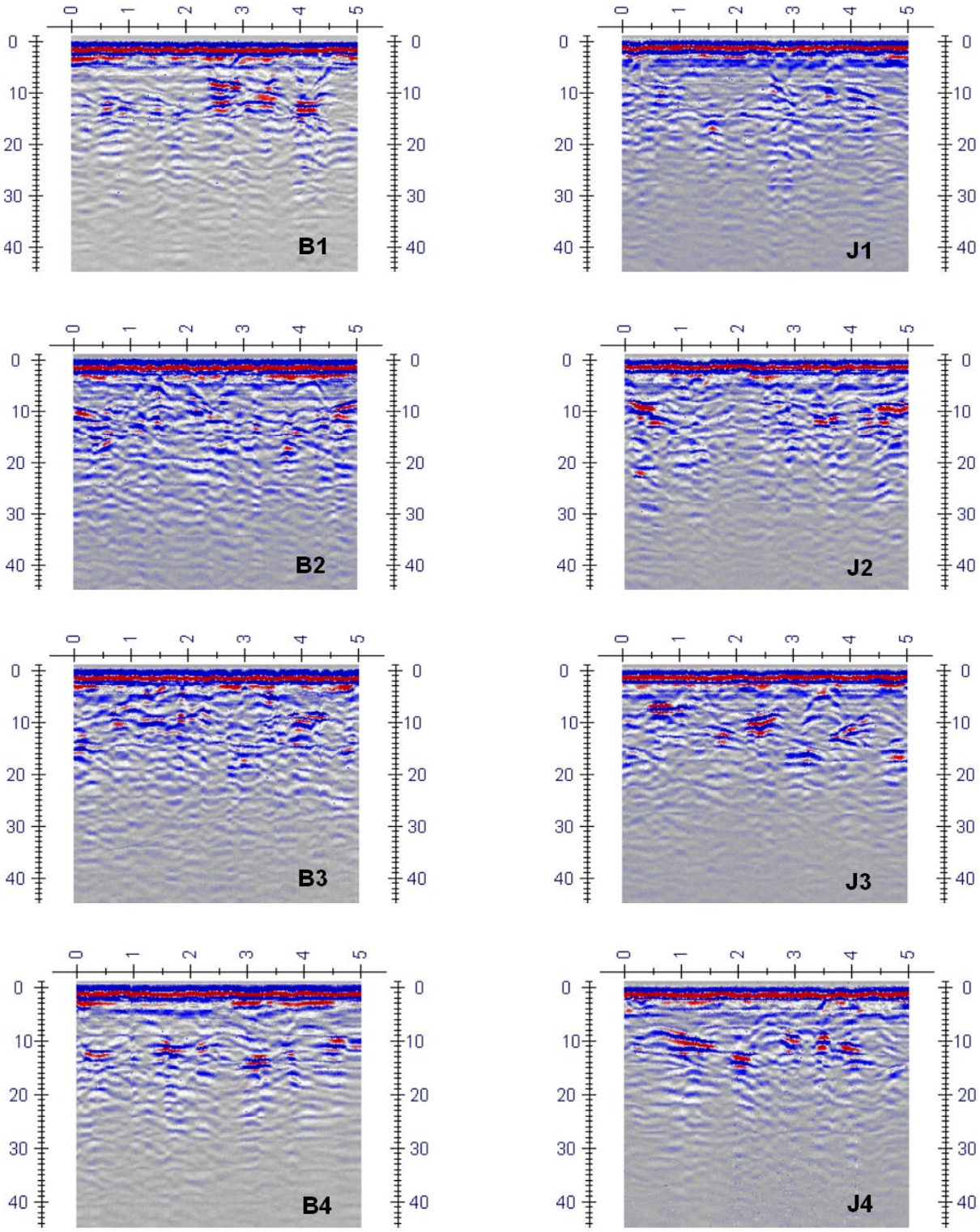

Radargrams of the left (B) and right (J) abutment front walls

Appendix 1: Radargrams /abutment front wall/

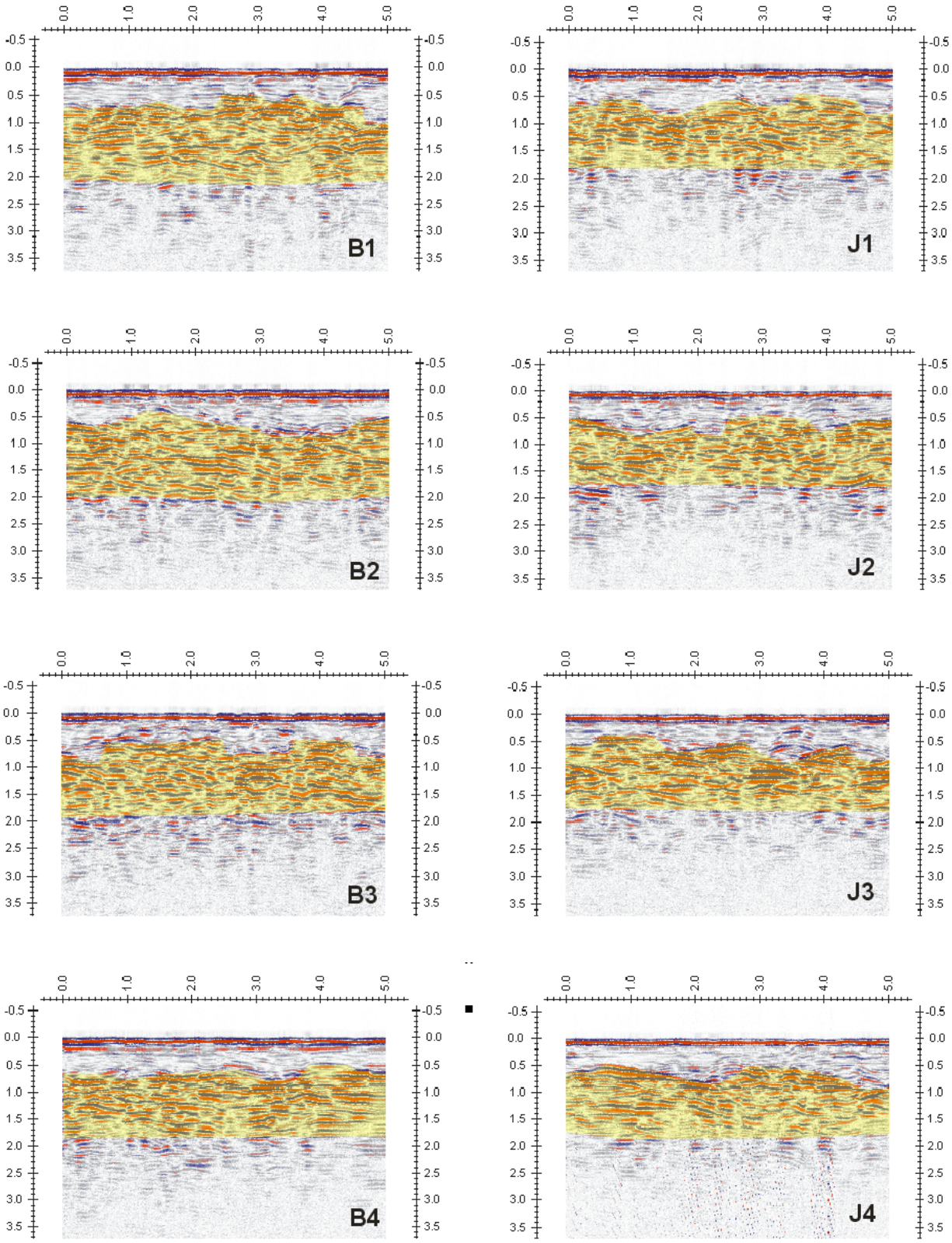

Processed radargrams of the left (B) and right (J) abutment front walls
Horizontal axle: distance (m), Vertical axle: depth (m)

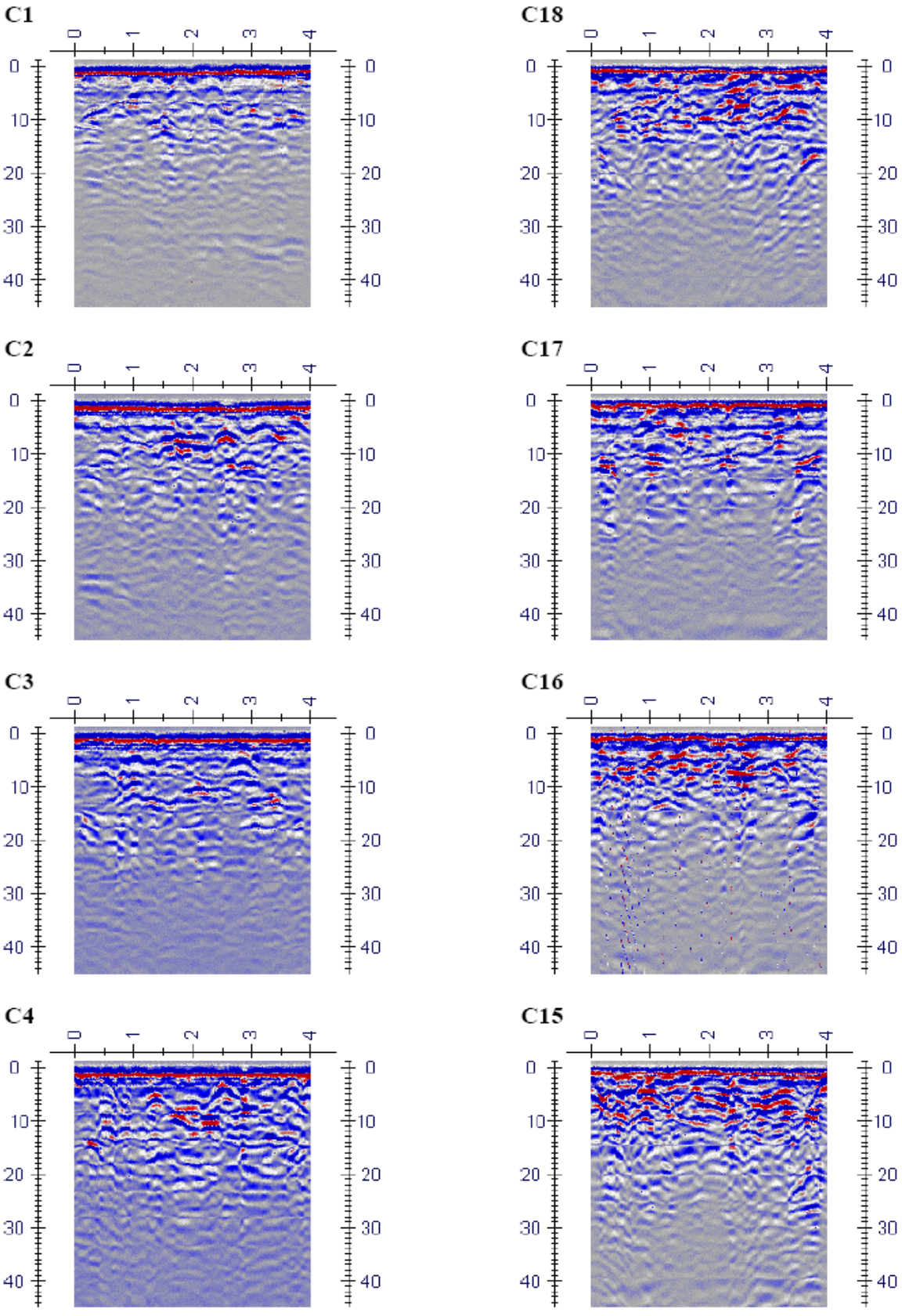
C1
C18
C2
C17
C3
C16
C4
C15

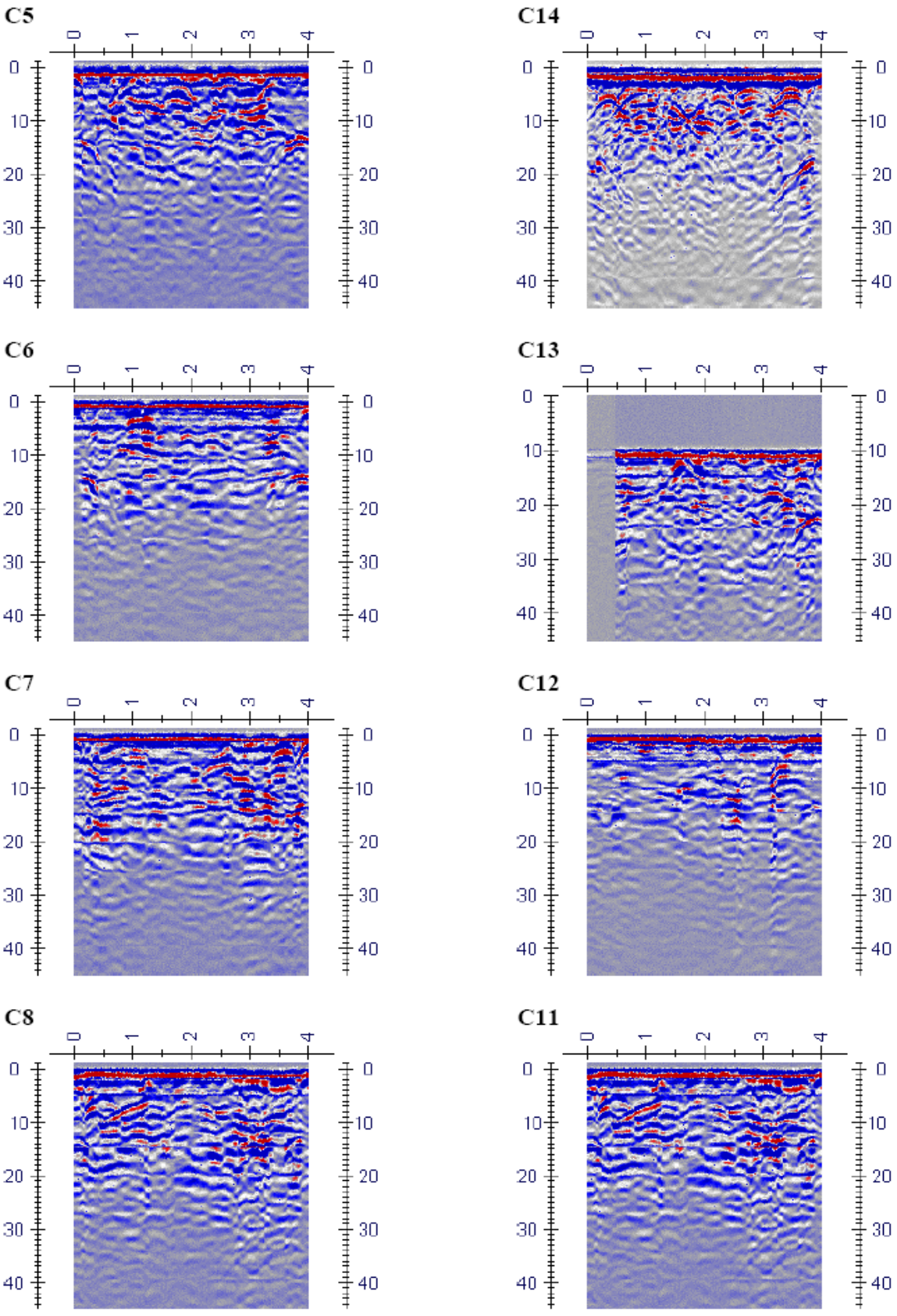
C5
C14
C6
C13
C7
C12
C8
C11
0
1
2
3
4
0
10
20
30
40

C9

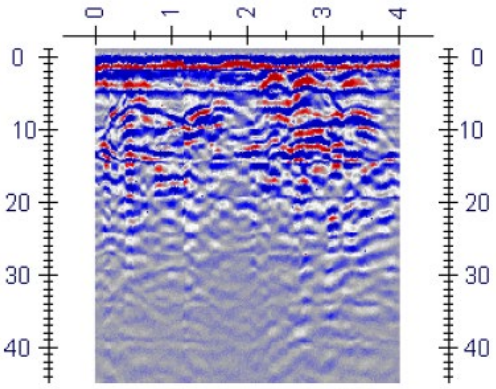

C10

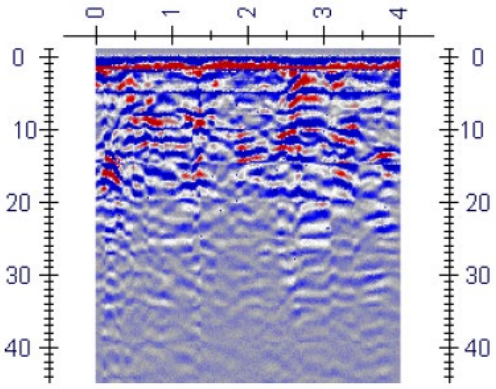

Appendix 2: Radargrams /internal arch/

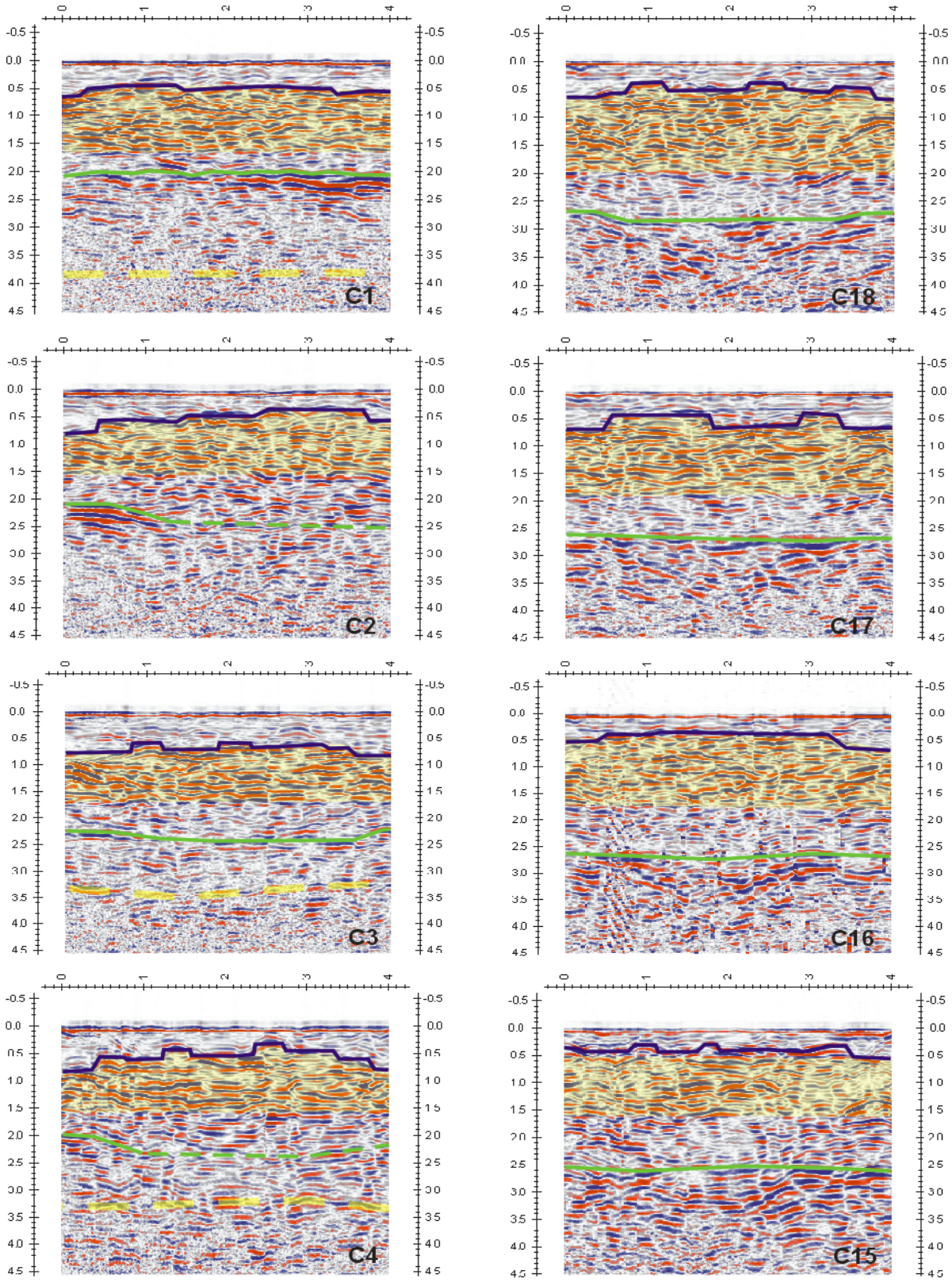

Processed radargrams of the internal arch
Horizontal axle: distance (m), Vertical axle: depth (m)

Appendix 2: Radargrams /internal arch/

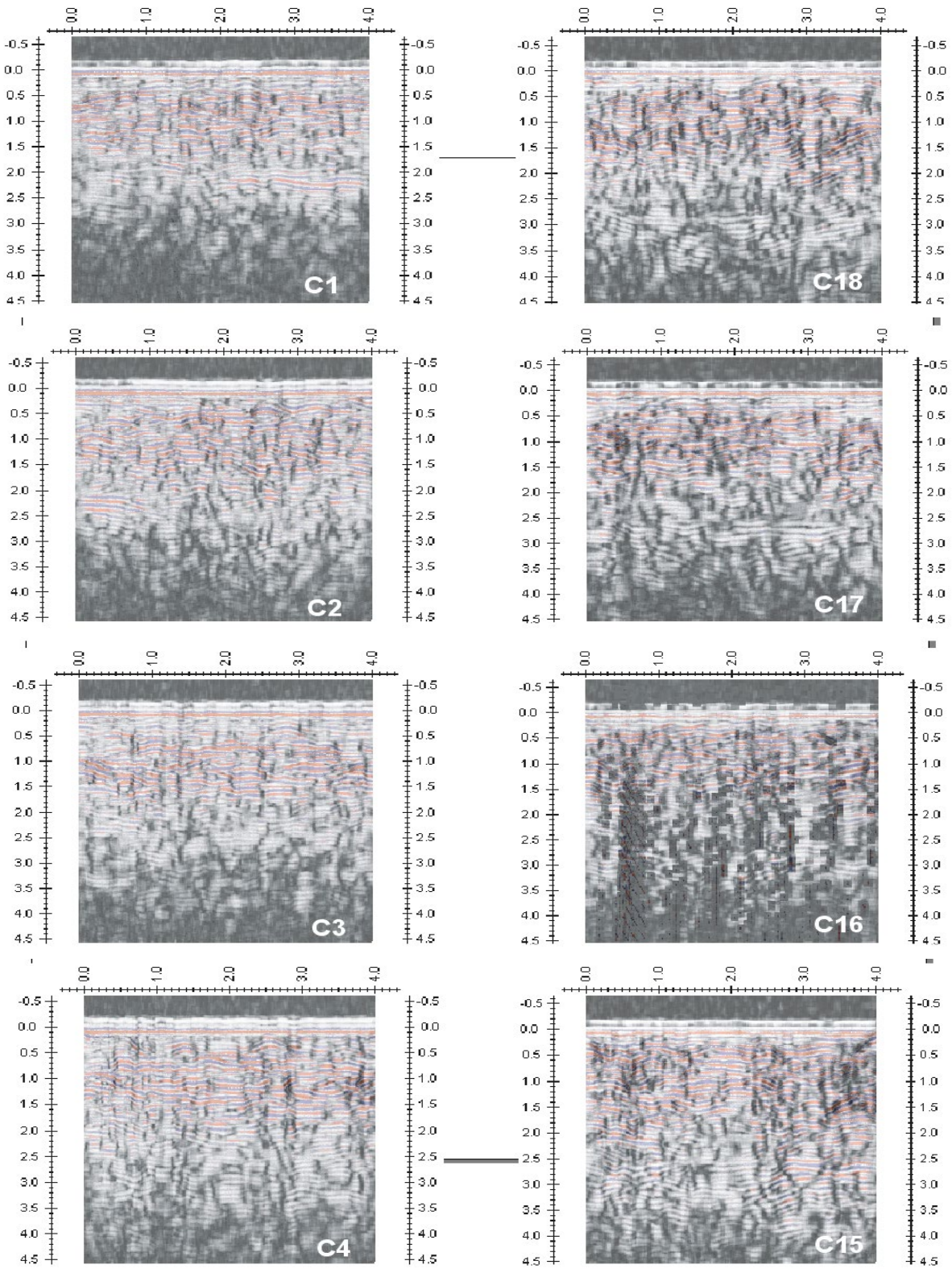

Radargrams of the internal arch after coherence analysis
Horizontal axle: distance (m), Vertical axle: depth (m)

Appendix 3: Anomaly map /internal arch barrel/

Measurements with 450 MHz antenna

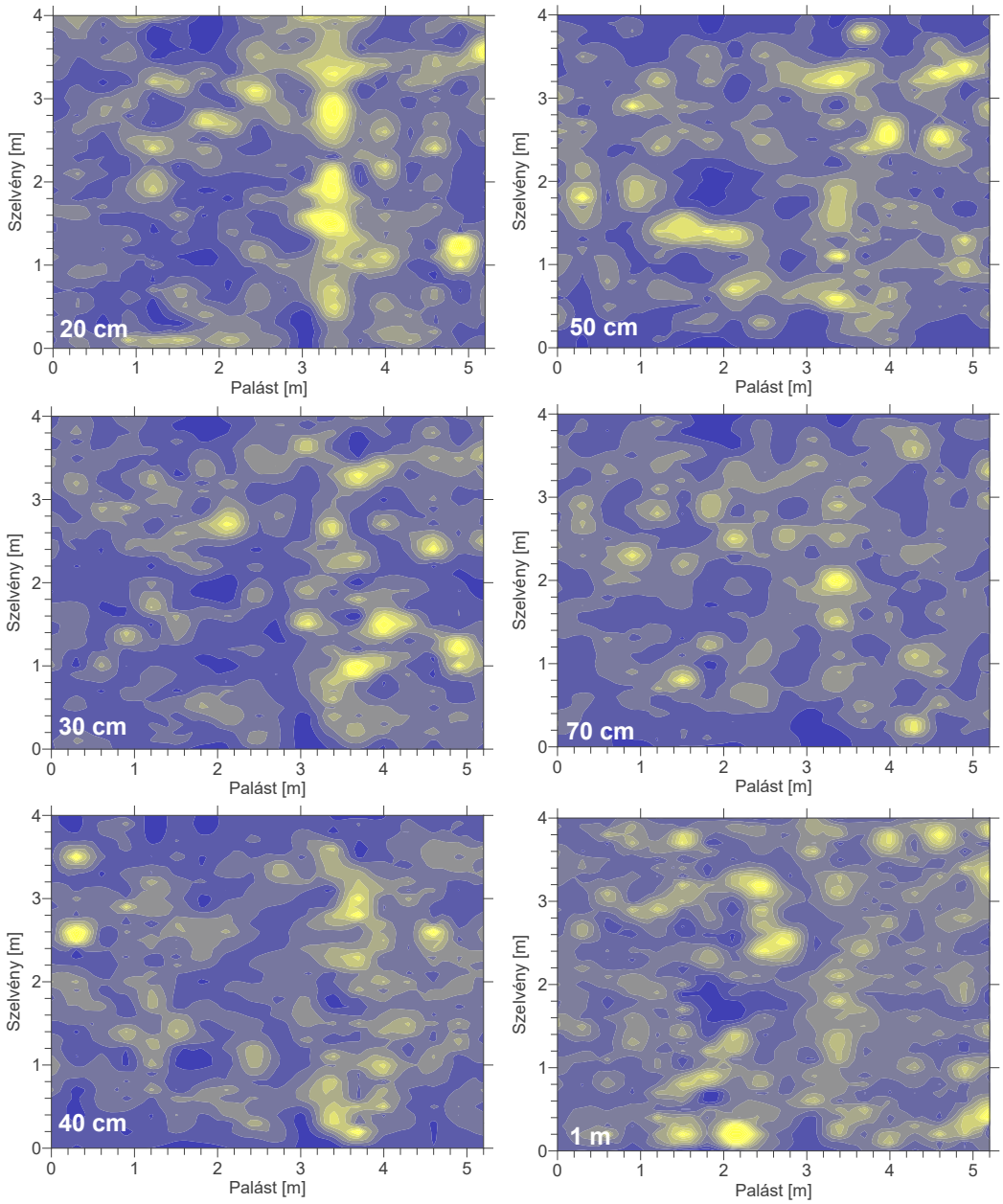

Anomaly map. 3D representation of measured data with slice technique.

The images show anomalies in masonry interior at various depths.
Light spots are considered areas with lower reflection.

Appendix 4: Thermal images

Image	Location
T01	Viaduct superstructure

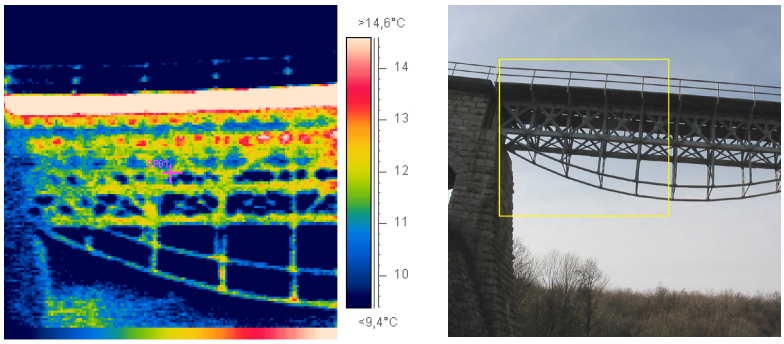

Image	Location
T02	Left abutment front wall – bottom region

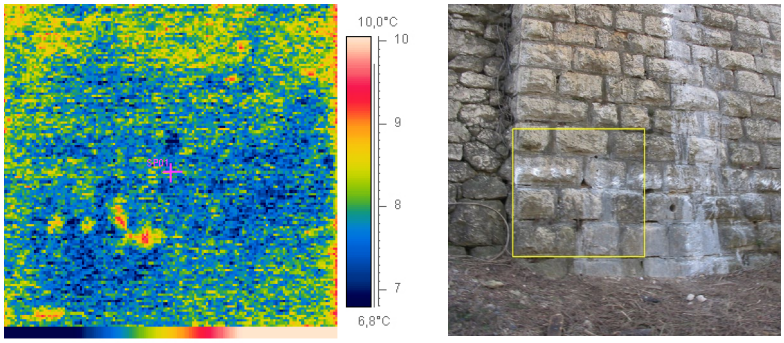

Image	Location
T03	Left abutment front wall – bottom region

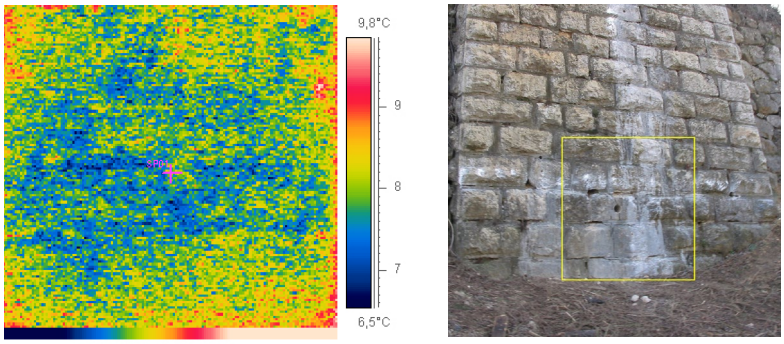

Image	Location
T04	Left abutment front wall – bottom region

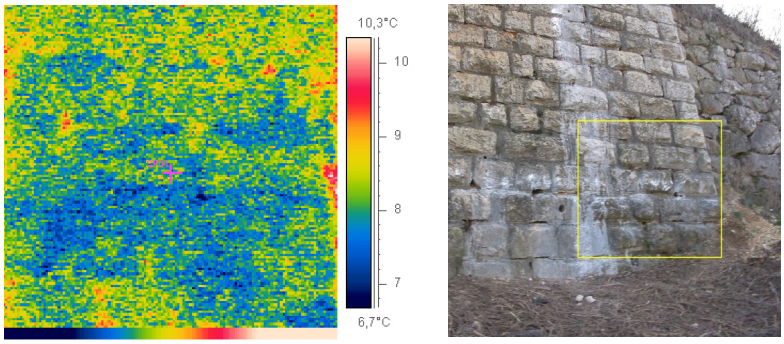

Image	Location
T05	Left abutment front wall – middle region

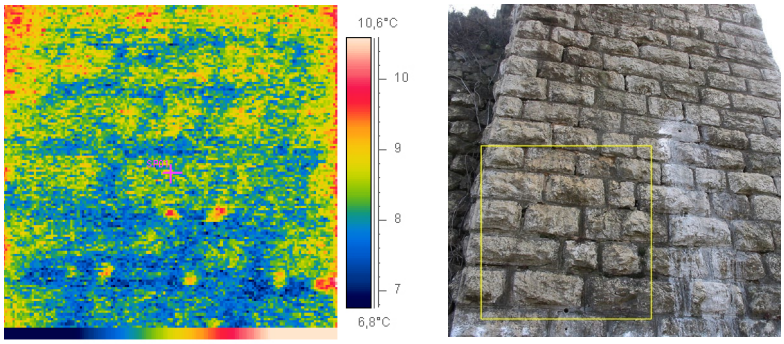

Image	Location
T06	Left abutment front wall – middle region

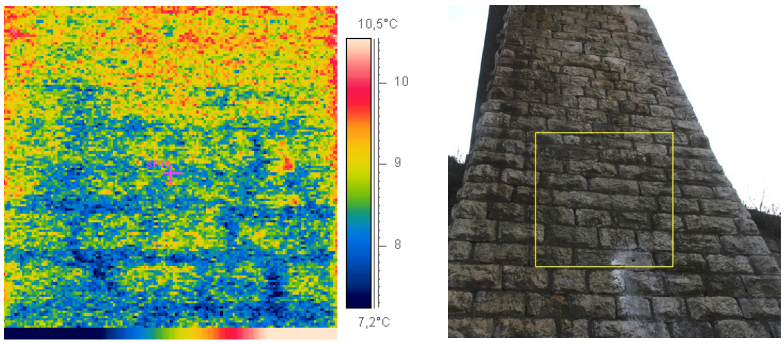

Image	Location
T07	Left abutment front wall – middle region

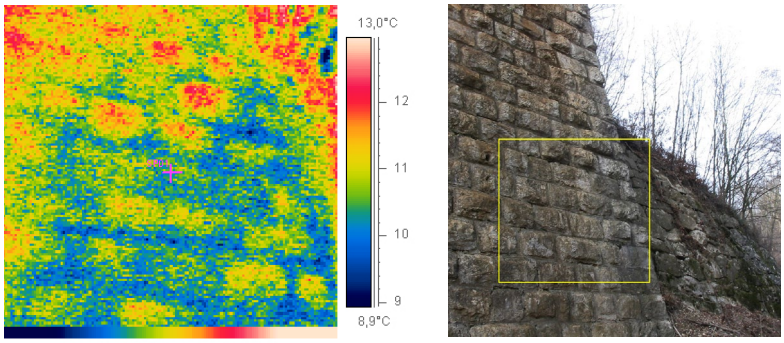

Image	Location
T08	Left abutment front wall – middle region

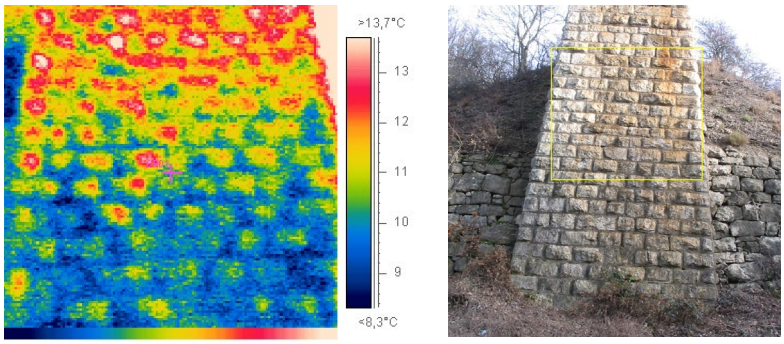

Image	Location
T09	Left abutment internal arch – barrel middle

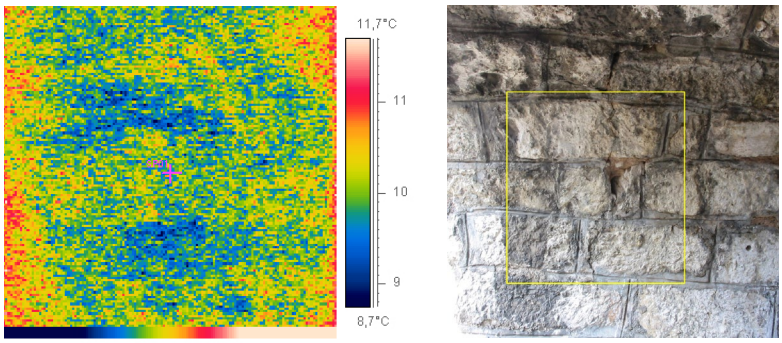

Image	Location
T10	Left abutment internal arch – barrel edge

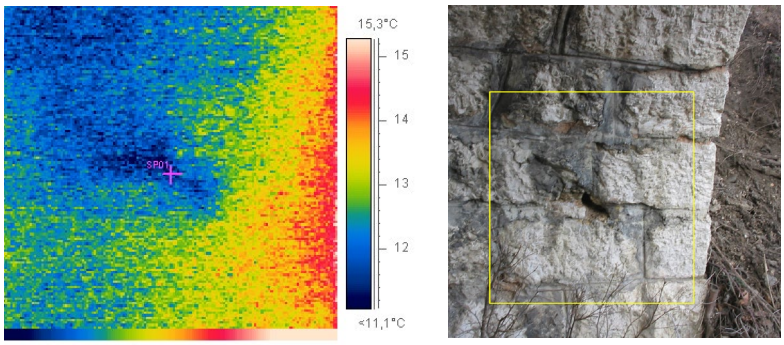

Image	Location
T11	Left abutment internal arch – side wall

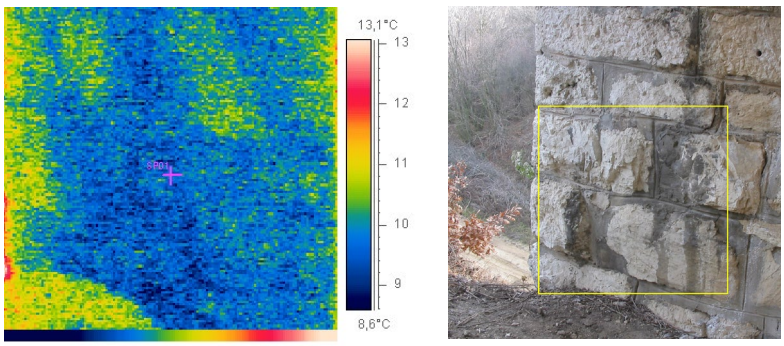

Image	Location
T12	Left abutment internal arch – barrel soffit

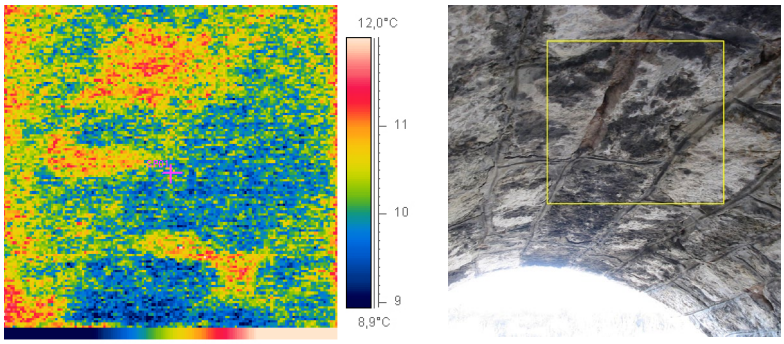

Image	Location
T13	Right abutment wing wall

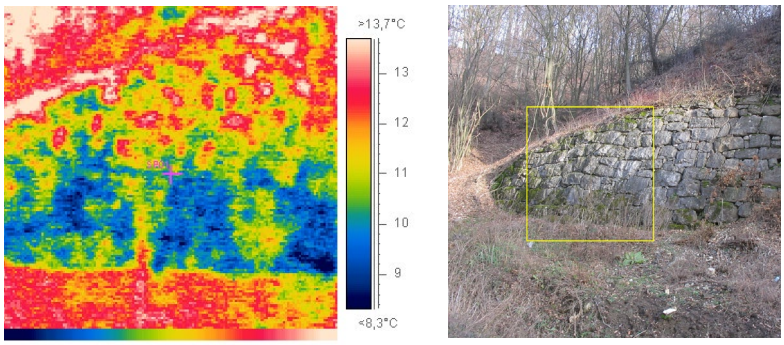

Image	Location
T14	Right abutment wing wall

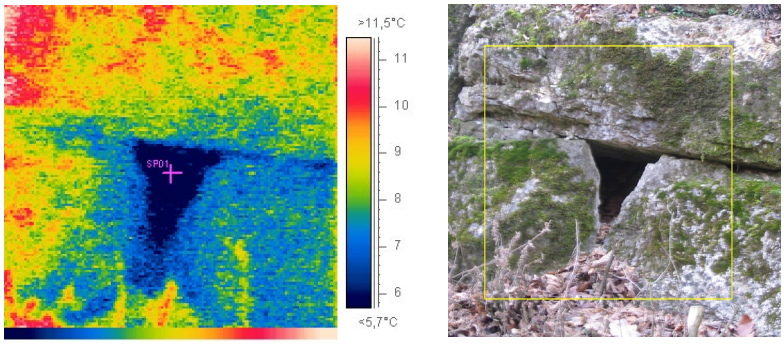

Image	Location
T15	Right abutment wing wall

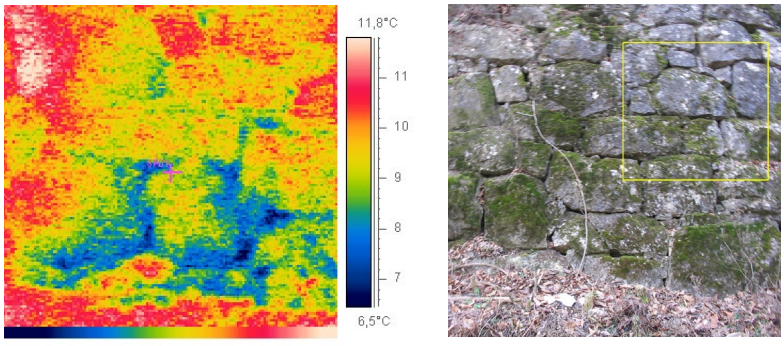

Image	Location
T16	Right abutment internal arch – side wall

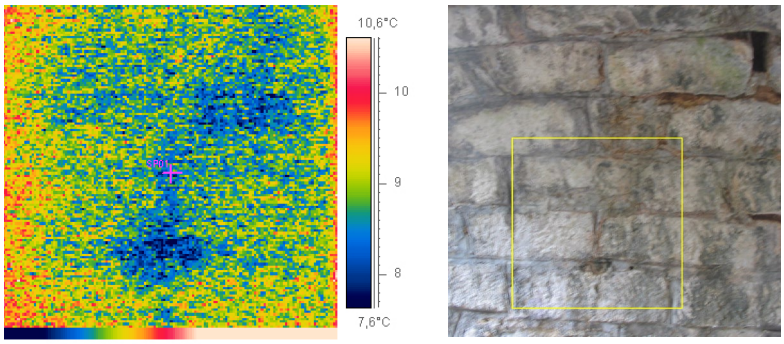

Image	Location
T17	Right abutment internal arch – side wall

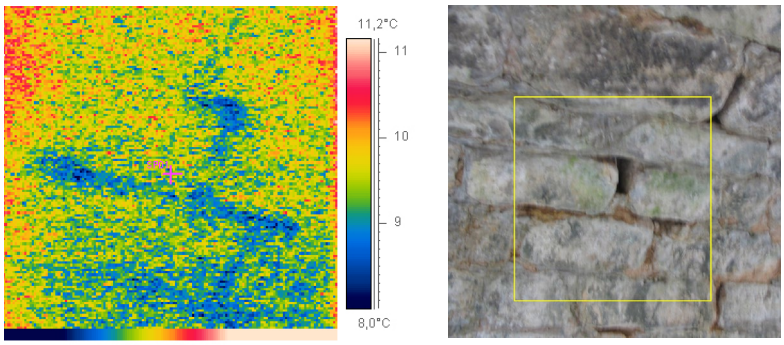

Image	Location
T18	Right abutment internal arch – barrel

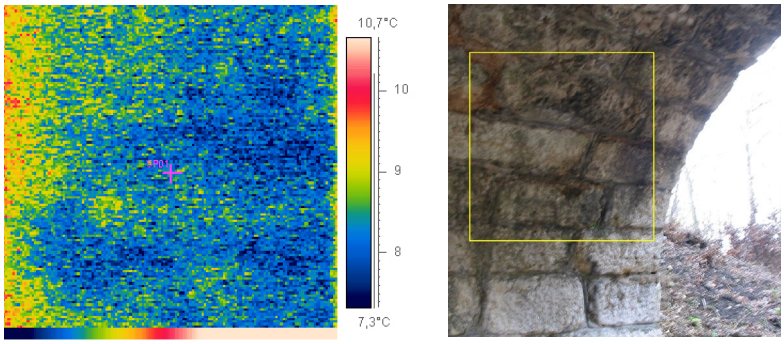

Image	Location
T19	Right abutment internal arch – barrel

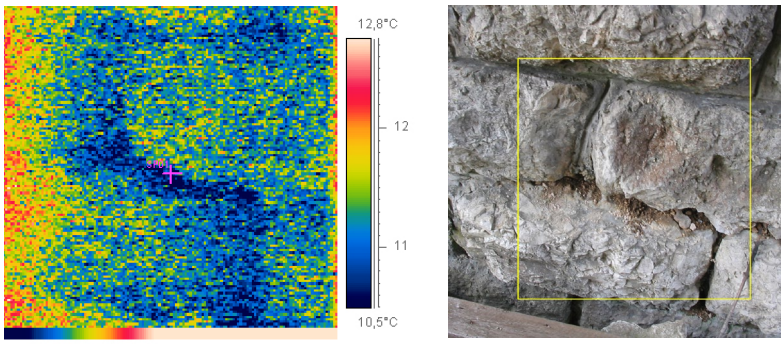

Image	Location
T20	Right abutment internal arch – barrel edge

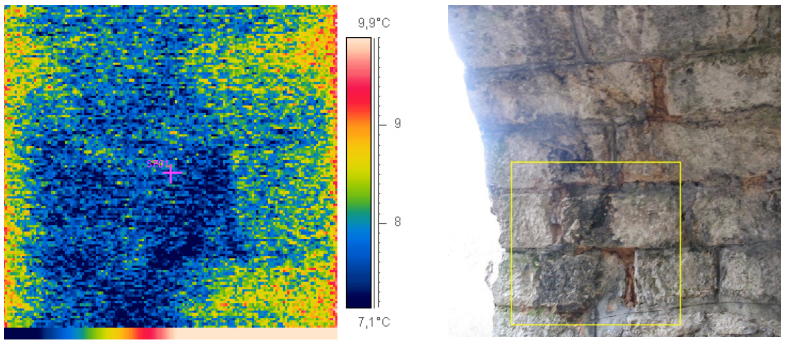

Image	Location
T21	Right abutment internal arch – barrel

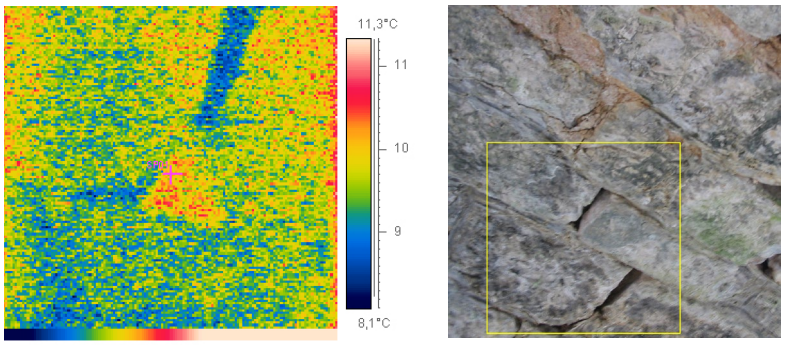

Image	Location
T22	Right abutment internal arch – side wall

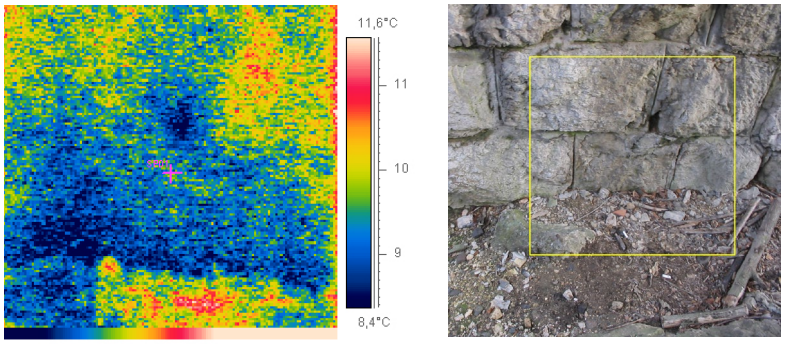

Appendix 5: Boroscopy images

Borehole number	Location of the borehole	Height from ground level (m)	Length of borehole (cm)	Diameter of borehole (mm)
B01	Right abutment front wall	1.40	80	100
B02	Right abutment front wall	1.25	65	50
B03	Left abutment front wall	1.00	60	50
B04	Left abutment front wall	1.60	60	50
B05	Right internal arch barrel	1.80	70	50
B06	Right internal arch barrel	1.20	70	50
B07	Right internal arch side wall	0.50	60	50
B08	Right internal arch side wall	1.00	60	50
B09	Right internal arch side wall	0.50	60	50

Borehole	Location
B01	Right abutment front wall

Depth = 0cm

Depth = 40cm

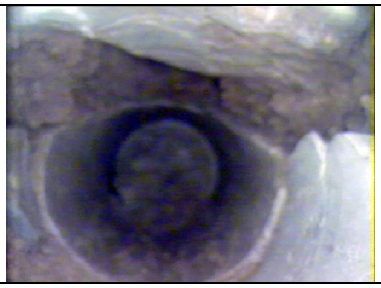

Depth = 60cm

Borehole	Location
B02	Right abutment front wall

Depth = 10cm

Depth = 30cm

Depth = 50cm

Borehole	Location
B03	Left abutment front wall

Depth = 5cm

Depth = 15cm

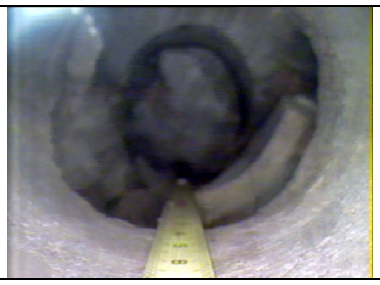

Depth = 45cm

Borehole	Location
B04	Left abutment front wall

Depth = 10cm

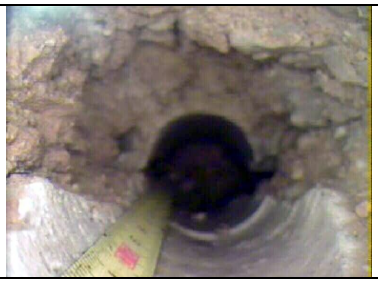

Depth = 40cm

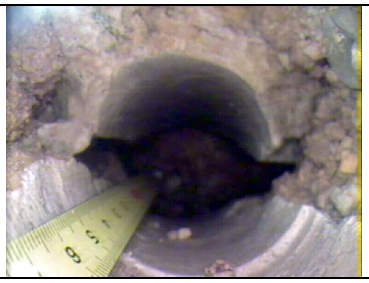

Depth = 50cm

Borehole	Location
B05	Right internal arch barrel

Depth = 0cm

Depth = 15cm

Depth = 40cm

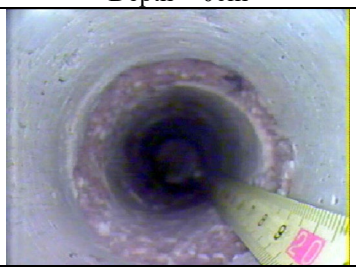

Depth = 50cm

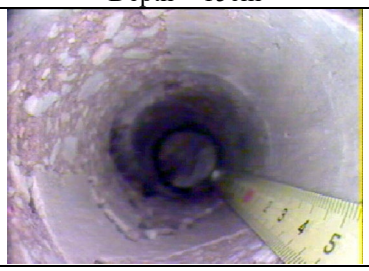

Depth = 55cm

Depth = 60cm

Borehole	Location
B06	Right internal arch barrel

Depth = 20cm

Depth = 30cm

Depth = 40cm

Depth = 45cm	Depth = 50cm	Depth = 55cm

Borehole	**Location**
B07	Right internal arch side wall

		
Depth = 10cm	Depth = 40cm	Depth = 40cm

Borehole	**Location**
B08	Right internal arch side wall

		
Depth = 2cm	Depth = 10cm	Depth = 25cm
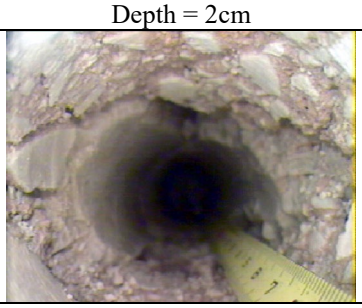	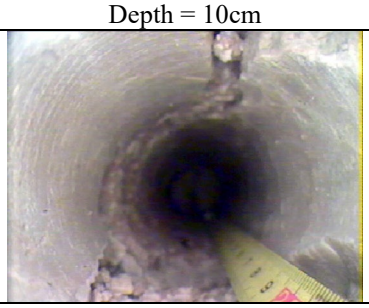	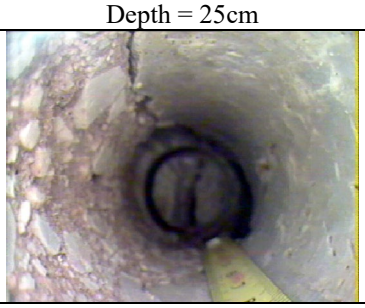
Depth = 37cm	Depth = 42cm	Depth = 55cm

Borehole	**Location**
B09	Right internal arch side wall

		
Depth = 5cm	Depth = 30cm	Depth = 40cm

Case Study 6

Mapping the foundation of two masonry bridges with NDT methods

1. Background

The condition, construction material and depth of the foundations of existing railway bridges are often unknown although the knowledge of these information is essential for their assessment. Assessment of foundations is particularly important when foundation damages are suspected or when increase in loading is expected. The failure of foundation may lead to the failure of the entire bridge, their inspection therefore is of utmost importance in many cases. The inspection of foundations is difficult in most cases as they are not directly accessible. Conventional techniques for the inspection of foundations are mainly based on simple visual inspection of their uppermost parts and do not provide any information on their depth, geometry, integrity and the quality of the surrounding soil. Other conventional techniques for mapping foundations, such as excavations, can be expensive and not feasibe in most cases.

Non-destructive investigation of existing bridge foundation has gained ground in recent years although the available experience and references in this field are yet limited. Various NDT techniques have been developed and tried. These include the borehole radar method, the parallel seismic method, the borehole sonic method, cross-borehole sonic tomography and the dynamic foundation response method.

The following chapters provide information on two promising and easily applicable methods, the borehole radar and parallel seismic methods. The execution of pilot tests is demonstrated that were carried out at two masonry bridges in Hungary.

2. Description of the methods

2.1 Parallel Seismic method (PS)

The Parallel Seismic (PS) method is a borehole test method for determining depths of foundations. The method can also detect major anomalies within a foundation as well as provide the surrounding soil velocity profile. The method requires the installation of a borehole close to the foundation being tested. The method can be used also when the foundation tops are not accessible or when the piles are too long and slender to be testable by other techniques. Basic Concept: The Parallel Seismic (PS) method involves hammer impacts at any part of the exposed structure that is connected to the foundation (or impacting the foundation itself, if accessible). A hydrophone or a three component geophone located in a nearby borehole records the compressional and/or shear waves traveling down the foundation. Therefore, the PS test requires drilling a 5- to 10-cm-diameter hole as close as possible to the foundation being tested (preferably within 1.5 m). The borehole should extend at least 1 to 3 m below the expected bottom of the foundation. If hydrophones are used, the hole must be cased, capped at the bottom, and the casing and hole filled with water. For geophone use, the

hole must usually be cased (but not always) and grouted to prevent the soil from caving in during testing.
PS tests can be performed on concrete, wood, masonry, and steel foundations. Some portion of the structure that is connected to the foundation must be exposed for the hammer impacts. The principle of the method is shown on *Fig. 1.*

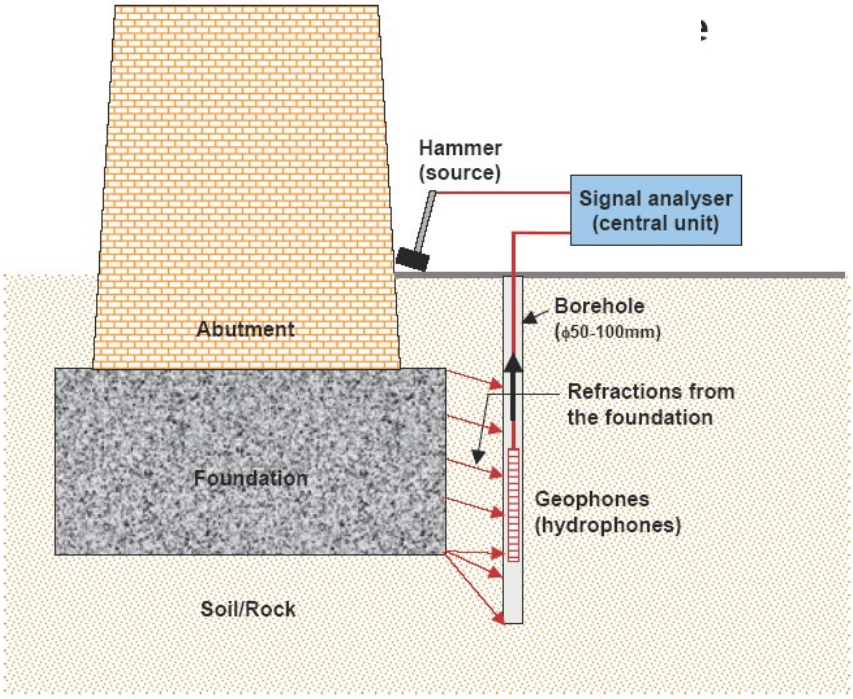

Fig.1: Principle of the Parallel Seismic (PS) method

Data Acquisition: In a PS test, a hammer strikes the structure, and the response of the foundation is monitored by a hydrophone or a geophone receiver placed in the borehole. A signal analyzer records the hammer input and the receiver output. The receiver is first lowered to the bottom of the hole, and a measurement is taken. Then, the receiver is moved up 10-50 cm, and the second measurement is made. This process is continued until the receiver has reached the top of the boring.
Data Processing: Analysis of the PS data is performed in the time domain. In PS tests, one relies on identifying direct arrival times of compressional and shear waves at the receiver locations, as well as the wave amplitudes. The PS tests are performed at 10 to 50 cm vertical receiver intervals in the borehole.
Data Interpretation: For hydrophone data, the time arrival of compressional waves is picked from the data for all receiver locations. A plot of the time arrival-versus-depth is prepared.
Advantages: The Parallel Seismic method is more accurate and more versatile than other nondestructive surface techniques for determining unknown foundation depths. The accuracy of the method depends on the variability of the velocity of the surrounding soil and the spacing between the borehole and the foundation element. Depths are normally determined with 95% accuracy or better.
Limitations: A borehole is needed for Parallel Seismic tests, which adds to the cost of the investigation (unless borings are also required for other geotechnical purposes). The borehole should be within 1.5 m of the foundation, which sometimes cannot be achieved. Note that for very uniform soils (such as saturated sands), a successful test can be performed with up to 4.5 to 6 m spacing between the source and the borehole. As the borehole moves away from the

foundation, interpretation of the PS data becomes more difficult, and the uncertainty in the tip depth determination becomes greater.
Interpretation of the signals can be difficult due to the various refraction possibilities of the seismic waves depending on the quality and layered configuration of the surrounding soil (*Fig. 2*). Interpretation of the results therefore requires skilled experts.

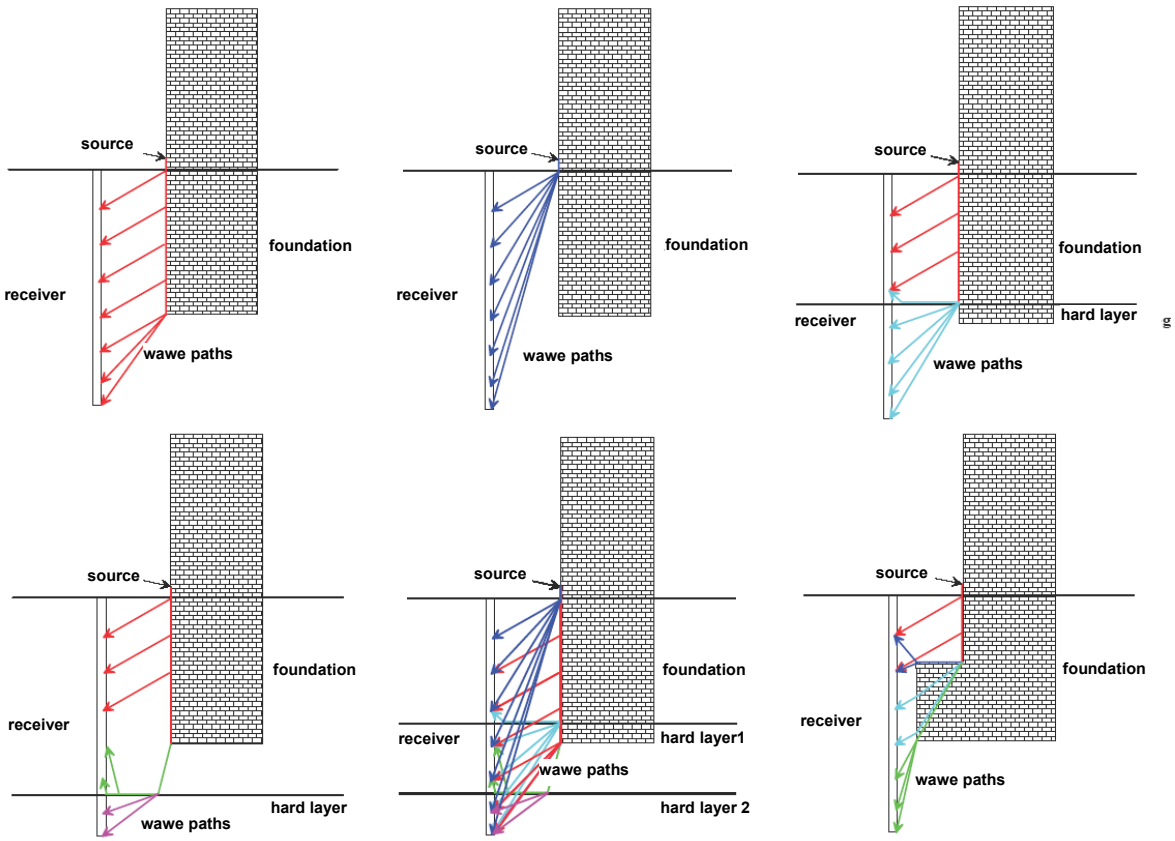

Fig. 2: Different refraction modes of seismic waves

2.2 Borehole Radar method

The Borehole Radar method uses a borehole ground penetrating radar (GPR) antenna to obtain reflection echoes from a foundation for the determination of unknown depth and geometry of foundation. The principle of the method is shown on *Fig. 3*.
Data Acquisition: In borehole radar, an antenna transmits radar energy into the surrounding rock and soil, and a receiver then records reflections that occur as the radar signals encounter and reflect from interfaces with different dielectric properties. The method is very similar to the borehole sonic method, where seismic waves are used rather than electromagnetic waves. Borehole radar can be used in reflection mode or in cross-hole tomography mode. The radar measurements are either directional or omnidirectional, depending on the type of equipment and antennas.
Radar uses radio waves with frequencies varying generally between 10 and 2,000 MHz. These waves are influenced primarily by the dielectric properties of the medium through which they are traveling and the electrical conductivity of the medium. Highly conductive materials attenuate the radar signals and limit its depth of penetration. Although the lower frequencies penetrate more than higher frequencies, they have less resolution.

In the unknown depth of foundation application, the borehole radar signal will be reflected from the foundation until the bottom of the foundation is reached. There will be no reflections beneath the foundation, except for those emanating from geologic conditions. The observed change in the reflected signal is used to locate the bottom of the foundation.
Limitations: Borehole radar requires a PVC-cased borehole; the method will not work if the hole is steel-cased. The depth of penetration is significantly influenced by the electrical conductivity of the rocks and soil surrounding the borehole, which may not be known before the radar survey is completed. Penetration up to about 10 m may
be achieved in resistive conditions. In conductive materials, since the penetration of the GPR signal will be limited, getting the borehole as close to the pile as possible will be advantageous.

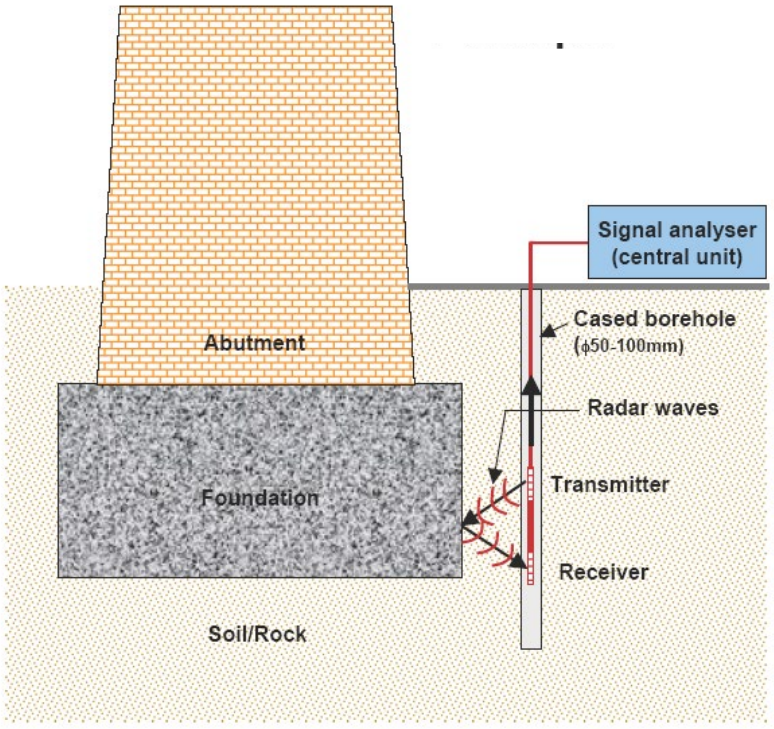

Fig.3: Principle of the Borehole Radar method

3. Field tests

Pilot tests have been carried out on two masonry bridges (Rátót viaduct and Eplény arch bridge) in Hungary in order to investigate the potential in the borehole radar and parallel seismic methods in mapping the unknown foundations of existing railway bridges. The foundations selected for the survey were constructed from different materials and had different depth. The foundation of the Rátót viaduct was made from concrete while the Eplény arch bridge had stone foundations.

Fig. 4. shows that there were controversial informations on the depth of the foundations of the Rátót viaduct. The original plan suggested 242,82m while on the reconstruction plan 241,60m was indicated. The latter was determined by an electro-acoustic technique many years ago.

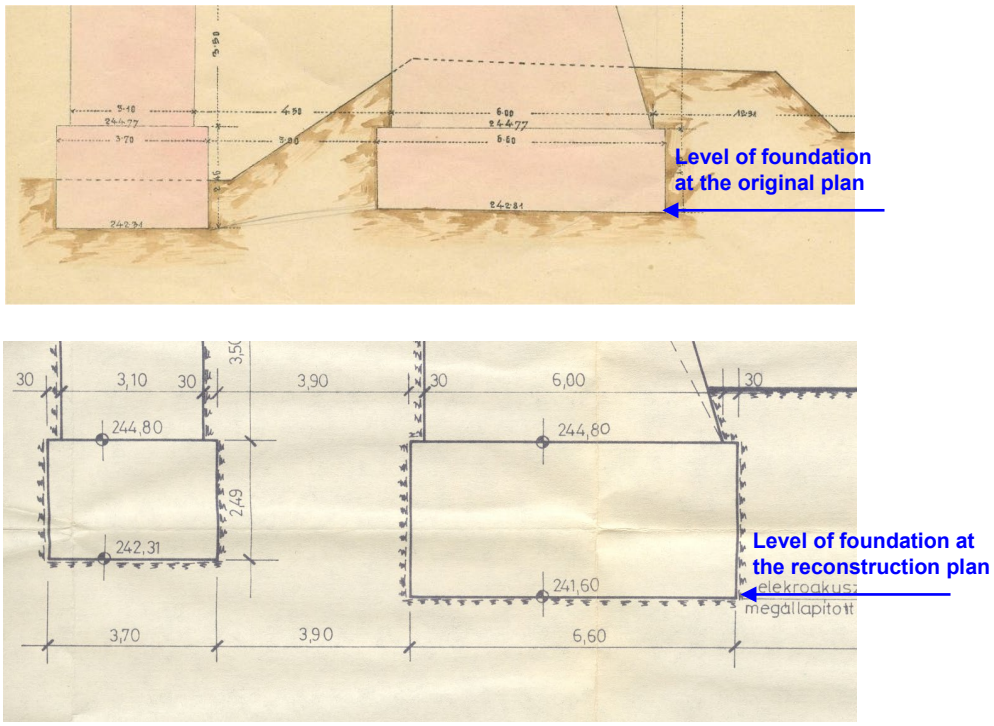

Fig.4: Existing information on the foundation of the Rátót viaduct.
top) original plan bottom) reconstruction plan

There were no exact information on the foundation depth of the Eplény arch bridge although according to experience on similar structures it was expected to be around 1,50m below ground level.

3.1 Tests with the borehole radar and parallel seismic methods

Two boreholes were drilled beside the foundation of each structure. Appendix 1 and the following Table demonstrate the steps that were followed during the borehole radar and parallel seismic measurements.

Step	Equipment used	Description	Remark
Step 1: Drilling of the boreholes	Simple rotary drill connected to petrol engine.	The drilling was carried out by 3 people. A boreholes were 60mm wide and were made 1m below the suspected foundation levels. The drilling operation took only a few minutes.	The operation is very quick in soft soil. In rocky soil heavier machinery could be needed.
Step 2: Removal and analysis of soil	-	Visual analysis and simple tests were made in order to view the layers and determine the type and wettness of soil.	If geotechnical data are required for the assessment, samples should be taken to laboratory for further testing.
Step 3: Casing of borehole	PVC tube	Rigid or flexible tubes can be used for casing the borehole. Flexible ones are more suitable for deeper boreholes.	PVC casing is needed only for the radar testing in order to stabilize the surface of the borehole. Metal tubes cannot be used.
Step 4: Testing with borehole radar	Borehole radar + central unit attached to a computer	The radar was slowly lowered down and pulled up in the borehole while the central unit received the signals.	The operation is very quick. There is no limitation in the depth of the borehole.

Step 5: Testing with the paralle seismic method	Geophones + signal analyser attached to a computer	The geophones were lowered down in the borehole. The series of geophones placed on a metal rod had physical contact with the soil surface of the borehole by detecting elements. During the operation the rod was pulled up in 10 cm steps while recordings were made at each step. A simple hammer was used for making strikes at the structure.	The operation is quick but a bit slower than the borehole radar method. There is no limitation in the depth of the borehole. If the surface of the borehole is stable there is no need for PVC casing.
Step 6: Processing and analysis of data	Computer	The received signals were analysed by appropriate software.	Skilled expert is required for the interpretation of measured data.

Results of the borehole radar measurements

Analysis of the soil samples taken out from the boreholes confirmed that the soil was clayey and wet around the foundation of both structures. In this environment no reliable interpretation of the borehole radar results was possible.

Results of the parallel seismic measurements

A plot of the arrival times -versus-depth has been prepared for both structures (Fig. 5 and Fig. 7). Changes in the physical properties of the medium lead to changes of the chracteristics of the plot (e.g. changes of the first arrival times result change of the slope of the curve) The top and bottom of the foundation and the hard rock layer are clearly noticeable on the 'time-depth' plots received from the abutment of the Rátót viaduct (Fig. 5).

Surprisingly the bottom of the foundation is approximately 1m above the hard rock layer according to the PS measurements. Measurements on the second borehole suggests the same level of foundation bottom, but the hard rock layer is found at lower depth. The PS tests confirm the correctness of the foundation data at original plan (Fig. 6).
Red arrows on the recordings received from the two boreholes drilled at the Eplény arch bridge (Fig. 7) point at the level of foundation bottom.

Time (ms)

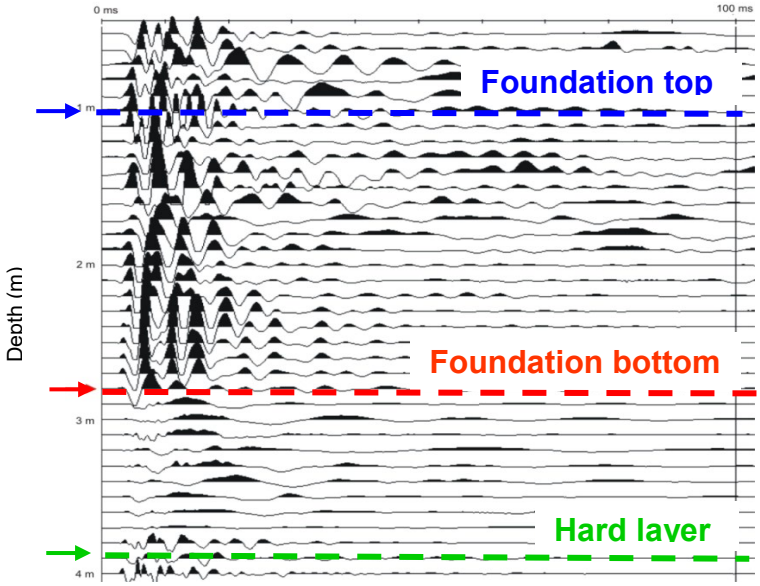

Fig.5: Interpretation of PS recording of the 1st borehole (Rátót viaduct)

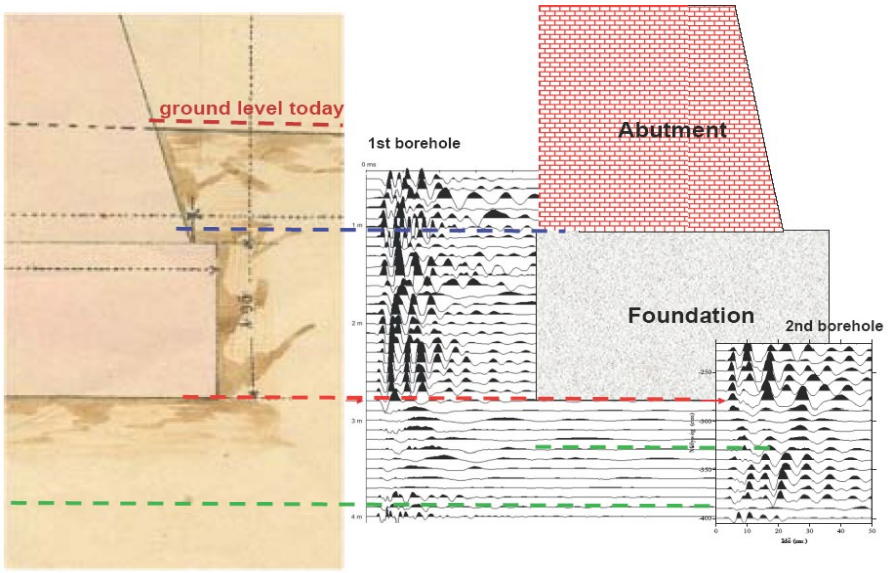

Fig.6: Confirmation of the original plan by the PS measurements (Rátót viaduct)

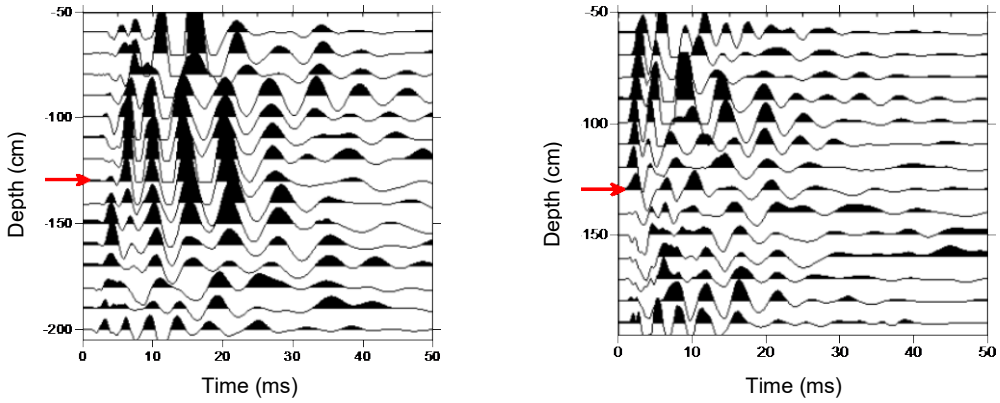

Fig.7: PS recordings at Eplény arch bridge

4. Conclusions

Both methods tried during the survey are promising tools for mapping unknown bridge foundations. Advantages of these methods are that they are relatively quick and inexpensive and can accurately determine the depth of foundations. The main limitations of the methods are that the measurement require a drilled borehole (in many cases cased too) and the accuracy depends on the soil properties and the distance of borehole to the foundation being investigated. Further limitations of the borehole radar method that it always requires a PVC cased borehole and the method is not applicable in electrical conductive environment such as clayey soil with high moisture content (unfortunately this was the case in the survey carried out). On the other hand it may provide results with better resolution than the parallel seismic method. It is thus recommended that both the borehole radar and parallel seismic methods are used for the mapping of bridge foundations and the interpretation is made by the utilisation of both results.